Sektion 3.3: Klimadynamik und Sedimente, GeoForschungsZentrum Potsdam

Paleoenvironmental changes in the Black Sea region during the last 26,000 years: a multi-proxy study of lacustrine sediments from the western Black Sea

Dissertation
zur Erlangung des akademischen Grades
Doktor der Naturwissenschaften (Dr. rer. nat.)
in der Wissenschaftsdisziplin Geologie

eingereicht an der Mathematisch-Naturwissenschaftlichen Fakultät
der Universität Potsdam

vorgelegt von
Olga Kwiecien
März 2008

Table of contents

ABSTRACT

Paleoenvironmental records provide ample information on the Late Quaternary climatic evolution. Due to the great diversity of continental mid-latitude environments the synthetic picture of the past mid-latitudinal climate changes is, however, far from being complete. Owing to its significant size and landlocked setting the Black Sea constitutes a perfect location to study patterns and mechanisms of climate change along the continental interior of Central and Eastern Europe and Asia Minor.

Presently, the southern drainage area of the Black Sea is characterized by a Mediterranean-type climate while the northern drainage is under the influence of Central and Northern European climate. During the Last Glacial a decrease in the global sea level disconnected the Black Sea from the Mediterranean Sea transforming it into a giant closed lake. At that time atmospheric precipitation and related with it river run-off were the most important factors driving sediment supply and water chemistry of the Black 'Lake'. Therefore studying properties of the Black Sea sediments provides important information on the interactions and development of the Mediterranean and Central and North European climate in the past.

One significant outcome of my thesis is an improved chronostraphigraphical framework for the glacial lacustrine unit of the Black Sea sediment cores, which allowed to refine the environmental history of the Black Sea region and enabled a reliable correlation with data from other marine and terrestrial archives. Data gathered along a N-S transect presented on a common time scale revealed coherent changes in the basin and its surrounding.

During the glacial, the southward-shifted Polar Front reduced moisture transport to the northern drainage of the Black Sea and let the southern drainage become dominant in freshwater and sediment supply into the basin. Changes in NW Anatolian precipitation reconstructed from the variability of the terrigenous input imply that during the glacial the regional rainfall variability was strongly influenced by Mediterranean sea surface temperatures and decreased in response to the cooling associated with the North Atlantic Heinrich Events H1 and H2. In contrast to regional precipitation changes, the hydrological properties of the Black Sea remained relatively stable under full glacial conditions.

First significant modification in the freshwater/sediment sources reconstructed from changes in the sediment composition, lithology, and $\delta^{18}O$ of ostracods took place at around 16.4 cal ka BP, simultaneous to the early deglacial northward retreat of the oceanic and atmospheric polar fronts. Meltwater pulses, most probably derived from the disintegrating European ice sheets, changed the isotopic composition of the Black Sea and increased the supply from northern sediment sources.

While these changes signalized a mitigation of the Northern European and Mediterranean climate, a decisive increase in local temperature was indicated only later at the transition from the Oldest Dryas to the Bølling around 14.6 cal ka BP. At that time the warming of the Black Sea surface initiated massive phytoplankton blooms, which in turn, induced the precipitation of inorganic carbonates. This biologically triggered process significantly changed the water chemistry and was recorded by simultaneous shifts in the elemental composition of ostracod shells and in the isotopic

composition of the inorganically-precipitated carbonates. Starting with the B/A warming and continuing through the YD cold interval and the Early Holocene warming, the Black Sea temperature signal corresponds to the precipitation and temperature changes recorded in the wider Mediterranean region.

Early Holocene conditions, similar to those of the Bølling/Allerød, were punctured by the marine inflow from the Mediterranean at ~9.3 cal ka BP, which terminated the lacustrine phase of the Black Sea and had a substantial impact on the chemical and physical properties of its water.

ZUSAMMENFASSUNG

Aus Paläoumweltdaten lassen sich detaillierte Informationen über die spätquartäre Klimaentwicklung gewinnen. Für die kontinentalen mittleren Breiten ist das Gesamtbild der Klimaänderungen während dieses Zeitraumes aufgrund seiner Vielfältigkeit allerdings noch immer unvollständig. Eine ideale Lokation, das Muster und die Mechanismen der Klimaänderungen in Osteuropa und Kleinasien zu untersuchen, ist das Schwarze Meer mit seiner bedeutenden Größe und seiner kontinentalen Lage.

Gegenwärtig ist das südliche Einzugsgebiet des Schwarzen Meeres durch ein mediterranes Klima geprägt, während die nördlichen Regionen von zentral- bzw. nordeuropäischem Klima beeinflusst werden. Als im letzten Glazial der Meeresspiegel so stark sank, dass das Schwarze Meer vom Mittelmeer abgetrennt und zu einem großen, abflusslosen See wurde, waren der atmosphärische Niederschlag und der damit verbundene Abfluss die wesentlichen Steuerfaktoren für Sedimenteintrag und Wasserchemie des Schwarzen „Sees“. Deshalb liefert die Untersuchung der Sedimente des Schwarzen Meeres wichtige Informationen über die früheren Zusammenhänge sowie die Entwicklung von mediterranem und zentral- bzw. nordeuropäischem Klima.

Das bedeutsamste Ergebnis meiner Doktorarbeit ist ein verbessertes Altersmodell für Sedimentkerne aus dem westlichen Schwarzen Meer; dieses erlaubt eine genauere Rekonstruktion der Entwicklungsgeschichte dieses Binnenmeeres und seiner Umgebung und ermöglicht einen fundierten Vergleich mit anderen marinen und terrestrischen Archiven. Daten, die entlang eines N-S Transektes im westlichen Bereich des Schwarzen Meeres erfasst wurden und auf einer gemeinsamen Zeitskala dargestellt werden, lassen die folgenden zusammenhängenden Entwicklungen im Becken und seiner Umgebung erkennen:

Während des Glazials war der Feuchtigkeitstransport zum nördlichen Einzugsgebiet des Schwarzen Meeres aufgrund der südwärts verlagerten Polarfront vermindert, so dass Süßwasser und Sedimente vorrangig aus dem südlichen Einzugsgebiet in das Becken gelangten. Die Rekonstruktion von Niederschlagsänderungen mit Hilfe von Schwankungen des terrigenen Eintrags zeigt, dass der regionale Niederschlag im Glazial stark von den Wasseroberflächentemperaturen des Mittelmeeres beeinflusst wurde und als Folge der Abkühlung während der nordatlantischen Heinrich-Ereignisse H1 und H2 abnahm. Im Gegensatz dazu blieb das Schwarze Meer während des Hochglazials hydrologisch relativ stabil.

Die Sedimentzusammensetzung, Lithologie und $\delta^{18}O$-Werte von Ostracoden zeigen, dass erste signifikante Änderungen im Frischwasser- und Sedimenteintrag zeitgleich mit dem frühglazialen nordwärtigen Rückzug der ozeanischen und atmosphärischen Polarfronten um 16.4 cal ka BP auftraten. Der Schmelzwassereintrag abschmelzender europäischer Eisflächen veränderte die Isotopenzusammensetzung des Wassers und erhöhte die Sedimentzufuhr aus den nördlichen Quellen.

Während diese Änderungen auf ein bereits milderes Klima in Nordeuropa und im Mittelmeerraum hindeuten, zeigt sich ein Anstieg der lokalen Temperaturen erst während des Übergangs von der

Älteren Dryas zum Bølling/Allerød um etwa 14.6 cal. ka BP. Zu diesem Zeitpunkt führte ein wahrscheinlicher Anstieg der Wasseroberflächentemperaturen im Schwarzen Meer zu einem massiven Phytoplanktonwachstum, welcher die Ausfällung anorganischen Karbonats zur Folge hatte. Dieser biologisch ausgelöste Prozess veränderte maßgeblich die Wasserchemie und spiegelt sich in simultanen Veränderungen der Elementzusammensetzung von Ostracoden und der Isotopenzusammensetzung von anorganisch ausgefälltem Karbonat wieder. Beginnend mit dem Bølling/Allerød, durch die Jüngere Dryas Kälteperiode und die frühholozäne Erwärmung hindurch, deckt sich das Temperatursignal des Schwarzen Meeres mit den Niederschlags- und Temperaturänderungen des weiteren Mittelmeerraumes.

Das Frühholozän war, ähnlich wie das Bølling/Allerød, durch das Einströmen salzhaltigen Meerwassers aus dem Mittelmeer gekennzeichnet (~9.3 cal. ka BP), welches die lakustrine Phase des Schwarzen Meeres beendete und einen erheblichen Einfluss auf seine chemischen und physikalischen Wassereigenschaften ausübte.

Acknowledgements

Founding his Fellowship, Gary Comer (1927-2006) believed that scientists of great knowledge and experience can unravel mysteries of Earth's changing climate. When I first came to Potsdam, having neither much knowledge nor experience, Professor Gerald Haug believed in my pure enthusiasm and offered me a PhD position. Decisions of these two men changed my life and let me spend four wonderful years in GFZ Potsdam.

Helge Arz! Thank you for showing me how THE climate works and how to open A core. You are the best mentor ever! I have learned a lot from you and I am both, lucky and happy that I had this chance.

Frank Lamy has always managed to untangle my twisted scientific concepts, and to straighten my even most unfortunate writing attempts. Gerald Haug (again) has taken care that these attempts were pretty frequent (Ja! Ich habe heute schon publiziert!) Thank you!

André Bahr – I use to think of you as an older scientific brother – thank you for you patience and competence and hours of stimulating discussions.

Birgit Plessen! You have measured meters and meters of Black Sea mud, tireless and always with a smile. I am very grateful for your constant faith in the significance of our not necessarily breathtaking results and in my abilities to make a story out of them.

My project would not have been possible without the support of many people who helped me with the analytical work. Gabi Arnold, Dieter Berger and Michael Köhler prepared blocks and thin-sections. Peter Dulski and Brigitte Richert run μXRF measurements. Heike Pfletschinger and Ursula Röhl from University Bremen taught me how to run the XRF scanner. Katrin Wolff sieved and grinded hundreds of my samples while Petra Meier showed me how to prepare them for mass spectrometers. Andreas Hendrich provided not only maps for my publications but also solutions for many graphic problems. Juliane Herwig and Helga Kemnitz introduced me to SEM facility. Last but not least Christine Gerschke often saved me from falling into the black hole of bureaucracy, so there was still some time left for science.

Christian, Clara, Gergana, Hans, Iris, Stefan and Susanne – you helped me to find myself in the German reality and to discover the beauty of German language. Most of all big thanks for all the fun and after-work activities we had together.

To all of my good 'old' friends – though the good 'old' times are gone and now you are dispersed all over the world – I do appreciate you have never forgotten about me! Asko, Dominiko, Magdo, Marto, Weroniko (Swinio moja kochana!) i Wojtku! I am glad to have friends like you!

My family has always believed in the success of all of my enterprises. Without this belief, I wouldn't have been who I am.

Sebastian kochanie! You were always there for me through all my ups and downs. I cannot imagine a better companion. Thank you.

1. Introduction

Understanding the past climate variability is essential in order to accurately predict the future behavior of the climate system. The past climatic oscillations are well documented in Antarctic and Greenland ice cores (e.g. Grootes et al., 1993; Petit et al., 1999) and in marine sediment cores from the across the oceans (e.g. Bond et al., 1993; Jaccard et al., 2005; Lamy et al., 2004). However, these records are often dominated by global-scale signals, like changes in circulation and composition of the atmosphere or ocean heat transport, and offer only limited information with respect to regional climate variability in other, in particular mid- and low-latitudinal continental parts of the globe.

Terrestrial climate archives like lake sediments, cave deposits or tree rings are of a different nature. Terrestrial sequences record spatially discrete climate conditions, superimposed on the hemispheric trend, but explicit for their locality. The role of local/regional features, for example altitude, topography or vegetation cover is highly significant; they can easily either suppress or amplify a hemispheric climate signal. Terrestrial archives allow tracing propagation of the climate signal into the continental interior. Due to their uniqueness, they offer an important advantage for testing the sensitivity of different components of the ecological system against climate change. Moreover, the integration and comparison of terrestrial records with ice core and marine data enables an assessment of possible leads and lags in the climate system. Therefore, continental archives are an excellent substance to evaluate geographic extent, magnitude, and timing of climatic oscillations.

1.1. Study area

Coupled atmosphere-ocean-land studies of a past climate were very successful in the Western Mediterranean (Cacho et al., 2006; Combourieu Nebout et al., 2002; Sanchez Goni et al., 2002). Due to its geographical position the whole Mediterranean region plays a communicator role between low- and high-latitude climatic systems (Fig. 1.1.1).

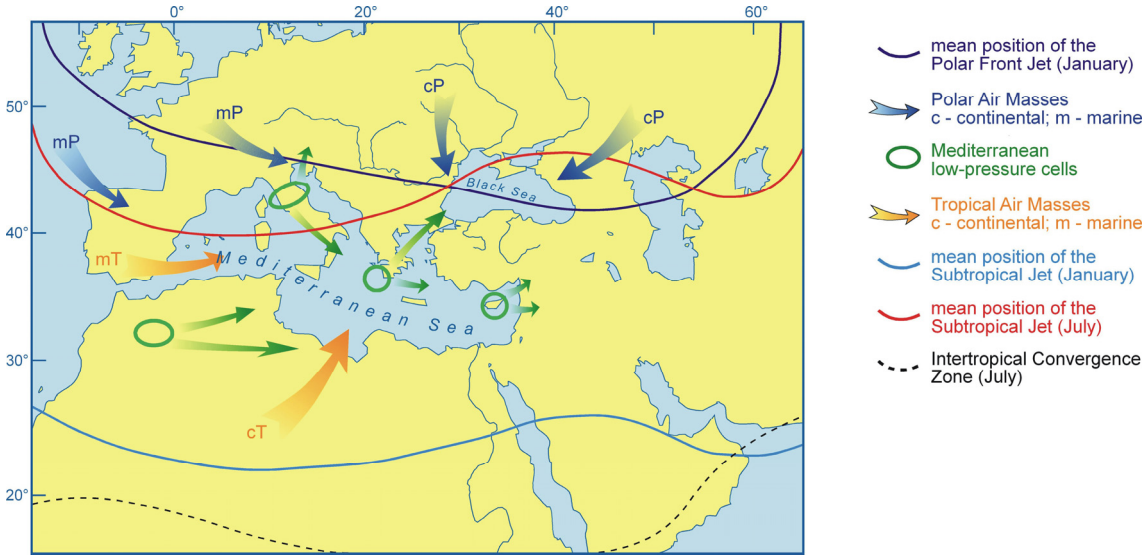

Figure 1.1.1: A Scheme of the atmospheric circulation patterns influencing climate in the Mediterranean region (after Wigley and Farmer, 1982). Mediterranean low-pressure cells represent modern regions of cyclonogenesis. Principal cyclone tracks are indicated by green arrows.

During summertime, the Mediterranean climate is influenced by subtropical high-pressure cells, with subsiding air bringing warm and dry conditions over the region. During winter, the strengthened and expanding Siberian High pushes the atmospheric jet stream systems equatorward. The Polar Front Jet replaces the southward-shifted Subtropical Jet and allows mid-latitude storms (low pressure cells) originating from the open Atlantic Ocean to enter the Mediterranean region. Here, the relatively warm water provides a secondary moisture source so that the storms may maintain or renew their strength as they move eastward (Fig.1.1.2).

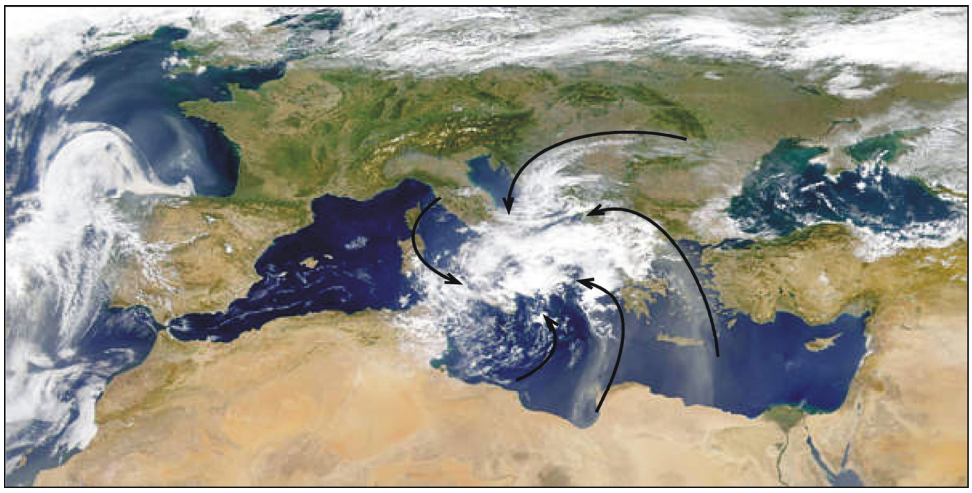

Figure 1.1.2: A low-pressure cell developing over the Central Mediterranean. Map source: http://visibleearth.nasa.gov

Today the Black Sea (Fig. 1.1.1) may be considered a satellite basin of the Mediterranean, though its connection with the Mediterranean Sea was not always stable in the past. The Black Sea forms an enclosed depression, located between southeastern Europe and Anatolia. Since its opening as a back-arc basin dated back to Cretaceous times (Cloething et al., 2003), the Black Sea has undergone a complex tectonic evolution. Being one of the Tethys remnant basins (together with closed basins like the Caspian Sea and the Aral Sea), today the Black Sea can be seen as the most distant arm of the North Atlantic Ocean. Within the last 3 Ma, however, the dual nature of the Black Sea is reflected in its changing hydrologic conditions. During glacial times when the global sea level is low, the Black Sea is a closed basin containing freshwater, while during sea-level high-stands in interglacials, the Black Sea – North Atlantic Ocean connection is regained via the Mediterranean Sea (Schrader, 1979). This cyclic entrance of saline Mediterranean water during interglacials resulted in periods where the Black Sea developed a strong stratification with bottom water anoxia. Today, the basin constitutes an excellent natural laboratory to study processes characteristic for an oxygen-free environment and most of the recent investigation concentrate chiefly on the youngest marine stage of the Black Sea. In 1997 the hypothesis of Ryan and Pitman (Ryan et al., 1997) proclaiming the Black Sea a potential scene for the biblical deluge (Noah's flood) won a renaissance of interest for the basin's hydrological past. Still, the highest attention was paid to the timing and the mechanism of the last reconnection with the Mediterranean Sea.

Only recently works of Major et al., (2002; 2006) and Bahr et al., (2006; 2005) highlighted the potential of the lacustrine Black Sea sediments as climate archive and contributed greatly to unveil the Last Glacial history of the basin itself and the adjacent continents. The geographical setting of the Black Sea is very attractive for paleoenvironmental reconstructions. Considering the Black Sea a lake, its enormous size and landlocked position perfectly qualifies it to record environmental and

hydrologic changes in the continental interior of Central and Eastern Europe and Asia Minor (Fig. 1.1.1). Southern - Mediterranean and northern - European drainage basins of the western Black Sea differ in topography, geology, and precipitation regime. The steep southern hinterland composed partly of carbonates is strongly affected by the Mediterranean climate and receives most of its precipitation during the winter. The more gentle northern hinterland composed mostly of cristaline rocks is characterized by continental climate with precipitation falling either all-year-long (in the west) or mostly in summer (in the east). Therefore, variations in the water chemistry and sediment composition of the Black Sea are strongly related to climate-related changes in the hinterlands.

1.2. Motivation of research

Previous reconstructions of the Black Sea climatic and hydrological evolution focused on the NW Black Sea (Major et al., 2002, 2006; Bahr et al., 2005, 2006). Lamy et al. (2006) conducted work in the SW of the Black Sea, however, they concentrated on the Holocene marine sediments (Fig. 1.2.1). The recovery of a new sediment core in the SW Black Sea (offshore Northwestern Anatolia, site MD04-2788/2760) completes the N-S transect of the western Black Sea basin (Fig. 1.2.1) and facilitates an integration of paleoclimatic data from the northern (European) and the southern (Mediterranean) drainage areas. Such a comparison is important for understanding the interactions between the Mediterranean and continental European climate in the past. The suite of Black Sea records covering the time span between 8 and 26 cal ka BP, allows now to concentrate on past climate changes in the continental mid-latitudes. These records not only provide information on the transition between two climate extremes, the Last Glacial and present interglacial, but deliver also insights into climate variability on millennial, centennial to interannual time-scales.

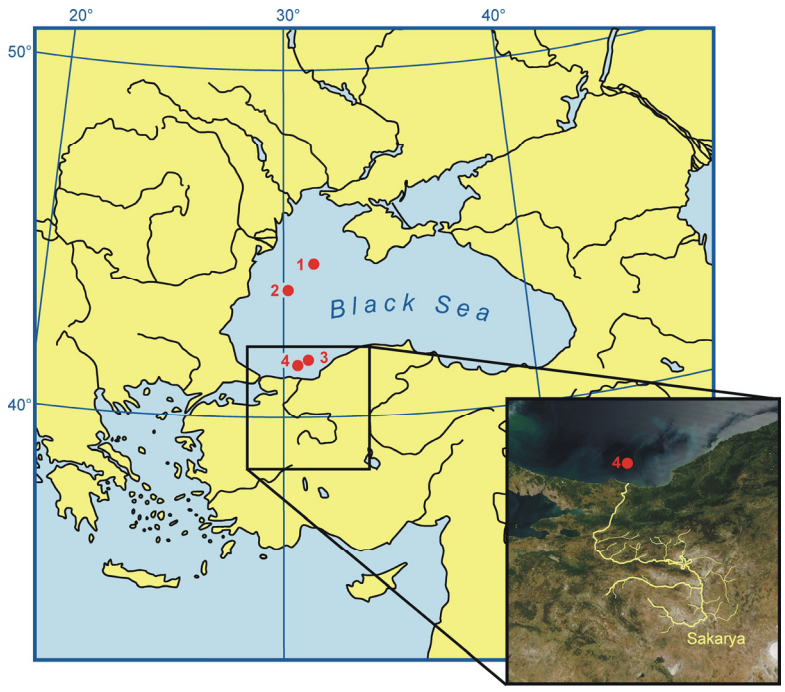

Figure 1.2.1: Sediment cores along a N-S Black Sea transect (1) Major et al., 2002; (2) Bahr et al., 2005; (3) Lamy et al., 2006; (4) new site MD04-2788/2760 (this study).

The objective of my work was to study in detail and comprehensively the environmental changes since the Last Glacial Maximum (LGM) in the Black Sea region. In order to fulfill this task I first focused on the advantages of the new coring site MD04-2788/2760 in the southwestern Black Sea:

- The proximity of the Mediterranean active volcanic domain provides independent time markers (tephra layers).

- Due to the location of the coring site next to the Sakarya River mouth (Fig. 1.2.1), terrigenous sediments derived from northeastern Anatolia constitute an inherent part of the deposits. Moreover, the vicinity of the river promotes exceptionally high sedimentation rates which result in a high temporal resolution.

- Consequently, the recovered sediments provide information on both the environmental changes in the drainage basin of the Sakarya, which is largely influenced by Mediterranean climate, and the general changes in the Black Sea basin itself.

- The almost continuously laminated glacial sediments display high-frequency changes in the sediment supply in response to interannual to decadal-scale climate variability.

A full exploitation of the paleoclimatic potential offered by the new site MD04-2788/2760 benefits from the integration of data available from other western Black Sea cores. Having a set of data from a complete N-S transect at my disposal, I addressed following issues:

- Constraining a reliable age model for the glacial Black Sea sediments
    - to enable the intercomparison with data from other marine and terrestrial records and place the environmental changes in the Black Sea basin and its vicinity in a wider context of Northern Hemisphere climate change.

- Tracing down alterations in terrigenous/freshwater input sources
    - to investigate factors controlling glacial precipitation/continental run-off in NW Anatolia,
    - to examine the pattern of regional climate change related to the purported shift in the atmospheric circulation regime at the onset of the deglaciation.

- Testing the sensitivity of the Black Sea hydrology to millennial-scale climate changes within the glacial and the deglaciation (MIS2 and transition to MIS1)
    - to examine the relationship between North Atlantic climate variability and the extent, amplitude, and timing of environmental changes in the Eastern Mediterranean/Black Sea region.

- Assessing the environmental background of decadal to centennial scale fluctuations in the laminated glacial sediments of the southwestern Black Sea.

1.3. Material

My work was based on the gravity core MD04-2788 and the corresponding piston core MD04-2760 retrieved in the southwestern Black Sea during the ASSEMBLAGE I cruise onboard of R/V *Marion Dufresne* in 2004 (Fig. 1.3.1, Tab. 1.3.1).

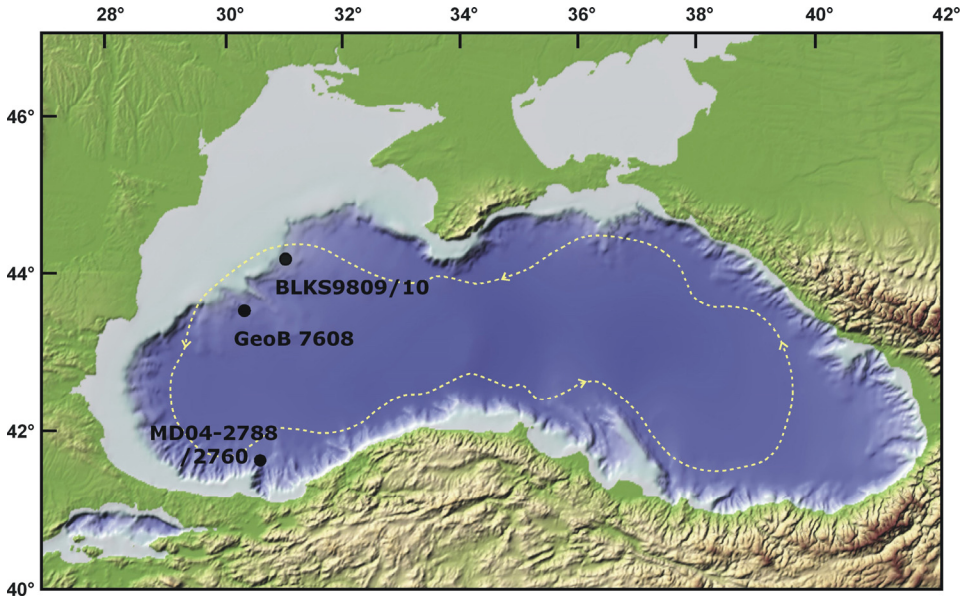

Figure 1.3.1: Study area with the location of the gravity and piston cores relevant for the present work. Yellow dashed line indicates the Black Sea rim current – a permanent counter-clockwise hydrographic feature of the modern Black Sea surface which is an important mechanism of sediment distribution in the basin.

Core	Latitude N	Longitude E	Water depth (m)	Core length (m)
MD04-2760[a]	41°31.7'	30°53.1'	1226	41.94
MD04-2788[a]	41°31.7'	30°53.0'	1224	6.00
GeoB 7608-1[b]	43°29.2'	30°11.1'	1202	6.85
BLKS9809[c]	44°05.2'	30°48.0'	240	8.40
BLKS9810[c]	44°04.0'	30°50.7'	378	7.59

Table 1.3.1: Geographical coordinates and length of the relevant gravity and piston cores ([a]this study, [b]Bahr et al., 2005; [c]Major et al., 2002).

The topmost meters of the piston core MD04-2760 were strongly disturbed (extended) during coring. However, a detailed comparison between high-resolution X-ray fluorescence (XRF) data allowed me to correlate the piston and gravity cores, and to construct a composite profile MD04-2788/2760. The composite profile MD04-2788/2760 is used as a master record for this study and has been complemented with proxy-records from two other sediment cores from the northwestern Black Sea (Fig. 1.3.1, Tab. 1.3.1). Core GeoB 7608-1, recovered during the R/V *Meteor* cruise M51-4 belongs to a down-slope transect in the northwestern Black Sea investigated by André Bahr during his PhD project (Bahr 2005). Cores BLKS9809, BLKS9810 (composite record BLKS9809/10) retrieved during the R/V *Le Suroit* cruise were analyzed by Candance Major and co-workers (2002; 2006). The detailed examination of the XRF Ca-intensity and $CaCO_3$ concentration allowed a precise

correlation of the MD04-2788/2760, GeoB 7608-1, and BLSK98-09,-10 records. Since the present work focuses on the lacustrine phase of the Black Sea, I confined my study to the time window before the reconnection with the Mediterranean Sea (8-26 cal ka BP). Within this time-span, all 3 records are presented, for the reasons of consistency, on the MD04-2788/2760 time scale.

According to the classic stratigraphy of Ross and Degens (1974), late Quaternary (~25 ka) Black Sea sediments are subdivided into two Holocene marine units: Unit I (finely laminated coccolith ooze) and Unit II (finely laminated sapropel), and the Glacial to Holocene lacustrine Unit III (clayly mud) (Fig. 1.3.2).

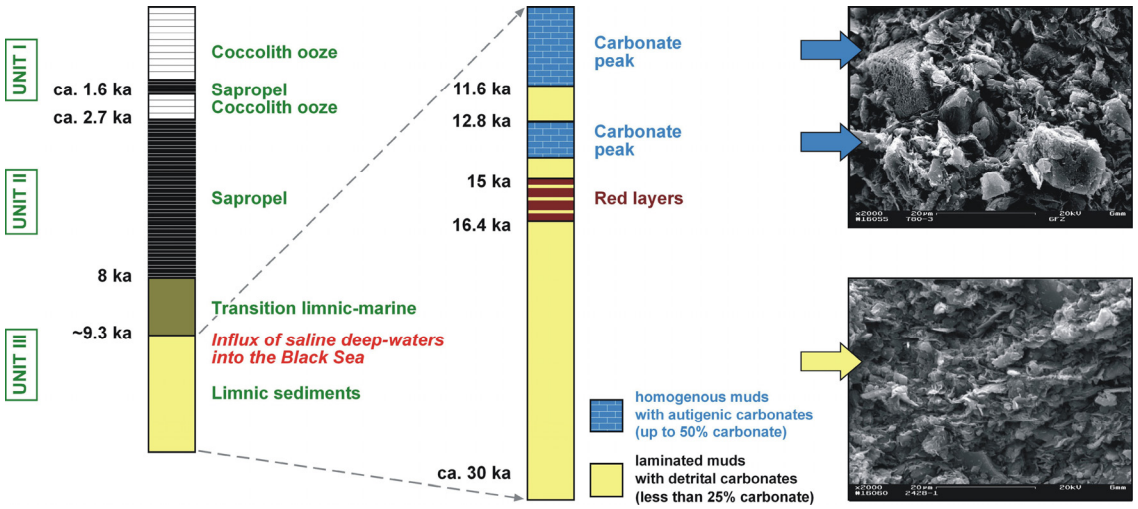

Figure 1.3.2: Stratigraphy of the glacial to Holocene Black Sea sediments (updated after Jones and Gagnon, 1994).

Glacial sediments of Unit III are generally represented by carbonate- and organic-poor terrigenous muds (Müller and Stoffers, 1974). A series of reddish-brown clays deposited in the Black Sea after ~16.4 cal ka BP, commonly called 'red layers' is most probably associated with a massive meltwater discharge at the onset of the deglaciation (Bahr et al., 2005; Major et al., 2002). The Bølling/Allerød warming, which followed after the deposition of the red layers, is recorded in the Black Sea sediments by high amounts of inorganically-precipitated carbonates (Bahr, 2005; Major et al., 2002). The carbonate precipitation diminished during the Younger Dryas cold interval, took up in the early Holocene, and continued until the reconnection with the Mediterranean Sea. The base of the Black Sea sapropel, traditionally marking the lacustrine/marine transition, is dated to ~8.0 cal ka BP (Lamy et al., 2006) but the first inflow of the Mediterranean water could have taken place as early as 9.5 cal ka BP (Bahr et al., 2006; Major et al., 2006).

1.4. Methods

Figure 1.4.1 presents the working scheme that guided my study. Non-destructive techniques like X-ray fluorescence (XRF) profiling measurements and digital imaging provided general information about the compositional and lithological changes of the investigated sediments. This first step helped to select intervals most suitable for dating and to optimize sampling resolution. All applied methods are briefly described below.

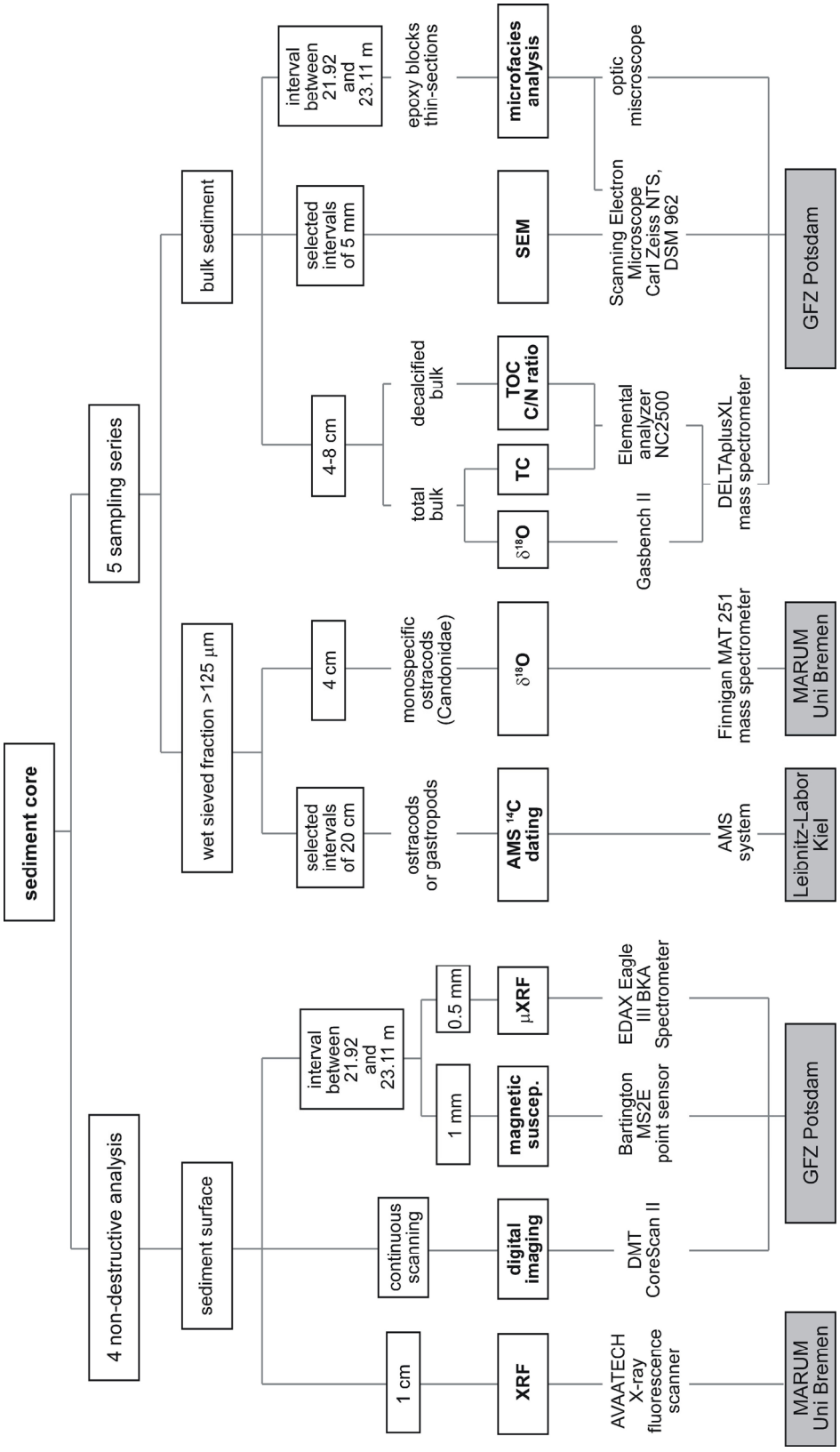

Figure 1.4.1: Flow-diagram depicting methods I have used.

X-ray fluorescence (XRF) scanning provides high-resolution semi-quantitative concentration of major elements in the sediment (e.g. Al, Si, S, K, Ca, Ti, Mn, and Fe) (Richter et al., 2006). This method has two advantages: it generates many data within a relatively short time-span and is non-destructive. Single element intensities may be calibrated by comparison with other methods (e.g. XRF Ca-intensity with the $CaCO_3$ content). Element ratios have proven to be useful parameters to distinguish whether biogenic or minerogenic components are the dominant fraction of the sediment (Arz et al., 1998), or to identify provenance of terrigenous material (Lamy et al., 2004). Due to its high resolution, XRF data provide a reliable tool for correlating different cores.

Magnetic susceptibility is a commonly used magnetic parameter directly proportional to the quantity and grain size of ferro- and ferri-magnetic materials in the sample (Verosub and Roberts, 1995). Magnetic susceptibility measurements are very useful for sediment studies as they can indicate temporal variation in the concentration and grain size of terrigenous material deposited in aquatic environment.

AMS ^{14}C dating is the most widely employed method for dating events within the last 50 ka. It is based on the concept of exponential decay rate of radioactive ^{14}C incorporated by the organisms during their lifespan. However, the atmospheric ^{14}C concentration may differ substantially from the concentration in local water reservoirs. Old 'dead' carbon eroded from carbonate rocks can be easily assimilated by acquatic organisms and provide diluted ^{14}C carbon. Admixture of old dissolved carbon (so-called hardwater effect) results in age offsets toward older ages and is a serious obstacle in constraining accurate chronologies. One way to estimate potential age offsets is the verification of the radiocarbon age model with independent time markers, like well-dated tephra layers.

During the lacustrine glacial phase the Black Sea water was predominantly of meteoric origin with the isotopic composition responding to changes in evaporation-to-precipitation ratio and modifications of atmospheric precipitation and/or run-off (Bahr et al., 2006). Both, temperature and isotopic composition of ambient continental water are reflected in stable oxygen isotope ratio ($\delta^{18}O$) of inorganically precipitated carbonates (Leng and Marshall, 2004). Therefore, $\delta^{18}O$ analysis of carbonatic material (like biogenic ostracod valves and authigenic calcite/aragonite) is a common method to reconstruct $\delta^{18}O$ variations of continental waters and to infer hydrological evolution of lacustrine systems. Ostracods, small crustaceans ubiquitous in terrestrial aquatic environments, are mainly benthic inhabitants building calcitic shells. As the building of a shell is a physiological process additional vital effects in the $\delta^{18}O$ of ostracod valves have to be considered. Fortunately, the vital offset tends to be relatively constant within closely related genera (Holmes and Chivas, 2002). On the contrary, authigenic carbonates are assumed to precipitate in isotopic equilibrium with the lake water. For my analysis, however, the carbonate subfractions (detrital and inorganic precipitates) were not isolated and $\delta^{18}O_{bulk}$ is actually a function of the two components. Consequently, in a first approach, our $\delta^{18}O_{bulk}$ record assisted by Scanning Electron Microscopy (SEM) imaging depicts changing proportions of detrital and inorganically-precipitated carbonates. Results of all $\delta^{18}O$ measurements are reported as ‰ relative to the VPDB standard.

Concentration of organic matter is reflected in the total organic carbon content (TOC weight %). The lake *in situ* productivity and/or detrital input may be sources for organic matter deposited in the lacustrine environment. The aquatic or terrestrial origin of organic matter can be generally inferred from its composition (e.g. using the C/N ratio; (Lamb et al., 2004; Lamb et al., 2007). After determining the total carbon content (TC weight %) I used the relation (TC - TOC) × 8.33 = $CaCO_3$ in order to calculate the dry weight percentages of calcium carbonate ($CaCO_3$).

Studying thin-sections under optical microscope provides general information about the texture and composition of finely laminated sediments. Complementary Scanning Electron Microscope (SEM) imaging of either bulk material or thin-sections brings valuable information on sedimentary microstructures. μXRF profiling of finely laminated sediments may provide a higher-resolution record of elemental distribution within consecutive laminae and therefore enables (i.e. in case of varved sediments) climate reconstructions on decadal to seasonal-scales.

1.5. Overview of manuscripts

My PhD thesis is based on four manuscripts, published or submitted to peer-reviewed international journals, and one additional preliminary study.

In the first manuscript 'Estimated reservoir ages of the Black Sea since the Last Glacial' (O. Kwiecien, H. W. Arz, F. Lamy, S. Wulf, A. Bahr, U. Röhl and G. H. Haug, *Radiocarbon*), I constrained the chronostratigraphical framework for the glacial Black Sea sediments and verified age models of already published records. Coupling AMS ^{14}C dating results with tephochronology, and comparing my results with age models of existing records, I was able to estimate changes in reservoir ages of the Black Sea from 26 to 8 cal ka BP. This manuscript established the chronological backbone of the subsequent paleoenvironmental studies.

The main focus of the second manuscript 'North Atlantic control on precipitation patterns in the Eastern Mediterranean/Black Sea region during the Last Glacial: new insights from the Black Sea sediments' (O. Kwiecien, H. W. Arz, F. Lamy, B. Plessen, A. Bahr, and G. H. Haug, submitted to *Quaternary Research*) concerns relative changes in precipitation for NW Anatolia in the Marine Isotope Stage 2 (MIS2), reconstructed from variations in the terrigenous supply. Analyzing changes in the composition of the terrigenous fraction coupled with stable oxygen isotope records along a N-S western Black Sea transect, I identified modifications in the freshwater/sediment sources and linked them to the abrupt cold spells in the North Atlantic region and early deglacial northward retreat of atmospheric and oceanic polar fronts.

The third manuscript 'Abrupt changes of temperature and water chemistry in the late Pleistocene and early Holocene Black Sea' (A. Bahr, F. Lamy, H. W. Arz, C. Major, O. Kwiecien and G. Wefer, *Geochemistry Geophysics Geosystems*) introduces a novel method to infer the temperature-variability of the deep Black Sea during the last 26 ka using Mg/Ca and Sr/Ca data measured on ostracods. Combining new data with sedimentological and geochemical proxies this study addresses also the question of timing and mechanism of the reconnection with the Mediterranean Sea.

The fourth manuscript 'The last deglaciation as recorded in the western Black Sea: a multi-proxy study' (O. Kwiecien, H. W. Arz, F. Lamy, B. Plessen, A. Bahr, and G. H. Haug, to be submitted to Quaternary Science Reviews or Palaeogeography, Palaeoclimatology, Palaeoecology) is a summary of published records together with new data, and presents the most comprehensive approach to the environmental changes acting on the Black Sea basin and its drainage during the LGM and Late Glacial. Synthesized information from the Black Sea records is compared with records from the Mediterranean region to provoke discussion on the last deglaciation in a wider Mediterranean-mid-latitudinal context.

The fifth manuscript 'Laminated glacial sediments from the southwestern Black Sea – a preliminary study' (O. Kwiecien, H. W. Arz, F. Lamy, P. Dulski, N. Nowaczyk and G. H. Haug, draft) exploits

the nature of the lamination in the glacial sediments and its potential to reconstruct high-frequency climate variability.

2. Estimated reservoir ages of the Black Sea since the Last Glacial

Olga Kwiecien[1], Helge W. Arz[1], Frank Lamy[1,2], Sabine Wulf[1,3], André Bahr[4,5], Ursula Röhl[4] and Gerald H. Haug[1,6]

[1]*GeoForschungsZentrum Potsdam (GFZ Potsdam), Germany*
[2]*now at the Alfred Wegener Institute for Polar and Marine Research (AWI), Bremerhaven, Germany*
[3]*now at the University of Texas at Austin, Institute for Geophysics, Jackson School of Geosciences, Austin, USA*
[4]*MARUM - Center for Marine Environmental Research, University of Bremen, Germany*
[5]*now at IFM-GEOMAR, Kiel, Germany*
[6]*now at the Swiss Federal Institute of Technology (ETH Zürich), Switzerland*

Published in: Radiocarbon, 50, 99-118

ABSTRACT *AMS ^{14}C dating of ostracod and gastropod shells from the southwestern Black Sea cores combined with tephrochronology provides the basis for studying reservoir age changes in the Late Glacial Black Sea. The comparison of our data with records from the northwestern Black Sea shows that an apparent reservoir age of ~1450 ^{14}C yr found in the glacial is characteristic of a homogenized water column. This apparent reservoir age is most likely due to hardwater effect. Though data indicate that a reservoir age of ~1450 ^{14}C yr may have persisted till the Bølling/Allerød warm period, the comparison with the GISP2 ice core record suggests a gradual reduction of the reservoir age to ~1000 ^{14}C yr that might have been caused by dilution effects of inflowing meltwater. During the Bølling/Allerød warm period, soil development and increased vegetation cover in the catchment area of the Black Sea could have hampered erosion of carbonate bedrock, and hence diminished contamination by 'old' carbon brought to the Black Sea basin by rivers. A further reduction of the reservoir age most probably occured contemporary to the precipitation of inorganic carbonates triggered by increased phytoplankton activity and was confined to the upper water column. Intensified deep water formation subsequently enhanced the mixing/convection, and renewal of intermediate water. During the Younger Dryas (YD), the age of the upper water column was close to 0 yr, while the intermediate water was ~900 ^{14}C yr older. The first inflow of saline Mediterranean water, at ~8300 ^{14}C yr BP shifted the surface water age towards the recent value of ~400 ^{14}C yr.*

INTRODUCTION

One important issue regarding research performed on Late Glacial lacustrine sediments of the Black Sea is the lack of a reliable chronostratigraphy. Attempts to decipher the chronology of Quaternary Black Sea deposits are hindered by a lack of material adequate for dating. Rare reports on reservoir age of the Black Sea water display inconsistent sets of data, and consider only marine sediments covering not more than the last ca. 8000 yrs of the Black Sea history (e.g. Jones and Gagnon, 1994; Guichard et al., 1993). In many aspects, the Black Sea is an exceptional water body. It is the world's largest anoxic basin that has changed its character from freshwater to marine only 8000 yr ago, and is known to have been oscillating between a freshwater and a marine state for at least the last three million years (Schrader, 1979). Though lately it gained an increased scientific interest due to the 'Flood hypothesis' (Ryan and Pitman, 1997), little progress has been made in developing consistent age models for its Late Quaternary sediments. The stratigraphy of the longest Black Sea record, so far, core 380A of the DSDP Leg 42, reaches most likely back to Messinian, and was assigned

using the freshwater/marine-brackish flora assemblages, combined with the global sea level curve (Schrader, 1979). In general, Schrader (1979) associated freshwater stages with cold periods (glacial conditions, low global sea-level stand, and no connection to Mediterranean) while he saw marine-brackish floras as indicative of warm periods (interglacial conditions, high global sea-level stand, open connection to Mediterranean). Schrader (1979) also found out that transitions from freshwater to marine-brackish (glacial to interglacial) conditions were often followed by sapropel deposits, though not every sapropel marked a freshwater/marine transition. Some sapropels indicated only occasional spills (sudden influxes of marine Mediterranean water).

According to Ross and Degens (1974), late Quaternary (~25.000 yr) Black Sea sediments are subdivided into the Glacial to Holocene lacustrine Unit III (clayey mud) and two Holocene marine units: Unit II (finely laminated sapropelic sediments) and Unit I (finely laminated coccolith ooze). The transition from Unit III to Unit II is accompanied by laminated, inorganically-precipitated aragonite of variable thickness (from mm scale to ~10 cm). Transitions between the units are stratigraphic markers, which can be correlated on basin scale. The division into these three units, together with the first rough radiocarbon dating, was initially presented by Ross and Degens (1970, 1974) and later modified by Hay (1990). A depth-increasing discrepancy between the ^{14}C age of organic and carbonate fractions was first observed by Deuser (1972) and later confirmed by Ross and Degens (1974). The dating of the Unit II/III transition (Jones, 1991) showed that AMS ^{14}C dates of organic carbon give consistently younger ages than those of total carbonate. However, the problem of unreliable application of ^{14}C data to construct a consistent chronostratigraphy of the marine units had arisen earlier, with the discovery of a mismatch between the proposed varve chronology and radiometric measurements (Ross and Degens, 1974; Degens et al., 1980; Crusius and Anderson, 1992). In an attempt to constrain this controversy, Jones and Gagnon (1994) performed a very detailed study of the transitions between Black Sea units comparing results derived by AMS ^{14}C dating of various materials. Averaging over several dates obtained on carbonates and organic carbon, they calculated 7540±130 yr BP for the onset of the sapropel formation marking the Unit II/III boundary, 2720±160 yr BP for the first invasion of coccolithophorides marking the Unit I/II boundary, and 1635±60 yr BP for the final invasion of coccolithophorides. The recognition of the Z-2 tephra from the Minoan eruption of Santorini dated at 3595 yr BP (Hammer et al., 1987, lately revised to 3577–3550 yr BP, Friedrich et al., 2006), within sediments containing marine organic matter ~1200 yrs older than the tephra itself, confirmed and yet underlined the complexity of AMS ^{14}C dating in the marine Black Sea (Guichard et al., 1993). The difficulty of constraining the chronostratigraphy for the lacustrine Black Sea consists in a limitation of available dating methods; carbonate material suitable for ^{14}C dating is commonly very sparse and sediments are either non-laminated or vaguely but not annually laminated. Independent time markers like, for instance, tephra layers have not been identified so far.

Major et al. (2002) were the first to propose a detailed AMS ^{14}C-based chronostratigraphy of Late Glacial Black Sea sediments. Dating was performed on adult shells of *Dreissena rostriformis* from two sediment cores recovered at 240 and 378 m water depth in the northwestern Black Sea (in this study we refer to these depths as to the 'upper water column'), and no reservoir correction was applied to the dates obtained. The importance of reservoir corrections due to 'too old' ages of glacial Black Sea sediments was noticed by Bahr et al. (2005). Using various carbonate material, they dated two cores from a slope transect in the northwestern Black Sea. The stratigraphy based on ostracod and gastropod radiocarbon dates from a core from 1200 m water depth (Bahr et al., 2005) showed a significant and almost constant offset of 1000 ^{14}C yr with respect to previously published data based on bivalve radiocarbon dates (Major et al., 2002). On the contrary, oxygen isotope data from the shallower core (168 m water depth) in the same transect, dated using the same species as in the

study published by Major et al. (2002) (articulated shells of *D. rostriformis*), supported a 0-yr reservoir correction. In conclusion, Bahr et al. (2005) suggested that either the dating samples must have been contaminated by older carbonates, or that in the ancient Black Sea basin at least the upper 400 m must have been ventilated, while deeper water masses should have been permanently stratified. This hypothesis, however, is not confirmed by the stable oxygen isotope records coming from the same transect suggesting that stratification of the Black Sea waters only occurred after 14,500 yr BP (13,000 ^{14}C yr BP) (Bahr et al., 2006). Interesting enough, although the recent Black 'Sea' is not exactly an analog for a glacial Black 'Lake', measured ages of water from different depths, as well as modeled results were not always found consistent (e.g. Top and Clark, 1983; Östlund and Dyrssen, 1986; Murray and Top, 1991). Attempts to assess the reservoir effect are listed in Table 2.1. Taking advantage of a new radiocarbon-dated record from the SW Black Sea, with tephra deposits as independent time markers, we aim to shed light on the Late Glacial Black Sea stratigraphy puzzle. Comparing records from different water depths, we propose a potential model of the temporal and spatial evolution of the glacial Black Sea reservoir age.

reference / water depth in m		Top and Clark, 1983	Östlund and Dyrssen, 1986	Murray and Top, 1991	Guichard et al., 1993	Jones and Gagnon, 1994	Siani et al., 2000	Major et al., 2002	Bahr et al., 2005
surface and upper water column	**0-200**	Estimation of vertical exchange time of tritium concen. on 3-box model	AMS^{14}C dating on water samples (DIC) (surface samples could have been contaminated	Estimation of water residence time on box model ~1400 ^{14}C yr (0-50m)	AMS^{14}C dating on organics bracketing Z-2 tephra ~1280 ^{14}C yr	AMS^{14}C dating on sea water (DIC), and sediments, (TOC, TCC) ~460 ^{14}C yr	AMS^{14}C dating on pre-bomb molluscs ~415 ^{14}C yr		AMS^{14}C dating on *Dreissena rostriformis,* ~0 yr
upper water column	**200-400**		decreasing to 800 ^{14}C yr at 300 m			sea water (DIC), decreasing to ~800 ^{14}C yr at 200 m		AMS^{14}C dating on *Dreissena rostriformis,* ~0 yr	
inter-mediate water	**400-1400**	125 yr	decreasing to ~1000 ^{14}C yr at 1400 m			sea water (DIC) decreasing to ~1500 ^{14}C yr at 400 m			AMS^{14}C dating on ostracods and/or molluscs ~1000 ^{14}C yr
deep/ bottom water	**below 1400**	400 yr	~2000 ^{14}C yr			~2000 ^{14}C yr			

Table 2.1: Compilation of published results on Black Sea reservoir age estimation. In white results for marine Black Sea, in gray results for the lacustrine Black Sea. (DIC: dissolved inorganic carbon, TCC: total carbonate carbon, TOC: total organic carbon). 'Water depth' column refers to the depth for which the measurement/estimation is representative.

STUDY AREA

Gravity and piston cores studied in this paper were taken in the southwestern Black Sea from the upper slope off western Anatolia (Fig. 2.1, Tab. 2.2). The coring site, north of the Sakarya River mouth, is located on a topographical elevation (~1220 m water depth) that is not affected by turbidites. The Sakarya River with a total length of 824 km and a drainage area of 56.504 km^2 is the longest and the second largest Anatolian river discharging into the Black Sea (Algan et al., 2002). The southern shelf of the Black Sea, in contrast to the broad and shallow northern one, is very narrow and steep, which results in sediment transport directly to the deep basin. Today, the Coriolis-force-driven rim current sweeps sediments off the northern shelf and redistributes them to the southwestern slope next to the Anatolian coast (Sur and Özsoy, 1996). This, together with the proximal location to the Sakarya River mouth, results in very high sedimentation rates in our study area.

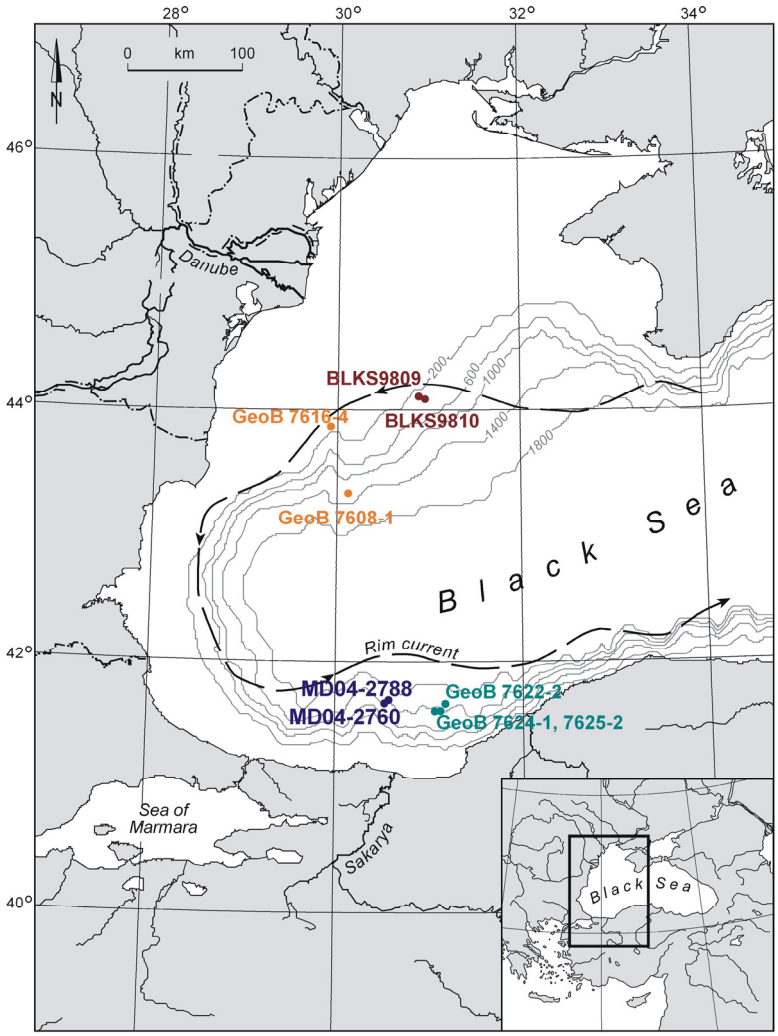

Figure 2.1: Study area with the locations of sediment cores MD04-2760, MD04-2788, and other cores relevant for this study (GeoB 7622-2, 7624-1, 7625-2 [Lamy et al., 2006]; GeoB 7608-1, GeoB 7616-4 [Bahr et al., 2005]; BLKS9810, BLKS9809 [Major et al., 2002]). Black dashed line indicates the western Black Sea rim current.

Core	Latitude N	Longitude E	Water depth (m)	Core length (m)
MD04-2760[a]	41°31.7’	30°53.1’	1226	41.94
MD04-2788[a]	41°31.7’	30°53.0’	1224	6.00
GeoB 7622-2[b]	41°32.1’	31°10.0’	1306	7.68
GeoB 7624-1[b]	41°30.0’	31°05.1’	1370	8.75
GeoB 7625-2[b]	41°26.7’	31°04.0’	1242	7.92
GeoB 7608-1[c]	43°29.2’	30°11.1’	1202	6.85
GeoB 7616-4[c]	43°41.0’	30°02.5’	168	9.16
BLKS9809[d]	44°05.2’	30°48.0’	240	8.40
BLKS9810[d]	44°04.0’	30°50.7’	378	7.59

Table 2.2: Location and the length of sampled cores ([a]this study, [b]Lamy et al., 2006; [c]Bahr et al., 2005; [d]Major et al., 2002).

MATERIAL AND METHODS

Material

The work presented here is based on the gravity core MD04-2788 (6 m) and the corresponding piston core MD04-2760 (41.94 m) retrieved at 41°31.67'N/30°53.09'E during the ASSEMBLAGE I cruise onboard of R/V *Marion Dufresne* in 2004. Both cores reveal the typical marine stratigraphic divisions of Unit I and II with a combined thickness of 3.23 m for MD04-2788 and 5.91 m for MD04-2760. The difference found in the thickness of Units I and II between the two cores is due to differential compaction/elongation within the gravity and piston core. In our case, the elongation factor is on average x2. The lowermost lacustrine Unit III consists of homogeneous and centimeter- to millimeter-scale laminated muddy clay of 2.67 m in the gravity core and 24.3 m in the piston core. The base of Unit III was not reached. The lowermost 11 m of sediment of the piston core suffered from deformation and bending during the coring procedure and were not used in present study.

Profiling measurements

After splitting, both cores were scanned in 1 cm resolution with an AVAATECH X-ray fluorescence scanner at the University of Bremen, Germany. Additionally, gravity core MD04-2788 was scanned in 2 mm resolution. The XRF-core scanner, developed at the Netherlands Institute for Sea Research, Texel, measures the bulk intensities of major elements (e.g. Al, Si, S, K, Ca, Ti, Mn, and Fe) on split sediment cores (Jansen et al., 1998; Röhl and Abrams, 2000). The Ca-intensity data obtained were used for correlation with bulk carbonate data and XRF-Ca data from previously published records (Major et al., 2002; Bahr et al., 2005).

Tephrochronology

Two distinct tephra layers have been identified in the sediment cores. One tephra, of 0.1 cm thickness was recognized in the Holocene marine Unit II in both cores MD04-2788 and MD04-2760 at 2.58 m and 4.4 m depth, respectively. A similar light-colored tephra was found in gravity cores GeoB 7622-2, GeoB 7625-2, and GeoB 7624-1 from the southwestern Black Sea at the same stratigraphic position (Lamy et al., 2006), representing the same eruptive event. The second tephra, reddish in color and 0.5 cm thick, was recognized in the glacial lacustrine part of the piston core MD04-2760 at 26.52 m depth. The tephra layers in cores GeoB 7622-2, GeoB 7625-2, GeoB 7624-1, and MD04-2760 were identified by means of major-element electron probe micro analyses (EPMA). Petrographical and chemical composition of both tephras was determined using polished thin sections. Sample preparation followed in its entirety that described in detail by Wulf et al. (2002).

Radiocarbon dating

AMS ^{14}C dating of lacustrine sediments (Unit III) was performed on shells of either ostracods (mixed samples of *Loxoconchidae* and *Candonidae*), or benthic gastropods from the piston core MD04-2760 and on ostracod shells from the gravity core MD04-2788. A total of 14 radiocarbon samples (Tab. 2.3) were measured by AMS techniques at the Leibniz-Labor in Kiel, Germany (Nadeau et al., 1997).

Sample	Depth in the core (cm)	Corrected depth in the core (cm)[a]	Depth in the composite profile (cm) MD04-2788/2760	^{14}C age (yr BP)	Marine ΔR[b] / Applied reservoir correction[c]	Calibrated age[d] (yr BP) +/- 1σ	Material /source
Core GeoB 7622-2							
KIA 25671	57	57	15.4	1170 ± 35	70[b]	630-687	Lamy et al., 2006
KIA 25749, final invasion	137	137	77	2090 ± 30	70[b]	1529-1624	Lamy et al., 2006
KIA 25672, first invasion	233.5	233.5	152.8	2385 ± 35	70[b]	1879-1975	Lamy et al., 2006
KIA 25751	323	323	208.6	3080 ± 35	70[b]	2737-2813	Lamy et al., 2006
Z-2 / Minoan tephra	400	400	248	3331 ± 10	-	3550-3577	Friedrich et al., 2006
KIA 25674	478	478	289.4	4609 ± 55	70[b]	4675-4819	Lamy et al., 2006
KIA 19273	520	520	306.6	5719 ± 25	70[b]	5383-5464[e]	Lamy et al., 2006
KIA 25675	555	555	317.6	6590 ± 70	70[b]	6951-7133	Lamy et al., 2006
KIA 25753, UnitII/UnitIII	564.5	564.5	322	7625 ± 55	70[b]	7945-8074	Lamy et al., 2006
Core MD04-2788							
Z-2 / Minoan tephra	258	248	248	3331 ± 10	-	3550-3577	Friedrich et al., 2006
KIA 28419	463-470	453-460	674-684	13,220 ± 70	900[c,f]	14,069-14,408	ostracods
Core MD04-2760							
Z-2 / Minoan tephra	440	420	248	3331 ± 10	-	3550-3577	Friedrich et al., 2006
KIA 26698	643	609	341	8505 ± 45	900[c,f]	8374-8428	gastropod
KIA 26699	665-685	631-651	363-383	8820 ± 55	900[c,f]	8634-8780	gastropod
KIA 25679	665-685	631-651	363-383	8910 ± 45	900[c,f]	8861-8920	ostracods
KIA 26700	832-852	798-818	530-550	11,105 ± 60	900[c,f]	11,813-12,044	gastropod
KIA 26701	945-965	911-931	643-663	13,050 ± 70	900[c,f]	13,919-14,094	gastropod
KIA 25676	1540-1560	1506-1526	1238-1258	14,800 ± 100	1000[c,f]	16,207-16,656	ostracods
KIA 25684	1680-1700	1632-1652	1374-1394	16,120 ± 90	1450[c,g]	17,135-18,217	ostracods
KIA 25685	1815-1835	1777-1797	1509-1529	17,090 ± 110	1450[c,g]	18,591-19,348	ostracods
KIA 25686	2535-2555	2363-2383	2095-2115	19,390 ±110	1450[c,g]	20,772-21,879	ostracods
Y-2 / Cape Riva tephra	2652	2461	2192	18,310 ± 380[h]	-	21,270-22,290[i]	Pichler and Friedrich, 1976, Erikson et al., 1990
KIA 25687	2800-2820	2563-2583	2295-2315	20,240 ± 130	1450[c,g]	21,744-22,916	ostracods
KIA 25754	3025-3045	2765-2785	2497-2517	21,030 ± 160	1450[c,g]	22,720-23,863	gastropod
KIA 25688	3025-3045	2765-2785	2497-2517	21,460 ± 140	1450[c,g]	23,353-24,527	ostracods
KIA 25678	3310-3332	2995-3017	2726-2748	22,340 ± 190	1450[c,g]	24,521-25,595	ostracods

[a] excluding core gaps
[b] for marine samples, (ΔR) value according to the Marine Reservoir Correction Database, available at http://depts.washington.edu/qil/marine
[c] for lacustrine samples
[d] calibrated date range calculated by Calib Rev. 5.0.1 (Stuiver et al., 2005); ages of marine samples was calibrated using the Marine04 calibration curve (Hughen et al., 2004); ages of lacustrine samples was calibrated using the Intcal04 curve (Reimer et al., 2004)
[e] measurement on organic carbon target corrected for detrital carbon after Jones and Gagnon (1994) prior to calibration
[f] reservoir correction applied according to the results of the complex model presented herein. Reservoir correction was inferred by comparison to other Black Sea records and GISP2 record, therefore no error estimation is given
[g] estimated reservoir correction. The error estimation calculated according to the formula $(\sigma_{lacustrine}^2 + \sigma_{atmospheric}^2)^{1/2}$ falls into range 390 – 425 ^{14}C yr and gives an average value of 400 ^{14}C yr
[h] mean and standard deviation of original dating series
[i] mean and standard deviation of calibrated ranges of original dating series

Table 2.3: Details on age-control points used to construct age model for the composite profile of cores MD04-2788 and MD04-2760. All radiocarbon ages are calibrated using the Calib 5.0.1 software (Stuiver et al., 2005).

RESULTS

Composite profile MD04-2788/2760

In order to make a core-to-core comparison, we first corrected the original depths of both cores for core gaps. XRF-scanning results allowed a detailed correlation of the piston core MD04-2760 and the gravity core MD04-2788. Since the uppermost 5.91 m of the piston core were strongly disturbed (extended) during coring, we substituted the marine part of the MD04-2760 record (Units I and II, 0–5.91 m, corrected depth) with the respective part of the undisturbed MD04-2788 record (0-3.23 m, corrected depth). We then normalized the top of the lacustrine unit in the piston core MD04-2760 to the top of the lacustrine unit in the gravity core MD04-2788 by applying a constant correction of -2.68 m (3.23 – 5.91 = -2.68) to each corrected depth-value of the lacustrine part of the piston core (original depth, corrected depth and composite profile depth values are provided in Table 2.3).

Tephrochronology

On a geochemical, petrographical, and stratigraphical basis, the Holocene tephra was correlated with the marine Z-2 tephra, which has already been found in previous Black Sea sediment records (Guichard et al., 1993; Lamy et al. 2006). This rhyo-dacitic ash is allocated to the Minoan eruption of Santorini and dates to 3331±10 ^{14}C yr BP (3550-3577 cal yr BP; Friedrich et al., 2006) (Fig. 2.2, Tab. 2.4).

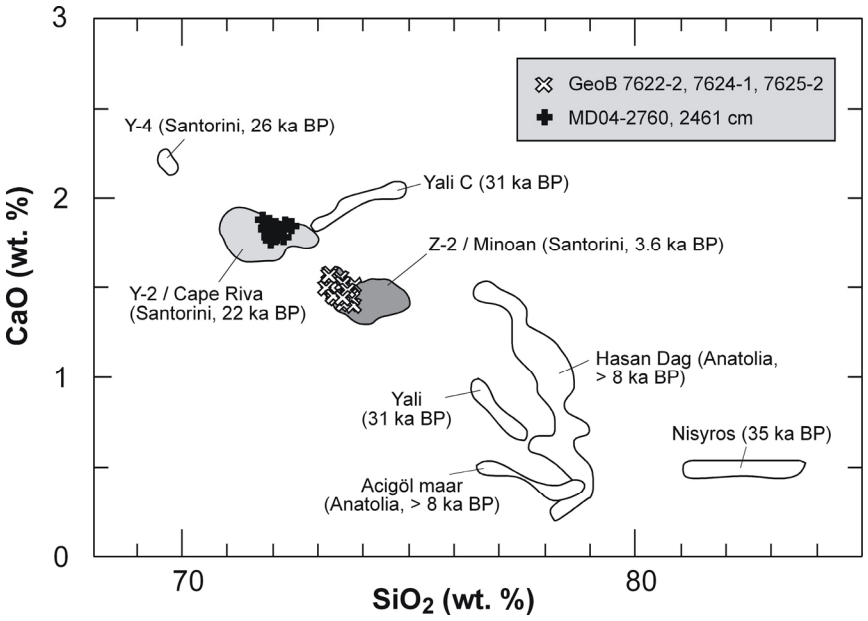

Figure 2.2: Chemical discrimination of the tephras found in cores GeoB 7622-2, 7624-1, 7625-2, and MD04-2760, and the prominent Quaternary tephra layers from Santorini, Yali, Nisyros, and Central Anatolia (for more details on discrimination of tephras in Mediterranean region see Vinci et al. [1985], Wulf et al. [2002, in press] and references therein). Please note that all data are normalized on an anhydrous basis.

Sample	GeoB 7622-2, 400cm	MD04-2760, 2461cm
Event	Minoan (Santorini)	Cape Riva (Santorini)
SiO_2	72.05 (0.70)	71.30 (0.59)
TiO_2	0.29 (0.03)	0.48 (0.03)
Al_2O_3	13.43 (0.18)	14.24 (0.17)
FeO	2.03 (0.06)	3.15 (0.12)
MnO	0.07 (0.04)	0.12 (0.03)
MgO	0.30 (0.01)	0.43 (0.04)
CaO	1.45 (0.04)	1.80 (0.03)
Na_2O	4.91 (0.10)	4.34 (0.24)
K_2O	3.17 (0.09)	2.82 (0.07)
P_2O_5	0.04 (0.04)	0.09 (0.02)
Cl	0.30 (0.02)	0.26 (0.02)
F	0.00 (0.00)	0.00 (0.00)
Total	97.99 (n=14)	98.97 (n=13)

Table 2.4: Mean values of major element chemistry obtained by microprobe analyses on single glass shards from respective tephra deposits. Numbers in parentheses represent the 1 sigma standard deviation, n = number of glass shards analyzed.

The glacial tephra in core MD04-2760 is similarly rhyo-dacitic in its chemical composition but corresponds most likely to the Late Glacial marine Y-2 tephra. Y-2 has been detected in numerous deep-sea cores of the Aegean Sea, the Levantine Basin (e.g. Keller et al., 1978; Federman and Carey, 1980; Vinci, 1985), and the Sea of Marmara (Wulf et al., 2002), and correlates with the Cape Riva eruption of the Santorini volcano (Fig. 2.2, Tab. 2.4, for more details on discrimination of tephras in Mediterranean region see Vinci et al., [1985]; Wulf et al., [2002; in press] and references therein). Dating of Cape Riva deposits on land (dating wood intercalated with tephra deposits) provided a series of four ^{14}C dates: 18,050±340, 18,165±210, 18,880±230 yr BP (Pilcher and Friedrich, 1976) and 18,150±200 yr BP (Eriksen et al., 1990). For further calculations, we applied an age of 18,310±380 ^{14}C yr BP (21,270-22,290 cal yr BP) for the tephra representing the mean value and standard deviation obtained from the 4 dates.

Chronology

A ^{14}C-based age model was constrained for the composite profile including both, gravity core MD04-2788, for the marine part, and piston core MD04-2760, for the lacustrine part of the record. In order to improve the age model, we further used the Z-2 tephra time marker and additional age points from the recently dated and nearby core GeoB 7622-2 (Lamy et al., 2006) (Fig. 2.1, Tab. 2.2 and 2.3). All radiocarbon ages determined on core GeoB 7622-2 could be exactly transferred to core MD04-2760 by careful visual inspection of the lamination pattern. Moreover, the comparison with the GeoB 7622-2 record revealed that the uppermost ~64 cm of our record (extrapolated on the basis of sedimentation rate), covering the last ~1000 yr were lost during the coring procedure (Fig. 2.3).

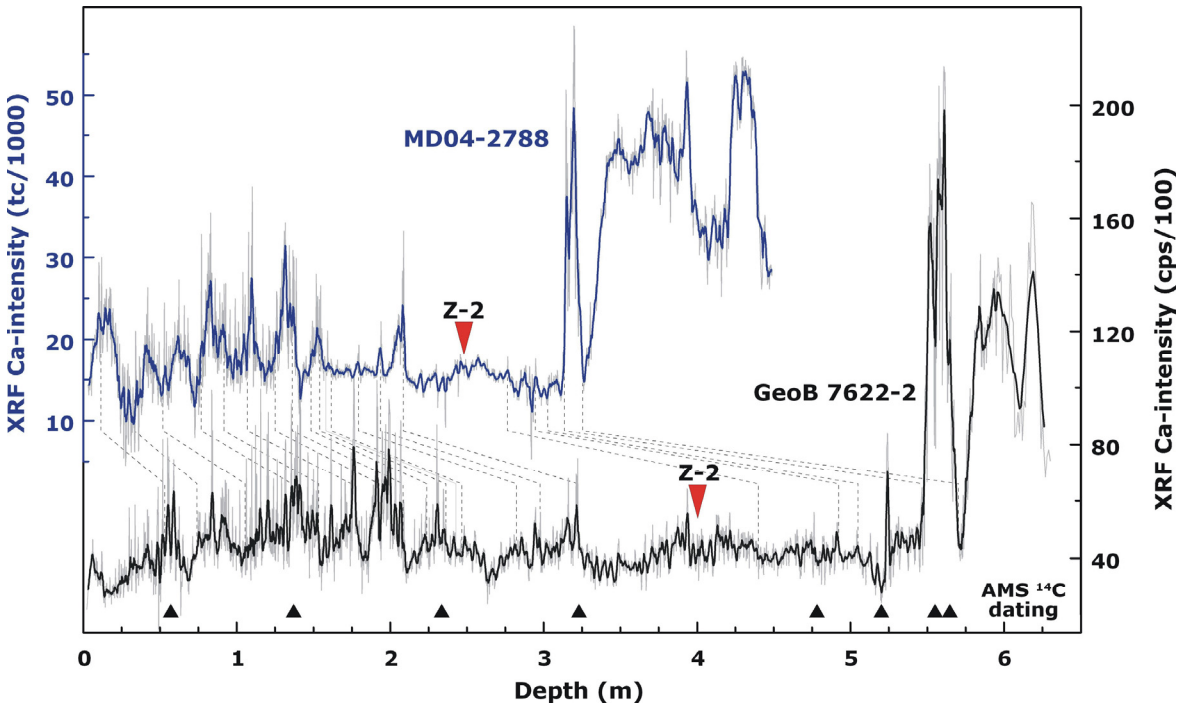

Figure 2.3: XRF Ca-intensity record and dating points from core GeoB 7622-2 (Lamy et al. 2006). XRF Ca-record from MD04-2788 displays very similar pattern. The dashed lines represent correlation levels. Thin lines represent original data and bold lines represent a 9-point moving average. The two cores were measured using different XRF core scanners providing counts per second (cps) for the GeoB 7622-2 and total counts (tc) for the MD04-2788. Accordingly, the values for the Ca-intensity differ in order of magnitudes. AMS ^{14}C dating indicated with black triangles was performed on the core GeoB 7622-2.

We performed a linear interpolation between the age-control points imported from GeoB 7622-1, the ^{14}C age of the Z-2 Minoan Ash obtained from terrestrial deposits (Friedrich et al., 2006), and the age control points from the lacustrine part (consisting of 13 dates derived from the MD04-2760, and 1 date transferred from MD04-2788) (Fig. 2.4a). Since the linear interpolation of the Y-2 tephra age derived an age 1450 ^{14}C yr older than a mean value of the original dating series (Pilcher and Friedrich, 1976; Eriksen et al., 1990), this tephra was not directly included in the radiocarbon age model (see discussion below). Only after applying a reservoir correction to the AMS ^{14}C dating results (see discussion below), the mean calibrated age of Y-2 tephra was included in the calibrated age model (Fig. 2.4b). Calibrated ages were calculated with a 1-sigma standard deviation. In two cases, when two dates were available from the same interval (ostracods and gastropods, from 3.63 – 3.83 m and 24.97 – 25.17 m composite depth; Tab. 2.3), we used a mean value for constraining the age model. Considering the relatively large volume of sample material required for each dating due to the extremely high sedimentation rates and therefore dilution of the benthic 'in situ' material, these ages were in good agreement considering their dating uncertainties.

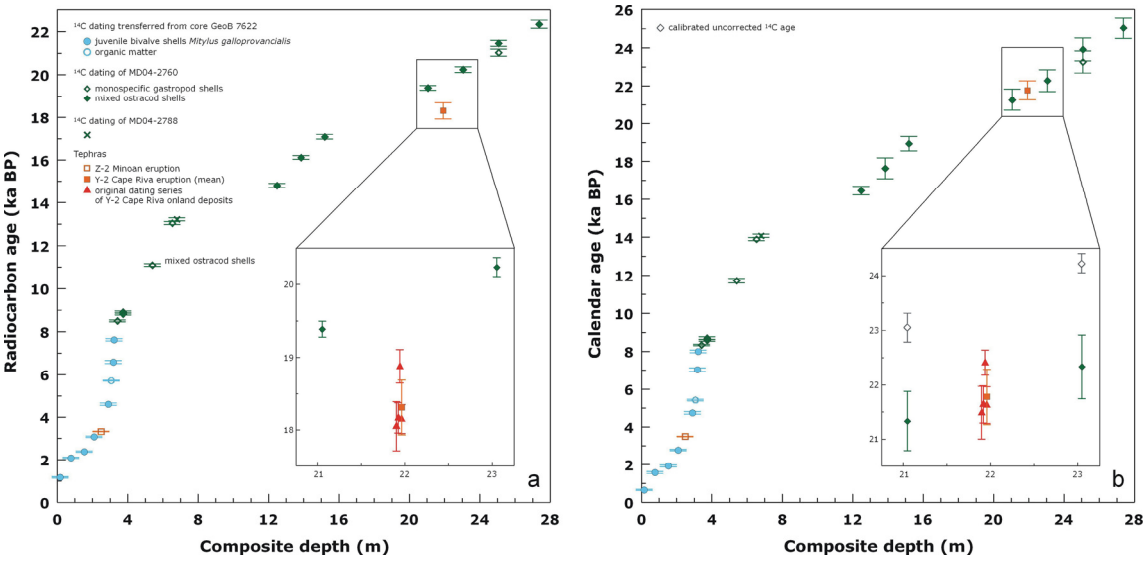

Figure 2.4: Age-depth model of the composite profile. (a) shows the radiocarbon age versus the composite depth. The zoom-in box shows the original dating series of the Y-2 Cape Riva tephra on-land deposits (Pichler and Friedrich, 1976; Eriksen et al., 1990) located between two bracketing samples of core MD04-2760. (b) shows the calendar age (with 1sigma standard deviation) versus composite depth. Reservoir corrections (for comparison check Table 2.3) were applied to all ages prior to calibration. The zoom-in box shows the calibrated results of Pichler and Friedrich (1976) and Eriksen et al. (1990). For comparison the calibrated uncorrected ages of the two samples bracketing the Y-2 tephra are shown. Because of the relatively big sample volumes required for each dating, the dating results should be viewed as time frame not for a certain depth point but for a certain depth range.

Sedimentology

XRF data obtained on composite core MD04-2788/2760 give a time resolution ranging from 3 to 17 years. The Ca-signal reflects a basin-wide sedimentation pattern and is comparable with a lower resolution XRF Ca-record from the northwestern Black Sea (Bahr et al., 2005; core GeoB 7608-1) and a low-resolution record of $CaCO_3$ content from bulk carbonates (Major et al., 2002; core BLKS9810) (Fig. 2.5).

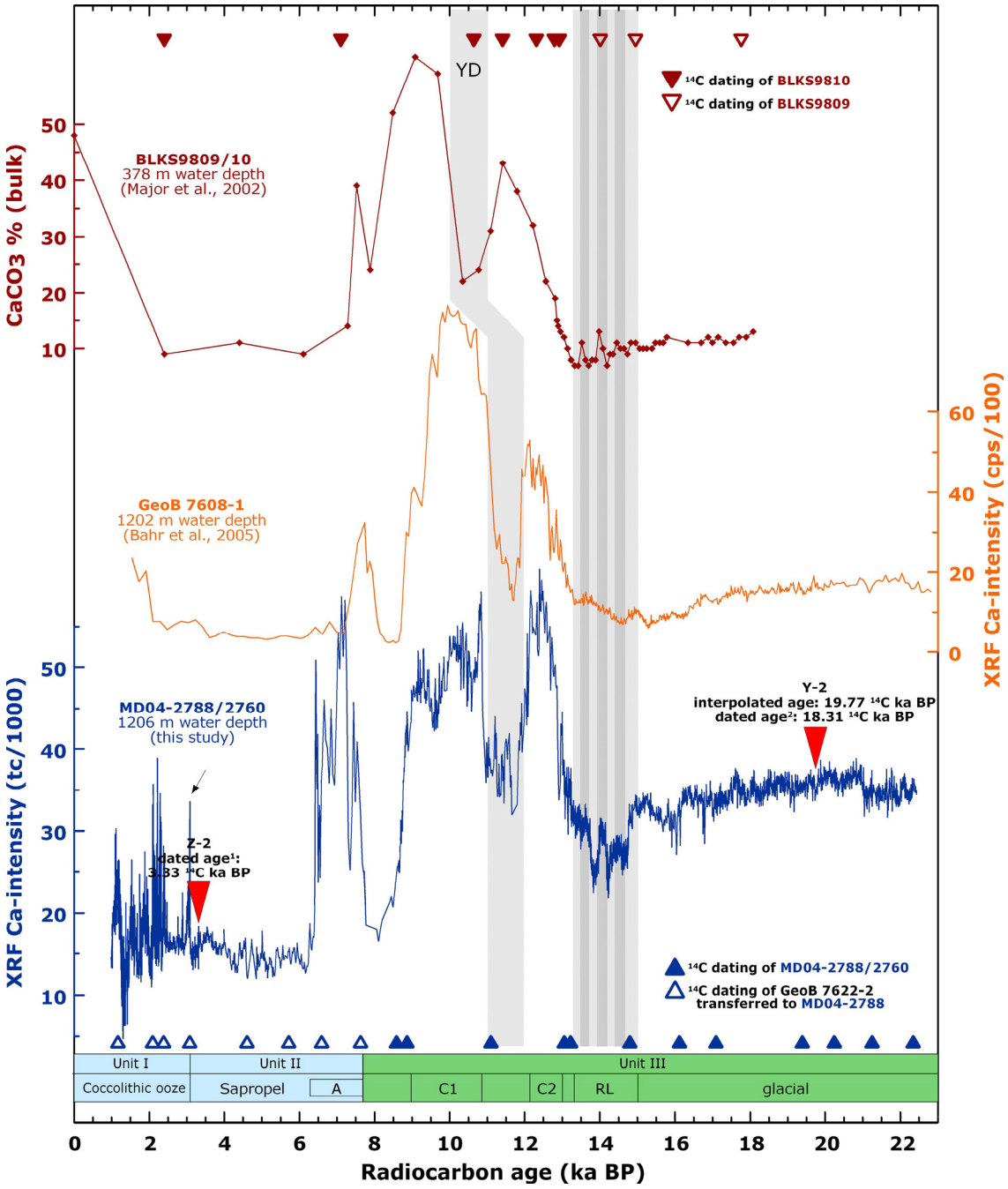

Figure 2.5: Juxtaposition of the Black Sea carbonate content/ Ca-intensity records (NS transect) showing a good agreement until 13 ^{14}C ka (the 'red layers' interval is indicated by light and dark gray bars) and a subsequent significant offset between the records from shallow and intermediate water depths. A maximum offset occurs during the Younger Dryas and is indicated by a light gray bar. AMS ^{14}C dating results are labeled with empty blue triangles for core GeoB 7622-2, filled blue triangle for MD04-2788/2760, filled red triangles for BLKS9810, and empty red triangles for BLKS9809. The dated age[1] of the Z-2 Minoan Ash is given according to the AMS ^{14}C dating of Friedrich et al. (2006). The dated age[2] of the Y-2 tephra is given according to the AMS ^{14}C dating of Pilchner and Friedrich (1976) and Eriksen et al. (1999). The age of the Y-2 Cape Riva tephra is marked according to the linear interpolation between the two neighboring ^{14}C dates. The legend bar shows the major stratigraphic units including the 'red layers' (RL) and carbonate peaks (C1, C2) in the lacustrine unit, and the aragonite peak (A) and the sapropel and coccolith ooze in the marine units. The nomenclature for the lacustrine peaks is after Major et al. (2002). Please note the legend bar refers to the stratigraphy of MD04-2788/2760. The small black arrow indicates the first appearance of *E. huxleyi* in the Black Sea.

The Last Glacial period is characterized by relatively stable and low Ca-values which are interrupted at 14,800 ^{14}C yr BP by a series of Ca-minima reflecting a change in the input sources. This interruption is known as 'red layer interval' and was previously interpreted as the result of an outflow of the Caspian Sea into the Black Sea via the Manych depression, caused by increased glacial meltwater discharge (Major et al., 2002; Bahr et al., 2005 and references therein). Alternatively, the deposition of the 'red layers' could be generally related to enhanced erosion associated with Late Glacial permafrost thawing (Major et al., 2002). The 'red layers', also described as brown muds (Major et al., 2002), are enriched in terrigenous components embedded in a silty to claysh matrix. The timing of the 'red layers' in our record is in disagreement with dates proposed by Bahr et al. (2005, GeoB 7608-1) (Fig. 2.5). However, some results of Bahr et al. (2005) could have been biased by dating material containing older reworked shells. Notably, when tuned to the MD04-2760 XRF Ca-intensity record, the XRF Ca-signal from the core GeoB 7608-1 reveals congruent patterns (Fig. 2.6).

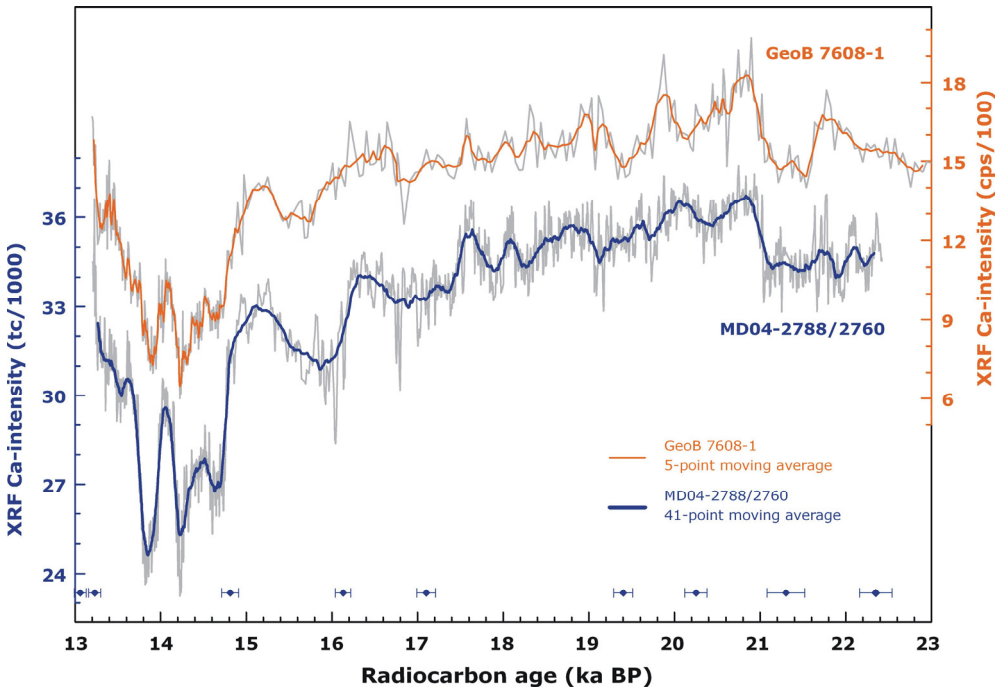

Figure 2.6: The XRF Ca-intensity of the MD042788/2760 plotted on the radiocarbon time scale. The XRF Ca-intensity of the GeoB 7608-1 was tuned to the MD04-2788/2760 signal. The diamonds indicate AMS ^{14}C dating (+/- dating error) of the MD042788/2760. For the GeoB 7608-1, the thin line represents the original data and the bold line represents a 5-point moving average. For the MD04-2788/2760, the thin line represents a 3-point moving average and the bold line a 41-point moving average. The two cores were measured using different XRF core scanners providing counts per second (cps) for the GeoB 7608-1 and total counts (tc) for the MD04-2788/1760.

Two distinct Ca-maxima, the carbonate peaks C2 and C1 occurring at 13,000-12,000 ^{14}C yr BP and 10,800-9000 ^{14}C yr BP, respectively, reflect high amounts of inorganically precipitated calcite (Fig. 2.5, nomenclature for the peaks C2 and C1 after Major et al. [2002]; for comparison see Bahr et al. [2005, 2006]). The Ca-minimum in between C2 and C1 (12,000-11,000 ^{14}C yr BP) represents reduced carbonate precipitation combined with an increase in terrigenous supply. The youngest Ca-maximum A, located in the core MD04-2788/2760 between 7770 and 6380 ^{14}C yr BP, corresponds to mm-scale layers consisting of authigenically precipitated aragonite. The base of the aragonite marks the onset of the marine Unit II (sapropel). Inorganic aragonite precipitation in the Black Sea is characteristic for the base of the Unit II. Thickness of the aragonite layer depends on the sedimentation rate and can vary significantly from a few mm to several cm (Ross and Degens,

1974). The aragonite peak in the marine part of our record is related neither to the Ca-maximum at 7520 ^{14}C yr BP described by Major et al. (2002) from the lacustrine Unit III, nor to the Ca-maximum at ~7600 ^{14}C yr BP described by Bahr et al. (2005), also from the Unit III (Fig. 2.5). The separate carbonate peak as described from core BLKS9810 can be either an artifact (it is represented by a single measurement only), or a continuation of the carbonate peak C1 (Major, personal communication, 2005), which is part of the basin-wide sedimentation pattern. Similarly, the Ca-peak in GeoB 7608-1 most probably is detached from the carbonate peak C1 due to the dilution by siliciclastic material (Bahr, personal communication, 2007).

Ca-values, which are very low in marine Unit II (sapropel), increase significantly in Unit I. This increase is related to the occurrence of coccolith-rich layers. The single Ca-peak at ~3080 ^{14}C yr indicates the first invasion of *Emiliania huxleyi* into the Black Sea, and marks the transition between Unit I and Unit II.

DISCUSSION

Reservoir age variations

The new ^{14}C ages, the presence of volcanic ash layers, and basin-wide sedimentological patterns suggest a significant and variable reservoir age for the Late Glacial Black Sea. The identification of the Y-2 tephra for the first time in the Black Sea sediments, turned out to be essential for the estimation of the water reservoir ages in the glacial. By definition the reservoir age represents the difference between the ^{14}C age of a marine/lacustrine sample and the ^{14}C age of a contemporaneous atmospheric sample. In core MD04-2788/2760 the Y-2 tephra is located between two radiocarbon dates. The linear interpolation between these two dates yields an age of ~19,760 ^{14}C yr for the tephra layer, which is 1450 ^{14}C yr older than the mean value of the reported Y-2 terrestrial ages (18,310 ^{14}C yr BP) (Tab. 2.3, Fig. 2.4a).

Considering the original Cape Riva dating series (Pilcher and Friedrich, 1976; Eriksen et al., 1990), the end members of the reservoir age estimate are 1720 ^{14}C yr and 890 ^{14}C yr (Fig. 2.4a) and the average reservoir age error is ~400 ^{14}C yr (Tab. 2.3). Another indication that a reservoir correction becomes necessary, is that the Ca-minimum at 12,000-11,000 ^{14}C yr BP most probably representing the Younger Dryas cold interval (Major et al., 2002) is about ~1000 ^{14}C yr older than the commonly assigned age for the YD (e.g. Hughen et al., 2000). Thus, the reservoir age seems to decrease from about 1450 ^{14}C yrs close to the Last Glacial Maximum to ca. 1000 ^{14}C yr during the YD. However, in the interval between ~15,000 and 13,500 ^{14}C yr BP, the 'red layers' interval, our record is in good agreement with the northwestern Black Sea record of Major et al. (2002) that was not corrected for any reservoir effect. According to the published δ^{18}O data (Bahr et al., 2006), the Black Sea was in hydrological steady state during the glacial. Therefore, it is reasonable to assume a constant reservoir age over that time. The MD04-2788/2760 record suggests a subsequent reservoir age decrease towards the YD period to ~1000 ^{14}C yr that starts at ~13,000 ^{14}C yr BP and continues until the end of the lacustrine unit (Fig. 2.5). This shift from 1450 to ~1000 ^{14}C yr for the intermediate water reservoir age takes place within, or shortly after the deposition of the 'red layers'. At the same time, the reservoir age of the upper water column reaches a value close to 0 yr (Major et al., 2002; Bahr et al., 2005).

Additional support for the divergent trends in the reservoir ages of the different water masses comes from the observation of a temperature-dependent stratification of the Black Sea basin that started at ~13,000 ^{14}C ka BP and continued till the end of the lacustrine phase (Bahr et al., 2006).

The good agreement between the intermediate and upper water column records until 13,500 ^{14}C yr BP (Fig. 2.5) suggests that either: (1) there were no age differences at all and the reservoir age of the whole water column was ~1450 ^{14}C yr, or (2) that the age of the upper water column and intermediate water ware varying in the same way. To constrain our calibrated stratigraphy, we tested two hypotheses. A simple model assumes changes in the reservoir age only after the deposition of the 'red layers' (at 13,500 ^{14}C yr BP), but divergent for the upper water column and the intermediate water (change to 0 ^{14}C yr for upper water column and to 1000 14C yr for intermediate water) (Fig. 2.7, thin solid lines). A more complex model includes two changes of reservoir age: a first parallel change at the onset of the 'red layer' deposition (at ~15,000 ^{14}C yr BP) to 1000 ^{14}C yr reservoir age, and a second divergent change after the 'red layers' (after 13,500 ^{14}C yr BP) to 0 ^{14}C yr reservoir age for the upper water column and to 900 ^{14}C yr for the intermediate water (Fig. 2.7, dashed lines). After calibration of the corrected radiocarbon dates, we compared the results of our models with the GISP2 ice core chronology (Grootes and Stuiver, 1997). The first simple model shows a ~350 yr offset for the beginning of B/A, and an 150 yr offset for the YD. The second complex model provides more satisfactory results, producing a ~200 yr offset for the beginning of the B/A and a 0 yr offset for the YD (see Tab. 2.3). Based on the observations available for different water depths, we developed a rough model of estimated temporal changes in the Black Sea reservoir ages (Fig. 2.7, Tab. 2.3).

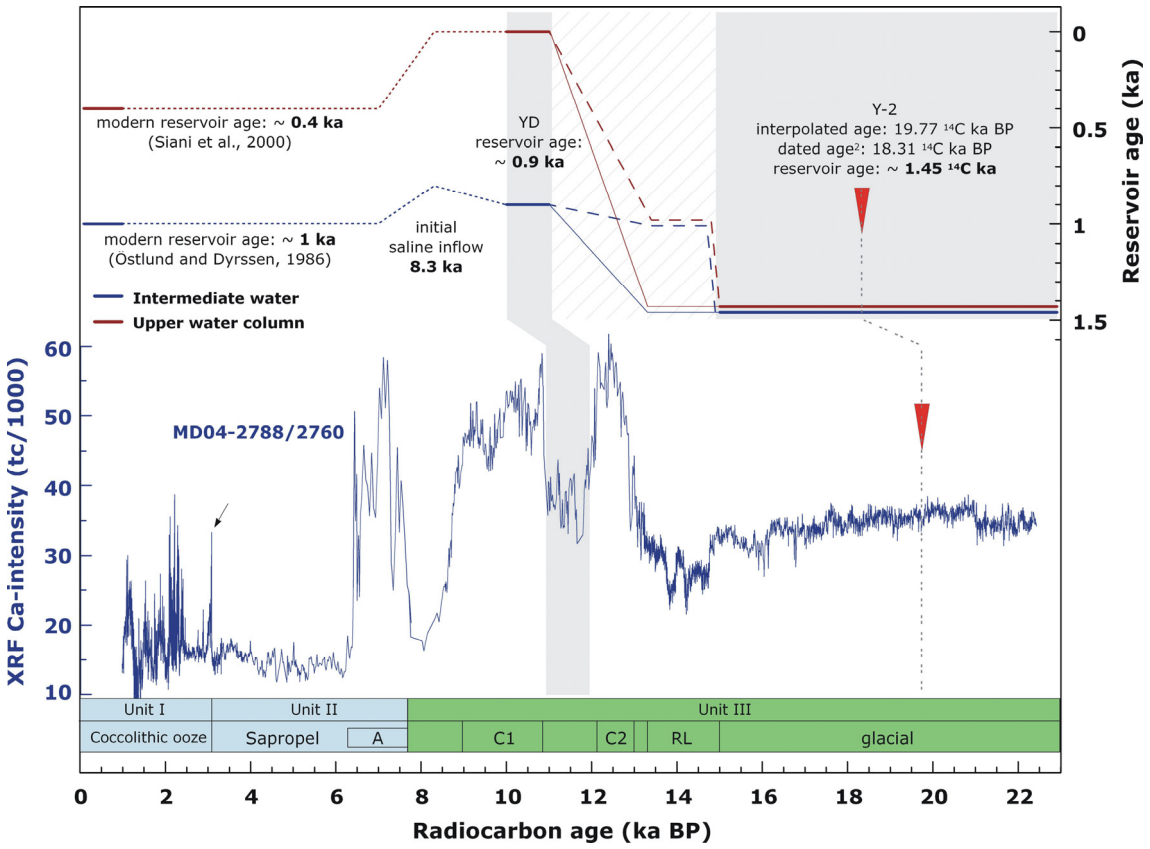

Figure 2.7: Model of temporal changes in the reservoir age of the Black Sea at different water depths juxtaposed to the MD04-2788/2760 XRF Ca-intensity record. Blue lines represent the intermediate water and red lines the upper water column. Bold solid lines show the evolution of the reservoir ages based on

observation. Between 15 ^{14}C ka BP and 11 ^{14}C ka BP thin solid lines show the possible evolution of the reservoir ages following a simple model, while dashed lines show the evolution of the reservoir ages suggested by a more complex model (see chapter 'reservoir age variations'). Dotted lines represent the possible evolution of the reservoir age after 10 ^{14}C ka BP. The age of the Y-2 Cape Riva tephra in MD04-2788/2760 is marked according to the linear interpolation between neighboring ^{14}C dates. The legend bar is the same as in Figure 2.5. The small black arrow indicates the first appearance of *E. huxleyi*.

Source of the age offset

The proposed reservoir age of 1450 ^{14}C yr for a probably well mixed water body in the glacial Black Sea, is unexpected and requires some explanation. The contamination of samples by older carbonates is rather unlikely due to a careful inspection and cleaning of the datin samples. The location of the core MD04-2788/2760 was intentionally chosen on an isolated bathymetric high in order to avoid potential turbidite tracks. The sampled material showed no signs of reworking and all dating results appear in stratigraphical order. Finally, dating different material from the same interval yielded reproducible results (Tab. 2.3).

Another explanation for the large age offsets involves a potential temperature-dependent stratification of the basin, undetectable in δ^{18}O record. If this had been the case, the temperature-signal might have been compensated by factors such as salinity, and changed δ^{18}O of atmospheric precipitation (Bahr et al., 2006). Murray et al. (1991) presented a similar scenario for the marine Black Sea. Their ventilation box model implied that 'old' deep water was upwelled to the surface, and subsequently cooled and removed from atmospheric contact to form a cold intermediate layer. Murray et al. (1991) referred to the depths between 25-100 m below the sea surface as to the cold intermediate layer (CIL). According to their model, the time of CIL formation was too short for the water to equilibrate its ^{14}C content with the atmosphere. Hence, due to the depletion of ^{14}C, both surface and intermediate water might have been 1400 ^{14}C yr old. This model, however, contradicts the results of radiocarbon measurements showing a reservoir effect of ~400 ^{14}C yr in the recent Black Sea (Jones and Gagnon, 1994; Siani et al., 2000), and was applied only for the marine Black Sea connected with the Mediterranean (regarding initial conditions and inflow of deep Mediterranean water).

A third, and in our opinion the most likely, explanation is the presence of an 'apparent' reservoir age due to hardwater effect. The hardwater effect has already been proposed by Ross and Degens (1974) and Top and Clark (1983) in order to resolve discrepancies between results of different dating methods applied to the Black Sea water and sediments. In the case of a hardwater effect, radiocarbon ages that are apparently 'too old' are the result of the admixture of older 'dead' carbon originating from the dissolution of old, radioactively 'dead' carbonates. Potential sources of dissolved carbon are numerous in the Black Sea region. Old $CaCO_3$-bearing rocks like limestones, marlstones, and sandy-carbonate flysch series are abundant all over the Black Sea drainage area. The Danube itself, which contributes 40% to the total Black Sea river runoff, drains through the Alpine domain dominated by old carbonatic rocks. Today, more than 70% of $CaCO_3$ brought into the Black Sea by rivers is carried in solution (Strakhov, 1951), however this might have been different in the glacial. During cold periods physical weathering is more pronounced than the chemical one, and this may affect the amount of DIC (dissolved inorganic carbon) transported by rivers. Nevertheless, a weakened effect of chemical weathering can be balanced by intensified erosion – typical for glacial conditions when the vegetation cover is reduced. Though Mg/Ca and Sr/Ca data on ostracods (Bahr et al., 2008; Major et al., 2006) point to a rather low alkalinity of the glacial Black Sea water, the possibility of hardwater effect is not eliminated. For example, Hajdas et al. (1995) reported hardwater effect in the softwater body of Lake Holzmaar (Eifel, Germany).

Timing and a mechanism of the reservoir age decrease

Assuming a hardwater effect as the reason for the age offset in the glacial calls for a mechanism to reduce this offset, latest at the beginning of the Allerød. A process is required to explain the reduction of the reservoir effect for the upper water column from ~1450 ^{14}C yr to nearly 0 yr (or at least less than 900 ^{14}C yr) within a fairly short time interval. The comparison of our data with the upper water column records of Bahr et al., (2005) and Major et al., (2002) limits the decrease in reservoir ages to the time interval between ~15,000 and ~13,000 ^{14}C yr BP. During this time span, two significant events contributed to the depositional history of the Black Sea: the 'red layer' deposition (from ~14,800 to ~13,500 ^{14}C yr BP), and an interval of widespread inorganic carbonate precipitation (commencing at ~13,000 ^{14}C yr BP).

The 'red-layer' deposition involves an important inflow of glacial meltwater (Bahr et al., 2005). It is conceivable that this inflow added 'younger' (in terms of radiocarbon content) water and diluted the hardwater effect 'renewing' the Black Sea water. Indeed, significant meltwater pulses are observed in the δ^{18}O ostracod record from core GeoB 7608-1 from 1202 m water depth (Bahr et al., 2006) indicating that the meltwater signal was transported deeper into the basin. This may explain why the reservoir age was changing parallel for the whole water column until ~13,500 ^{14}C yr BP (Fig. 2.7).

During the glacial, exposed carbonate-rich bedrocks provided carbonate-rich sediments as a potential source of DIC. With the postglacial climate amelioration, the vegetation cover and soil formation in the Black Sea drainage basins probably played an important role in the reduction of the 'old' carbon input. Karrow and Anderson (1975) describe a similar example from proglacial lakes in Canada. Beside the change in the 'old' carbon supply, the decrease in the apparent reservoir age may involve additional processes such as the precipitation of carbonates from the water column that are enriched in the lighter carbon isotopes. Inorganic carbonate precipitation occurred in wide parts of the Black Sea basin during the Allerød. The δ^{13}C record of Bahr et al. (2005) shows that the high amounts of inorganically precipitated calcite at the onset of Allerød were most likely linked to increased phytoplankton activity. Photosynthetic utilization of CO_2 dissolved in water is known to induce supersaturation with respect to calcite and can lead to authigenic precipitation of carbonates (Kelts and Hsü, 1978).

Since the reservoir age reduction takes place at the same time it seems plausible that these processes are related. Such carbonate formation decreases the amount of DIC in the water (Zeebe and Wolf-Gladrow, 2001) depleting the dissolved carbon pool and potentially reducing the hardwater effect. To what degree the carbonate formation itself can account for a decrease in the reservoir age, or other biological processes are involved stays unclear. Both, phytoplankton activity and authigenic calcite precipitation are taking place in the surface waters, affecting the age of the surface waters first. Subsequent winter convection and deep water formation (Bahr et al., 2006) could have introduced the surface signal into intermediate depths. Such a scenario would explain our observations after 13,000 ^{14}C yr BP (Fig. 2.7) but also for the onset of the Holocene (Fig. 2.7). This period is also characterized by authigenic calcite precipitation (C1 Ca-peak) and a readvance of the vegetation in the Eastern Mediterranean region (e.g. Zonneveld, 1996; Robinson et al., 2006).

Reservoir age of the marine Black Sea

The limitation of the glacial reservoir age reconstruction consists in an inability to test our hypothesis, since the reservoir age of the recent marine Black Sea does not constitute an analog for the reservoir age of its lacustrine precursor. Observations and models valid for the marine Black Sea are inaccurate for reconstructing conditions over the Black 'Lake', which had a significantly

different hydrology as a closed basin without any connection to the Mediterranean Sea. Reservoir ages directly after the reconnection with the Mediterranean (~8300 ^{14}C yr BP, Bahr et al., 2006) must have been derived from the previous Black 'Lake' state, as a result of the mixture of the 'old' deep and intermediate waters, 'young' upper column and surface waters, and inflowing saline Mediterranean water. After establishing the modern two-layer flow and permanent stratification, the Black 'Lake' hydrology was replaced by the recent marine Black Sea state. The total exchange time for the Black Sea water after reconnection was estimated to be ~2000 yr (Bourdeau and Leblond, 1989). This value fits well with the measured reservoir age of recent deep/bottom water (Östlund and Dyrssen, 1986; Jones and Gagnon, 1994). Recent AMS ^{14}C measurements on DIC in water samples show that deep/bottom water has a residence time of ~2000 ^{14}C yr, intermediate water ~1400 ^{14}C yr, while the reservoir age of surface water is ~400 ^{14}C yr, close to the mean global ocean reservoir age. As mentioned previously, rivers drain huge amounts of dissolved carbonates into the Black Sea. Hence, the hardwater effect cannot be excluded as a factor causing an apparent reservoir age also today. In contrast to the glacial conditions, however, the recent permanent stratification and isolation of the intermediate and deep waters from atmospheric CO_2 favor not an apparent but rather real reservoir age.

CONCLUSIONS

During the glacial, we conclude that there was no offset between the age of the shallow and the intermediate water of the Black Sea basin. As shown by radiocarbon measurements combined with tephrochronology, the Black Sea water was characterized by a uniform apparent age of ~1450 ^{14}C yr that was primarily caused by hardwater effect. An initial reduction of the reservoir age probably happened during the deglaciation due to diluting effects of the inflowing meltwaters, and might have shifted the apparent age of both, intermediate water and upper water column to ~1000 ^{14}C yr. Latest with the onset of the Allerød, the reservoir age started to decrease divergently for the upper water column and the intermediate water. The second decrease was coincident with the precipitation of inorganic carbonates triggered by intense phytoplankton activity, both suggesting a biologically triggered reduction of the hardwater effect in the surface/upper water column. Additional changes in the vegetation cover and postglacial soil development in the drainage areas of the Black Sea inhibited a intense erosion of carbonatic bedrocks reducing the 'old' carbon supply. During the Younger Dryas the age of the upper water column was close to 0 yr, while the intermediate water was about 900 ^{14}C yr older. The recent reservoir age of the Black Sea waters was established after the reconnection with the Mediterranean Sea being the result of processes clearly different from those of the closed, glacial Black 'Lake' basin.

ACKNOWLEDGMENTS

We thank the captain and the crew of the RV *Marion Dufresne* for their efficient support during the ASSEMBLAGE I cruise and the IPEV for logistic support (RV *Marion Dufresne*). We also thank to the two anonymous reviewers whose comments helped to improve the manuscript. This research was sponsored by Comer Science and Education Foundation (CS&EF).

3. North Atlantic control on precipitation patterns in the Eastern Mediterranean/Black Sea region during the Last Glacial: new insights from the Black Sea sediments

Olga Kwiecien[1], Helge W. Arz[1], Frank Lamy[2], Birgit Plessen[1], André Bahr[3,4] and Gerald H. Haug[5]

[1]*GeoForschungsZentrum Potsdam (GFZ Potsdam), Germany*
[2]*Alfred Wegener Institute for Polar and Marine Research (AWI), Bremerhaven, Germany*
[3]*MARUM - Center for Marine Environmental Research, University of Bremen, Germany*
[4]*now at IFM-GEOMAR, Kiel, Germany*
[5]*Swiss Federal Institute of Technology (ETH Zürich), Switzerland*

Submitted to: Quaternary Research

ABSTRACT *Based on different proxy records from western Black Sea cores, we provide a comprehensive study of climate change during the Last Glacial Maximum and Late Glacial in the Black Sea region. For the first time we present a record of relative changes in precipitation for NW Anatolia based on variations in the terrigenous supply expressed as detrital carbonate concentration. The good correspondence between reconstructed rainfall intensity in NW Anatolia and past Mediterranean sea surface temperatures (SSTs) implies that during the glacial the regional precipitation variability was controlled, like today, by Mediterranean cyclonic disturbances. Periods of reduced precipitation correlate well with low SSTs in the Mediterranean related to Heinrich Events H1 and H2. Stable isotopes ($\delta^{18}O$), lithological and mineralogical data from the Black Sea point to a significant modification in the dominant freshwater/sediment source concomitant to the meltwater inflow after 16.4 cal ka BP. This change implies the intensification of a northern sediment source controlled by the Central and Northern European climate. Together with other geomorphological (lake level) and pollen records from the Mediterranean region our data consistently suggest a reorganization of the atmospheric circulation pattern affecting the hydrology of the European continent. The early deglacial northward retreat of both, atmospheric and oceanic polar fronts was responsible for the warming also in the Mediterranean region, leading simultaneously to more humid conditions in Central and Northern Europe.*

KEYWORDS *Black Sea; Mediterranean; paleoclimate; precipitation; terrigenous input, Heinrich Events*

INTRODUCTION

Recent studies on glacial millennial-scale climate variability carried out in the Mediterranean Sea have demonstrated that this region reacted very sensitively to rapid climatic and oceanographic changes in the North Atlantic realm related to the well-known Heinrich Events (HEs) (e.g. Bond et al., 1993). The response to these cooling events was identified in both, marine (Cacho et al., 1999, 2001; Sierro et al., 2005; Cacho et al., 2006;) and terrestrial (Allen et al., 1999; Combourieu Nebout et al., 2002; Sanchez Goni et al., 2002) records from the Mediterranean region in a variety of proxies. For the Last Glacial Maximum (LGM) and Late Glacial, terrestrial and marine Mediterranean archives with reliable chronological control draw a similar picture; a generally positive hydrological balance marked by pronounced dry spells corresponding to HEs. Western Mediterranean marine records show decreased sea surface temperatures (Cacho et al., 1999), decreased deep water temperatures and intensified ventilation (Cacho et al., 2006) corresponding to

HEs. Pollen data from the Western and Central Mediterranean document that arid and cold conditions over Western Europe were synchronous to the response of the marine domain to the HEs (Allen et al., 1999; Combourieu Nebout et al., 2002; Sanchez Goni et al., 2002). There is a lack of glacial marine records from the Eastern Mediterranean but ample evidence from terrestrial archives like Lake Lisan (Bartov et al., 2003; Prasad et al., 2004) that indicate humid conditions punctuated by enhanced aridity linked to the North Atlantic coolings. Oscillations in the North Atlantic polar front and atmospheric Polar Front were suggested to transmit the high latitude signals to mid latitudes (Cacho et al., 2001). The generally positive glacial hydrological balance reconstructed for the Mediterranean region is in agreement with a postulated more southerly position of the jet stream and the associated westerlies during this time window (Prentice et al., 1992). A southward-shifted jet stream would lead to relatively wet conditions in Southern Europe and the Mediterranean, and relatively arid conditions in Northern and Central Europe. Similarly, a northward retreat of the polar fronts could explain early deglacial changes in the European hydrological cycle. These opposing trends in precipitation across the European continent during the LGM and Late Glacial could be best observed in the differences in North European and Mediterranean lake level record (Harrison et al., 1996). Only few direct precipitation reconstructions were published for the Eastern Mediterranean region and are either not long enough or of low resolution. For example, two quantitative approaches using stable oxygen isotopes, a stalagmite record from Israel (Bar-Matthews et al., 1997) and an authigenic carbonate record from a crater lake in central Anatolia (Jones et al., 2007) propose very similar precipitation changes over the Last Glacial but these records do not reveal sufficient temporal resolution in the Marine Isotope Stage 2 to distinguish the LGM from Heinrich Event 1 (H1). Higher resolution reconstructions based on tree rings reach not further than 900 yr back (e.g. Touchan et al., 2007).

Here we introduce a record of precipitation changes in western Anatolia over the last 25 cal kyr based on variability of the terrigenous supply. We analyze changes in the composition of the terrigenous sediment fraction in order to identify modifications in the sediment input sources related to rainfall changes. To our advantage, the southern drainage area of the Black Sea (western Anatolia) is presently characterised by a Mediterranean-type climate while the northern drainage is under the influence of Central European and North European climate. Tracing down the changes in composition of the terrigenous fraction provides a basis to reconstruct the relative contribution from these two regions and to understand interactions between the Mediterranean and Central and North European hydrological regimes in the past. Finally, we present a close comparison between our Black Sea precipitation/sediment source record and other Mediterranean records documenting major shifts in past atmospheric circulation patterns occurring concomitant to the North Atlantic climate changes.

THE LAST GLACIAL BLACK SEA HISTORY

As the most distant arm of the Atlantic Ocean, the Black Sea demonstrates an unparalleled feature: it oscillates between lacustrine and marine stages following, respectively, glacial-interglacial sea level changes (Schrader, 1979). Today, the Black Sea is the world's largest anoxic basin. Therefore most of the previous investigations focused on its modern marine history covering the last ~8 ka. Only recent studies shed light on the glacial history of the western Black Sea (Major et al., 2002; Bahr et al., 2005) and the evolution of the hydrological properties of the basin during the last ~30 ka (Mudie et al., 2002a; Bahr et al., 2006; Major et al., 2006). During the glacial, sedimentation in the Black Sea was dominated by terrigenous supply of siliciclastic material (Müller and Stoffers, 1974). Stable

isotopes (Bahr et al., 2006) and Mg/Ca and Sr/Ca data (Bahr et al., 2008) measured on ostracods all point to relatively stable hydrological conditions of the Black Sea over this time-interval . A series of reddish-brown clays occur in the sediments of the northern (Major et al., 2002; Ryan et al., 2003; Bahr et al., 2005) and the southern (Kwiecien et al., 2008) Black Sea after 16.4 cal ka BP. The intermission of the reddish-brown clays, commonly called 'red layers interval', was previously thought to represent meltwater pulses brought to the Black Sea by a Caspian spillover at the onset of the deglaciation (Bahr et al., 2005). This interpretation was supported by the similarity of the Black Sea red layers to the 'chocolate' clays representing glacial high stand of the Caspian Sea (Kroonenberg et al., 1997). Anomalies in the $\delta^{18}O$ signal (Bahr et al., 2006) and 87Sr/86Sr ratio (Major et al., 2006) of ostracod shells emphasized the significance of the melt/freshwater pulses on the Black Sea hydrology. As discussed in this paper, there are new findings that question the delivery of the red clays via the Caspian spillover. The Bølling/Allerød warming, which followed the deposition of the red layers, is recorded in the Black Sea sediments by a high amount of inorganically-precipitated carbonates (Major et al., 2002; Bahr et al., 2005). The inorganic carbonate precipitation was attributed to increased CO2 assimilation due to massive phytoplankton blooms (Bahr et al., 2005). The carbonate precipitation is interrupted by the Younger Dryas cold interval, restarted in the early Holocene and continued until the reconnection with the Mediterranean Sea. The base of the Black Sea sapropel, traditionally marking the lacustrine/marine transition, is dated to ~8 cal ka BP (Lamy et al., 2006) but the first inflow of the Mediterranean water could have taken place as early as 9.5 cal ka BP (Bahr et al., 2006; Major et al., 2006).

CLIMATOLOGICAL AND GEOLOGICAL SETTING

Site MD04-2788/2760 is located at the continental slope of the south western coast of the Black Sea (NW Anatolia) off the mouth of the Sakarya River (Fig. 1). Today this region is influenced mainly by Mediterranean moisture sources and receives most of its rainfall during the winter/spring season. The rainfall in the Eastern Mediterranean is primarily of cyclonic origin (Wigley and Farmer, 1982, Kostopoulou and Jones, 2007) (Fig. 3.1). Mediterranean SSTs play the key role in cyclogenesis; storms are formed along temperature gradient boundaries and are normally fed by moisture uptake from the relatively warm Mediterranean surface waters. Cyclones are more frequent and more intense during winter, when the atmosphere-sea surface thermal gradient (difference between the temperature of the air aloft and the sea surface) is steepest. Consequently, the sediment load of the Sakarya and other Anatolian rivers which follow the regional precipitation pattern shows a strong seasonal component (Algan et al., 1999) (Fig. 3.2a).

The major part of the Sakarya River's catchment (the upper river course composed of clastic continental rocks) is located in the Central Anatolia Plateau characterized by a dry to semi dry climate (Fig. 3.2b). In contrary, a carbonate-bearing rocks domain is situated in the costal mountain area (lower river course) (Fig. 3.2b). The orographic effect causes a steep gradient between the rainfall amount received by the lower and by the upper course of the Sakarya River (Fig. 3.2b). The contribution of the lower course of the Sakarya River receiving more rainfall over the year is therefore more sensitive to changes in precipitation.

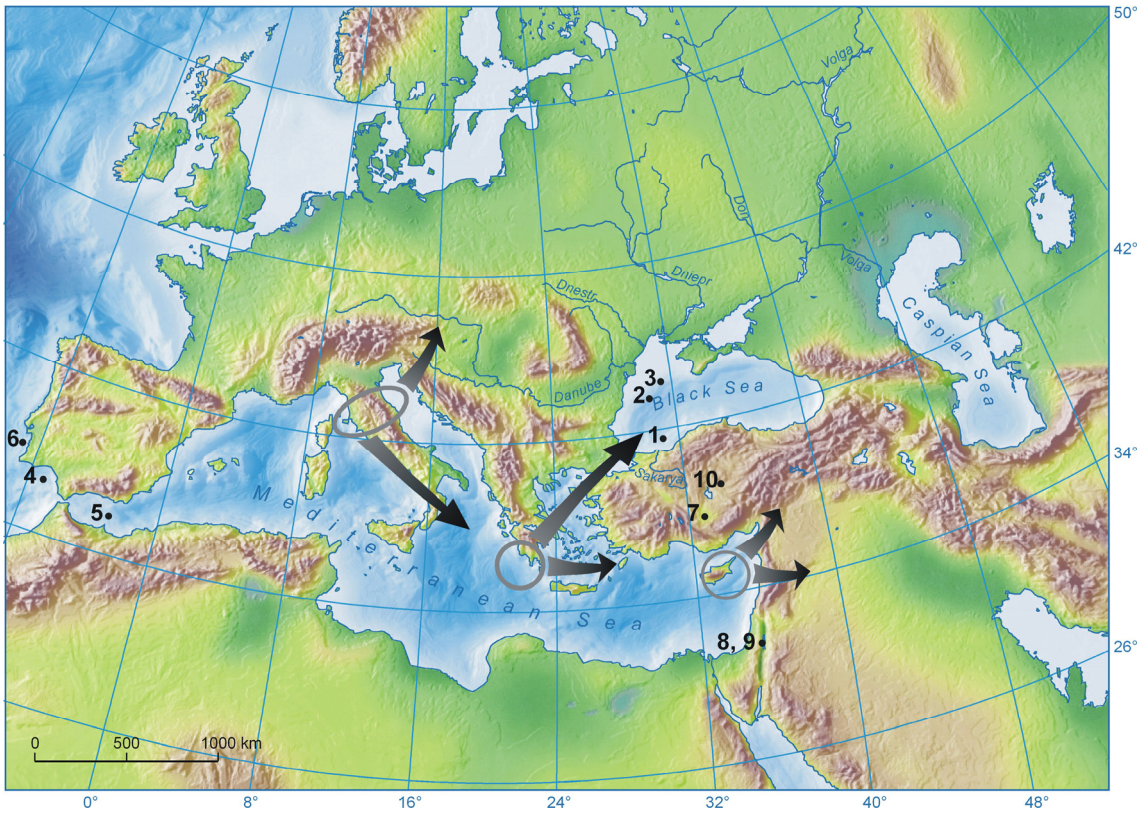

Figure 3.1: Regions of cyclonogenesis (Mediterranean low-pressure systems) and principal cyclone tracks (based on Wigley and Farmer, 1982) together with locations of the sites relevant for the study. 1) MD04-2788/2760 this study; 2) GeoB 7608-1 (Bahr et al., 2006); 3) BLKS9810, BLKS9809 (Major et al., 2002); 4) MD95-2043 (Cacho et al., 2000); 5) M39-008 (Cacho et al., 2000); 6) SU8118 (Bard et al., 2000); 7) Konya Plain lakes (Fontague et al., 1998 and references therein); 8) Lake Lisan (Bartov et al., 2003); 9) Soreq Cave (Bar.Matthews et al., 1997); 10) Eski Acigöl (Jones et al., 2007).

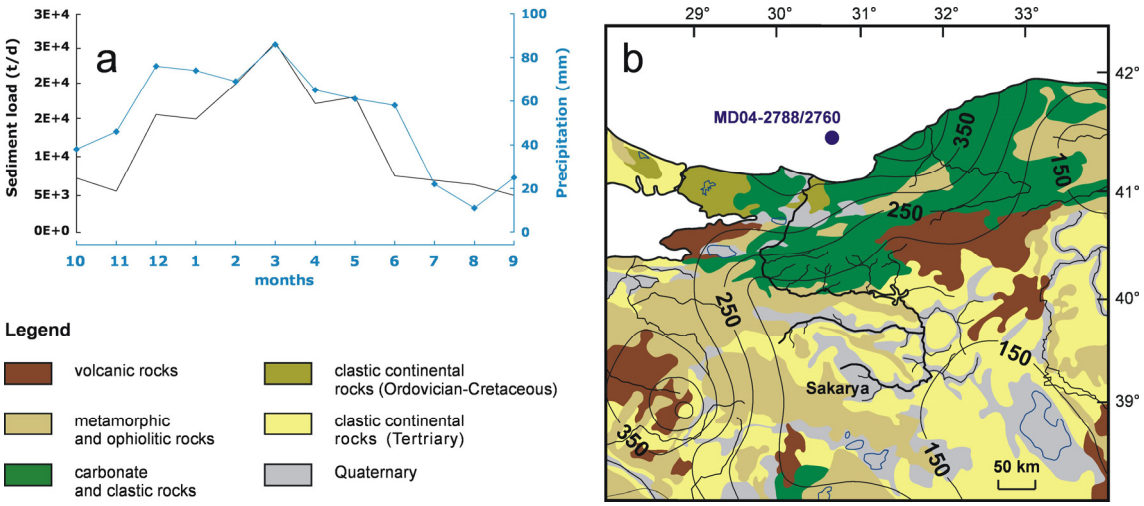

Figure 3.2: (a): Relation of sediment load transported by Sakarya River to the amount of regional precipitation (Algan et al., 1999). The data were obtained from the State General Directory of Electrical Research Works (EIE) data base (EIE, 1993). (b) The distribution pattern of long-term average winter precipitation (mm) (after Türkes and Erlat, 2005) superimposed on a simplified geological map of NW Anatolia (modified after Geological Map of Turkey, 2002).

MATERIAL AND METHODS

Material

The investigated record is a composite profile of the two sediment cores; MD04-2788 (gravity core - marine units) and MD04-2760 (piston core - lacustrine unit) (Kwiecien et al., 2008). Both cores were recovered from offshore northern Anatolia (Black Sea, 41°31.67'N; 30°53.09'E) at a water depth of 1200 m (Fig. 3.1) during the ASSEMBLAGE I cruise of the R/V *Marion Dufresne*. The proximity of the Sakarya River results in very high sedimentation rates at the study site. The glacial section with a sedimentation rate ranging from 1.5 m/ka to 2.5 m/ka is continuously laminated and shows 1 to 5 mm-scale alternations of light-colored clay to darker-colored clay/fine silt (or sporadically fine sand). The period between 15 and 16.4 cal ka BP is marked by a prominent intercalation of reddish-brown fine clay material. Starting at the Bølling/Allerød and continuing till the early Holocene, biologically triggered precipitation of inorganic carbonates suppresses the terrigenous signal. Therefore the younger part of our record (8-14 cal ka BP) is discarded for the purpose of this study.

Profiling measurements

After splitting, cores MD04-2788 and MD04-2760 were scanned in 1 cm resolution with an AVAATECH X-ray fluorescence scanner at the University of Bremen, Germany. The XRF-core scanner, developed at the Netherlands Institute for Sea Research, Texel, measures the bulk intensities of major elements (e.g. Al, Si, S, K, Ca, Ti, Mn, and Fe) on split sediment cores (Jansen et al., 1998).

$CaCO_3$ content

Samples were measured with an elemental analyzer (NC2500 Carlo Erba) at the GeoForschungsZentrum in Potsdam, Germany. Before the analysis the samples were freeze-dried and then ground and homogenized in an agate ball mill. Total carbon (TC) and total organic carbon (TOC) contents were determined in two separate runs. In the sediment samples for the organic carbon the carbonate fraction was removed by addition of a 20% HCl solution. Sample duplicates show a reproducibility of 0.2%. TC and OC were measured every 8 cm resulting in an average time resolution of ~40 yr. Starting at the first occurrence of the red layers (16.4 cal ka BP), the sampling resolution was increased to 4 cm giving a time resolution of ~16 yr. In order to calculate dry weight percentages of calcium carbonate ($CaCO_3$) we used the relation: $CaCO_3 = (TC - TOC) \times 8.33$.

Stable isotopes

Stable isotope analysis ($\delta^{18}O$) was performed on ostracod valves belonging to the genus *Candona* spp. (C. schweyeri and C. angulata). Either 5-8 valves of juvenile ostracods or 1-2 valves of adult ostracods were hand-picked from wet-sieved samples and analyzed at the University of Bremen using a Finnigan MAT 251 mass spectrometer with an automated carbonate preparation device. The ratio of $^{18}O/^{16}O$ is given in ‰ relative to the VPDB standard. Analytical long-time standard deviation is about ±0.07‰ VPDB. For the stable isotopes analysis we sampled the core MD04-2760 in 4 cm intervals however, not all samples provided enough material for the measurement.

Chronology

Presently, MD04-2788/2760 is the best-dated Black Sea record available for the LGM and Termination I, going back to ~25 cal ka BP. The chronological framework for the period of this study is based on calibrated AMS ^{14}C ages corrected for the reservoir effect, and a clearly identified tephra layer (Tab. 3.1) (Kwiecien et al., 2008). The discovery of the Y-2 tephra, for the first time in the Black Sea sediments, turned out to be essential for the estimation of the reservoir effect during the glacial. Subsequent comparison of the calibrated MD04-2760 record with the Greenland ice core (GISP2) chronology (Grootes et al., 1993) suggests that the glacial reservoir age of 1450 ^{14}C yr decreased to 900 ^{14}C yr before the onset of the Bølling. The detailed examination of the Ca-intensity XRF signal allowed a precise correlation of the MD04-2788/2760 record with previously published records from the western Black Sea (Kwiecien et al., 2008). For the reason of consistency, Black Sea records from other publications presented herein are tuned to the MD04-2788/2760 time scale.

Sample	Original depth in the core (cm)	Depth in the composite profile (cm) MD04-2788/2760	^{14}C age (yr BP)	Applied reservoir correction	Calibrated age[a] (yr BP) +/- 1σ	Material /source
Core MD04-2788						
KIA 28419	463-470	674-684	13,220 ± 70	900[b]	14,069-14,408	ostracods
Core MD04-2760						
KIA 26701	945-965	643-663	13,050 ± 70	900[b]	13,919-14,094	gastropod
KIA 25676	1540-1560	1238-1258	14,800 ± 100	1000[b]	16,207-16,656	ostracods
KIA 25684	1680-1700	1374-1394	16,120 ± 90	1450[c]	17,135-18,217	ostracods
KIA 25685	1815-1835	1509-1529	17,090 ± 110	1450[c]	18,591-19,348	ostracods
KIA 25686	2535-2555	2095-2115	19,390 ±110	1450[c]	20,772-21,879	ostracods
Y-2 / Cape Riva tephra	2652	2192	18,310 ± 380[d]	-	21,270-22,290[e]	Pichler and Friedrich, 1976 Erikson et al., 1990
KIA 25687	2800-2820	2295-2315	20,240 ± 130	1450[c]	21,744-22,916	ostracods
KIA 25754	3025-3045	2497-2517	21,030 ± 160	1450[c]	22,720-23,863	gastropod
KIA 25688	3025-3045	2497-2517	21,460 ± 140	1450[c]	23,353-24,527	ostracods
KIA 25678	3310-3332	2726-2748	22,340 ± 190	1450[c]	24,521-25,595	ostracods

[a]calibrated date range calculated by Calib Rev. 5.0.1 (Stuiver et al., 2005) using the Intcal04 curve (Reimer et al., 2004)
[b]reservoir correction was inferred by comparison to other Black Sea records and GISP2 record. therefore no error estimation is given.
[c]estimated reservoir correction. The error estimation calculated according to the formula $(\sigma_{lacustrine}^2 + \sigma_{atmospheric}^2)^{1/2}$ falls into range 390 – 425 ^{14}C yr and gives an average value of 400 ^{14}C yr
[d]mean and standard deviation of original dating series
[e]mean and standard deviation of calibrated ranges of original dating series

Table 3.1: Details on age-control points used to construct age model for the composite profile of cores MD04-2788 and MD04-2760 (Kwiecien et al., 2008). All radiocarbon ages are calibrated using the Calib 5.0.1 software (Stuiver et al., 2005).

RESULTS

Profiling measurements and $CaCO_3$ content

Very high sedimentation rates at the study site result in low-amplitude changes in the composition of the terrigenous fraction. The high resolution XRF Ca-intensity record is reproduced by bulk $CaCO_3$ measurements (Fig. 3.3A) suggesting that Ca primarily represents carbonates. We ascribed the apparent difference between the two records at 19.5-18 cal ka BP to the intense water condensation during the XRF profiling (Tjallingii et al., 2007) and corrected the XRF data in this interval using a linear relationship between XRF Ca-intensity and CaCO3 content. The $CaCO_3$ content ranges from 25 and 16.3 weight %. Both, $CaCO_3$ content and XRF Ca-intensity show 3 minima at 24.5-23.5 cal ka BP, 18-17 cal ka BP, and 16.4-15 cal ka BP. The last and most pronounced carbonate minima at 16.4-15 cal ka BP is coeval to the period of the ‘red layers’ deposition. After 15 cal ka BP the

carbonate content gradually increases and at 14 cal ka BP reaches the values observed for the period between 23 and 18 cal ka BP.

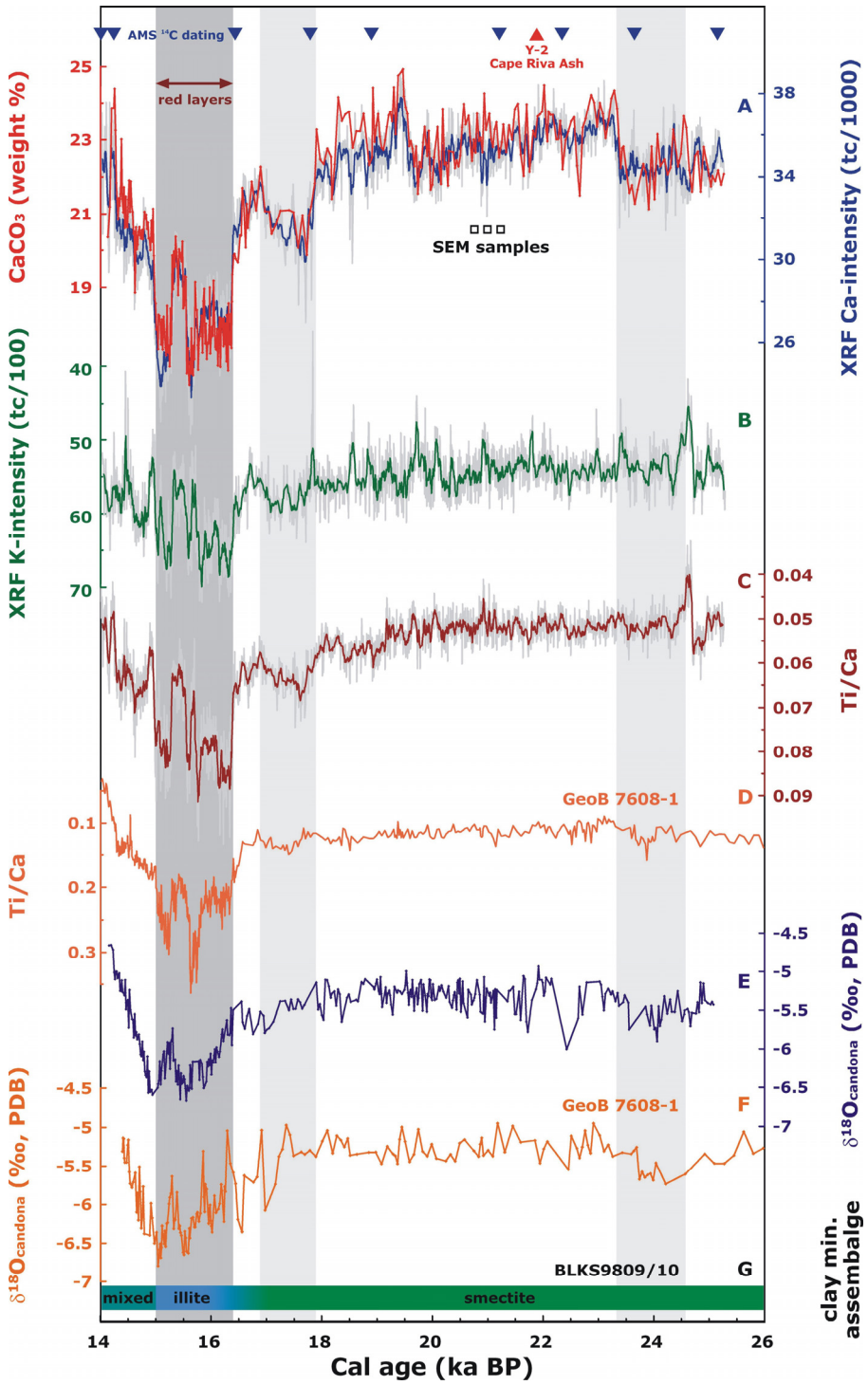

Figure 3.3: Paleoclimate records from different cores in the Black Sea. The chronology of core MD04-2788/2760 is based on reservoir-corrected calibrated ^{14}C ages (Kwiecien et al., accepted). (A-C, E) data from the MD04-2788/2760, in case of XRF data thin gray lines represent original data and thick color lines represent a 7-point moving average. (A) Corrected XRF Ca-intensity record (tc/1000) in blue, $CaCO_3$ (weight %) in red. (B) XRF K-intensity record (tc/100). (C) XRF Ti/Ca ratio. (D) XRF Ti/Ca ratio from the core GeoB 7608-1 (Bahr et al., 2005); (E) $\delta^{18}O$ measured on ostracods. (F) $\delta^{18}O$ measured on ostracods from the core GeoB 7608-1 (Bahr et al., 2006); (G) Clay mineral assemblage from the cores BLKS9809/10 (Major et al., 2002). Gray bars indicate periods of reduced carbonate supply.

Fe, Ti and K-intensities are commonly linked to siliciclastic components. Ratios of Fe, Ti or K to Ca can be used to represent variations in the relative proportion of siliciclastic and biogenic carbonate sedimentation. However, carbonates from the glacial sediments of the Black Sea are known to be dominantly detrital (Müller and Stoffers, 1974). Scanning Electron Microscope (SEM) analysis and sieving proved that throughout the glacial a dominant portion of the carbonate fraction is of detrital origin and was transported to the study site in the clay/silt fraction (Fig. 4) together with siliciclastics (a negligible amount of non-detrital carbonate fraction consists of gastropod and ostracod shells, Fig 4b). We have chosen the K-intensity and Ti/Ca ratio to trace changes in the composition of the terrigenous fraction. A significant part of K must come from K-rich clay minerals (e.g. illite) and K-feldspars which are characteristic for the northern sediment provenance of the Black Sea (Müller and Stoffers, 1974). K-intensity (Fig. 3B) and Ti/Ca ratio (Fig. 3C) stay on moderately stable level throughout the glacial and both abruptly increase after 16.4 cal ka BP. The period of increased K-intensity and Ti/Ca ratio correlates with the occurrence of red layers. Comparable enrichment in Ti and K during the red layers deposition can be observed in the cores from the northern transect (Bahr et al., 2005). The Ti/Ca ratio from core MD04-2788/2760 shows very similar pattern to the GeoB 7608-1 record from the northwestern Black Sea (Bahr et al., 2005) (Fig. 3D) but with generally lower values (~3 fold decrease). The change in the elemental composition in the MD04-2788/2760 and GeoB 7608-1 starting at 16.4 cal ka BP coincides with the change in the clay mineral assemblage composition recorded in the northwestern Black Sea (Major et al., 2002) (Fig. 3G).

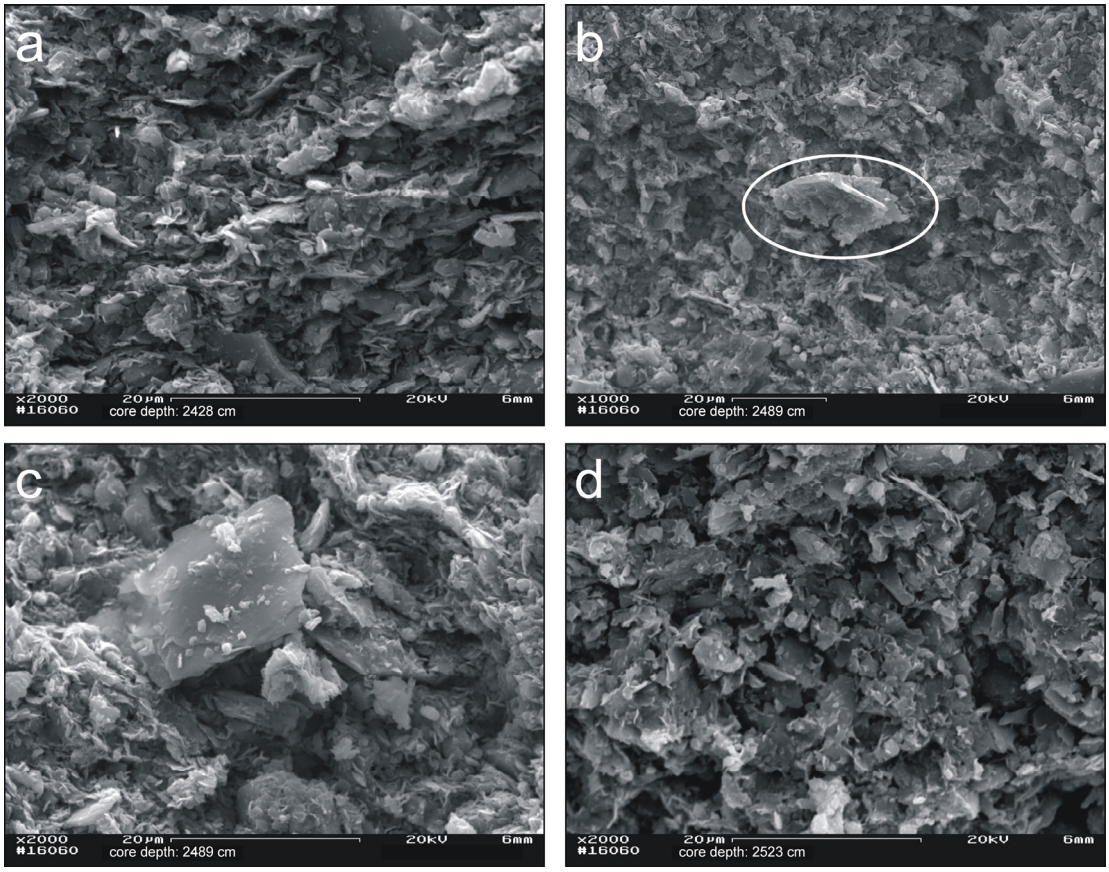

Figure 3.4: Scanning electron macrographs of sediment samples from selected intervals of the glacial section of the core MD04-2760. Original sample depth, magnification and scale are indicated on the picture. The age of the sampled intervals is also showed on the figure 3.3. The sediment is composed mostly of mud with sporadic bigger mica or feldspar crystals. Note a biogenic carbonate particle (fragment of ostracod shell) in the centre of picture (b), and a mica crystal in the centre of picture (c).

Stable isotopes

The isotopic composition of ostracod valves reflects the isotopic composition and temperature of the water mass at the time of valve calcification and therefore provides important information on the hydrology of the basin. $\delta^{18}O$ measurements from cores MD04-2788/2760 (Fig. 3.3E) reveal a relatively stable level during the glacial. Between 25 and 16.4 cal ka BP the $\delta^{18}O$ values oscillate around -5.3‰. A gradual but significant depletion of ~1‰ is observed during the deposition of the red layers between 16.4 and 15 cal ka BP. Within the thousand years after the deposition of the red layers $\delta^{18}O$ values rise back to their glacial level. Our results parallel very well the NW Black Sea record (core GeoB 7608-1) published by Bahr et al. (2006) (Fig. 3.3F). Only the two negative $\delta^{18}O$-excursions directly before the onset of the red layer are more pronounced in the GeoB 7608-1 than in the MD04-2788/2760.

DISCUSSION

Past rainfall variability

During the glacial, sedimentation in the isolated Black Sea was dominated by the fluvial input. Based on the very proximal core location to the river mouth, we assume that the major portion of the sediment was delivered to the MD04-2788/2760 site by the Sakarya River. Comparable XRF Ca-intensity patterns (Kwiecien et al., 2008) together with an enrichment in smectite (Major et al., 2002) (Fig. 3.3G) observed in the northern cores suggest that prior to 16.4 cal ka BP sediments from the southern provenance were penetrating further northward into the Black Sea.

Fluvial supply of terrigenous material is dependent on two factors: precipitation and the vegetation in the catchment area. Palynological investigations from Anatolia (Fontugne et al., 1999) suggest sparse vegetation cover and domination of steppe taxa throughout our study period (14-26 cal ka BP). With no alterations in the vegetation cover, changes in the terrigenous supply can be expressed as a function of past rainfall variability. Potential complications, for example, through an increased river runoff due to summer melting of mountain glaciers are unlikely, as there is no compelling evidence for the presence of glaciers during the late Pleistocene in western Anatolia.

Today, the sediment load of the Sakarya River follows the regional seasonal precipitation pattern (Algan et al., 1999) with the highest rainfall during the winter/spring months (Fig. 3.2b). The rainfall variability in western Anatolia will particularly affect the carbonate-bearing lower course of the Sakarya River and will be expressed as relative changes in the carbonate content of the sediment. A very good agreement between the high resolution XRF Ca-intensity and $CaCO_3$ concentration in our record (Fig. 3.3A) proves that Ca is bound in the calcium carbonates. We then assume that the $CaCO_3$ content in our record represent the contribution of the more rainfall-sensitive coastal mountain area and can thus be considered as an indicator for terrigenous supply from this region. With the modern relation of sediment load to regional rainfall pattern (Algan et al., 1999) as an analog, the $CaCO_3$ content in glacial times can be used as proxy for relative changes in the regional precipitation in the western Anatolia.

Link between the North Atlantic Heinrich Events and Black Sea precipitation

Today the south western coast of the Black Sea is influenced mainly by Mediterranean moisture sources and receives most of the rainfall during the winter season. The intensity of cyclones

supplying moisture towards the east is strongly related to the Mediterranean SSTs. In general relative precipitation changes in our glacial record (Fig. 3.5D) correlate well with the Mediterranean SST records (Cacho et al., 2001) (Fig. 3.5B, C) suggesting that during the glacial the regional rainfall variability was, similar like today, controlled by the Mediterranean cyclonic disturbances (low-pressure cells, Fig. 3.1). SST minima in the Mediterranean (Fig. 3.5B, C) (Cacho et al., 2001) are related to Heinrich Events H1 and H2 (Grootes et al., 1993), (Fig. 3.5A, timing of the H1 and H2 after [Bard et al., 2000]). During the glacial, extended continental ice sheets and sea ice resulted in a southward expansion of the polar zone which strengthened the westerly jet, displaced it equatorwards, and increased the temperature gradient between mid- and low-latitudes (Chapman and Maslin, 1999). A southward-shifted jet stream would have led to relatively wet conditions in Southern Europe and the Mediterranean, leaving the Central and Northern Europe relatively drier. Both, polar water and polar air masses, reached a maximum southward expansion during Heinrich Events (Rohling et al., 1998). This southward migration of the North Atlantic polar front and atmospheric Polar Front was related to the calving of sea ice and the waxing of continental ice sheets, respectively. SST minima recorded during Heinrich Events in the Western Mediterranean (Fig. 3.5B, C) were related either to the entrance of cold water from the Atlantic Ocean (Cacho et al., 1999; 2001; Sierro et al., 2005) and/or to the atmospheric conditions over the Mediterranean Sea, like intensified flow of dry and cold winds (Rohling et al., 1998; Cacho et al., 2000; 2006).

Although the temperature gradient between mid and low latitudes stayed high and the westerly jet stayed south, cooler Mediterranean SSTs occurring during HEs would have decreased the atmosphere-sea surface thermal gradient resulting in a weakening of the Mediterranean low-pressure systems. Subsequent less frequent and less intense storms would have led to significantly reduced precipitation in the Eastern Mediterranean/Black Sea region. Additionally, decreased air temperatures would have reduced the water vapor capacity thus hindering an eastward moisture transport. A similar scenario has already been proposed to link arid episodes in the Eastern Mediterranean with the Heinrich Events (Bartov et al., 2003). Enhanced aridity during Heinrich Events is documented by pollen records in the Western Mediterranean (Combourieu Nebout et al., 2002; Sanchez Goni et al., 2002) and by low lake levels in the Eastern Mediterranean, like e.g. of Lake Lisan (Bartov et al., 2003) and other Turkish lakes in the Konya Plain (Fontugne et al., 1999, and references therein). Thus, the precipitation decrease interpreted from our record during H2 can then be directly linked to the cooling of the Mediterranean.

Mixed nature of H1 and switch in the dominant sediment source

The signature of the Black Sea records during H1 (*sensu* Bard et al., 2000) is more complex. The initial decrease in carbonate concentration at ~18 cal ka BP indicating a decrease in northeast Anatolian precipitation is followed by a more pronounced decrease in carbonate content at 16.4 cal ka BP. The latter coincides with prominent changes in the composition of the terrigenous fraction and with a series of meltwater pulses reflected by the $\delta^{18}O$ signal (Fig 3.3E, F). Unlike the two previous carbonate concentration minima, this period starting at 16.4 cal ka BP is characterized by high sedimentation rates (not shown) and corresponds to a the rise of Mediterranean SSTs (Fig 3.5B, C).

The abrupt decrease in the $CaCO_3$ content at 16.4 cal ka BP (Fig. 3.3A) accompanied by an increase in XRF K-intensity and the Ti/Ca ratio (Fig. 3.3B, C) could imply either a drastically reduced carbonate supply (reduced rainfall) and/or an intensification of a previously less active source. In the north of the Black Sea, the concomitant increase of the Ti/Ca ratio during the red layers interval (Fig. 3.3D) was linked to the enrichment of fine clay material brought by meltwater inflow coming

from the north (Bahr et al., 2005). This interpretation was further strengthened by $\delta^{18}O$ data (Bahr et al., 2006) showing temporary isotopic depletion subsequent to each of the meltwater pulses (Fig. 3F) represented by Ti/Ca peaks (Fig. 3.3D). Our Ti/Ca record displays very similar fluctuations but of somewhat lower magnitude which could be explained by the northwards-decreasing amount of the detrital carbonates (Müller and Stoffers, 1974). Changes in our Ti/Ca ratio and XRF K-intensity correlate well with changes in the dominant sediment source at 16.4 cal ka BP also recorded as a shift in the clay mineral assemblage data (Major et al., 2002) (Fig. 3.3G). Therefore we interpret the Ti/Ca and K-variability during H1 in terms of changes in the relative contribution of a southern (Sakarya River) versus a northern sediment source.

The modification in the freshwater sources after 16.4 cal ka BP is recorded by the $\delta^{18}O$ data. The congruent isotope pattern from the north and the south of the Black Sea (Fig. 3.3E, F) indicates that the hydrological response to the meltwater injection was uniform on a basin-scale, and suggests that the water column was well mixed at the time of the inflow. Moreover the very good agreement between $\delta^{18}O$ records of MD04-2788/2760 and GeoB 7608-1 provides an independent proof for the accuracy of the Ca-signal-tuned chronology.

Several factors consistent with reconstructions of Central and North European climate can explain the suppression of sediment supply from the northern Black Sea provenance until ~16 cal ka BP. During the LGM cold and arid conditions prevailed in the northern and western drainage areas of the Black Sea (Florineth and Schluchter, 2000; Atanassova, 2005) and soils in the northern catchment remained partly frozen (Renssen and Bogaart, 2003). The retraction of Scandinavian Ice Sheets (Rinterknecht et al., 2006) and Alpine glaciers (Florineth and Schluchter, 2000) during the LGM suggests that the mid-latitudes may have suffered from moisture starvation at that time. Lake level data from Northwestern Europe indicate similar dry conditions (Harrison et al., 1996). Low precipitation would result in reduced fluvial runoff of the northern (Don, Dniepr, Dniester) and western (Danube) rivers while permafrost could have inhibited the erosion in the catchment. Dry conditions in Northern Europe during the glacial are consistent with the more southerly position of the polar fronts and westerlies, and wetter Southern Europe and Mediterranean region.

The intensification of the northern sediment/freshwater source after 16.4 cal ka BP is contemporary with the onset of deglacial warming in Europe. It roughly corresponds to the time when the Scandinavian Ice Sheet (SIS) blocked the drainage towards the Baltic Sea (Mangerud et al., 2004; Svendsen et al., 2004). Meltwater from a considerable sector of the SIS was proposed to have flown to the watershed of the Volga River (Mangerud et al., 2004). Enhanced Volga runoff would cause the Caspian Sea to overflow along the Manych Depression to the Black Sea (Bahr et al., 2005; Mangerud et al., 2004). The possibility of the Black Sea – Caspian Sea connection during the Late Glacial was challenged by Major et al. (2006) arguing that $^{87}Sr/^{86}Sr$ ratio of the modern Caspian Sea is too low to account for the $^{87}Sr/^{86}Sr$ changes seen in the Black Sea during the deposition of the red layers. Initial investigation of new cores retrieved from the northeastern Black Sea basin south of the Sea of Azov (R/V *Meteor* cruise 72/5, unpublished data) revealed no presence of red layers at the expected depth. This could imply that red layers are confined only to the western Black Sea basin which would in turn exclude their relation to the potential Caspian outflow. In addition, the rerouting of North European river systems and the direction of the meltwater discharge from the SIS is still a matter of debate. Meltwater could have been directed not only to the south, as initially suggested by Mangerud et al. (2004) but also towards the Baltic Sea, much farther west to the Bay of Biscaye (Menot et al., 2006), or the Arctic Ocean in the north (Demidov et al., 2006). Noteworthy, in case if the SIS advanced into the watersheds of the Volga River (Mangerud et al., 2004) a similar process could have taken place in the watershed of the Dniepr River (Kalicki and Sanko, 1998). Feeding of

the Dniepr River by thawing glaciers would usher a meltwater flow directly into the Black Sea without the necessity of the Caspian Sea basin as an intermedium. Alternatively, as first proposed by Major et al. (2002), thawing of the permafrost in the Dniepr River watersheds could have led to increased runoff in the northern drainage area and enhanced sediment transport of fine clay particles.

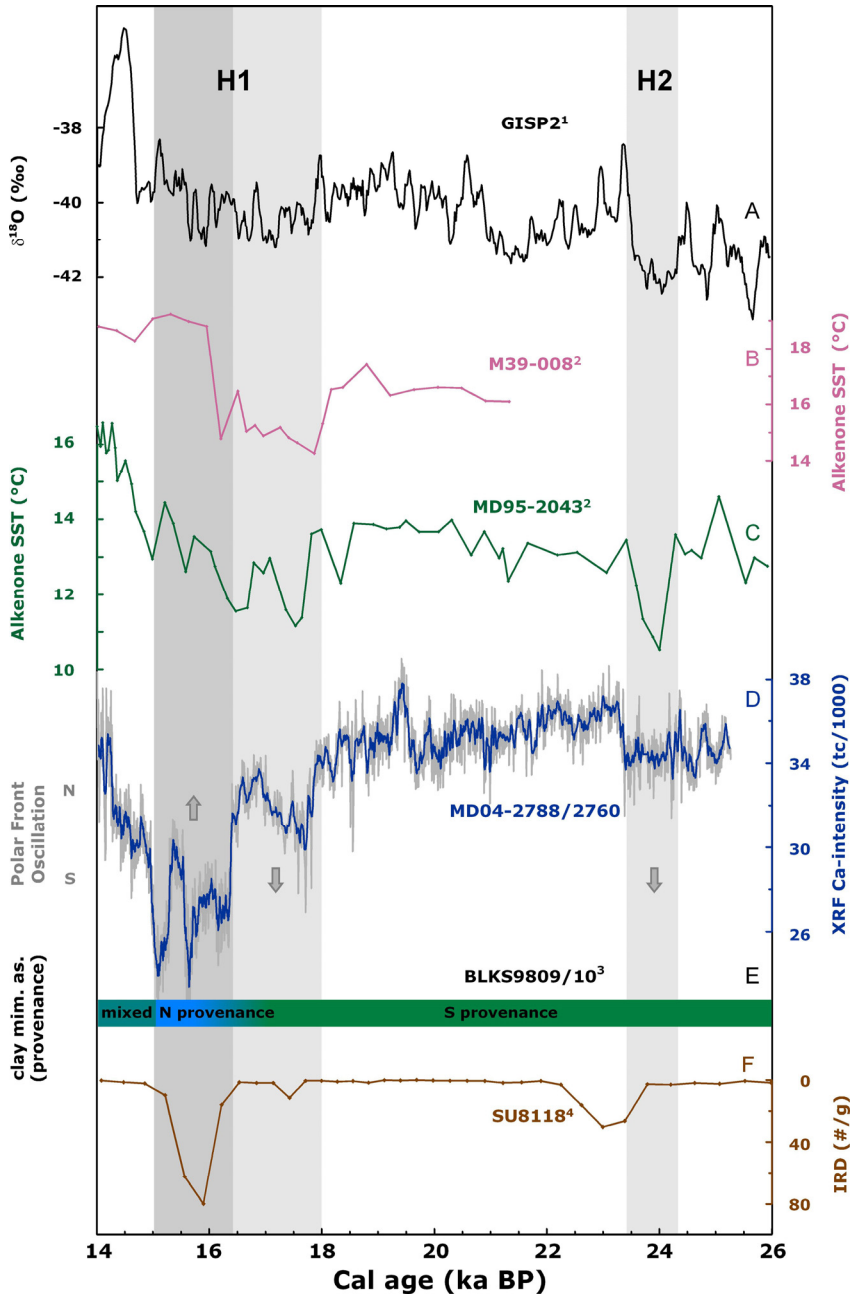

Figure 3.5: Juxtaposition of different climatic records covering LGM in the Mediterranean region (B–F) and GISP2 stratigraphy given for comparison (A). The gray arrows indicate inferred direction of the latitudinal displacements of the polar fronts. XRF Ca-intensity record from MD04-2788/2760 was corrected using the linear relation to $CaCO_3$ weight procentage. [1]Grootes et al. (1993); [2]Cacho et al. (2001); [3]Major et al. (2002); [4]Bard et al. (2000). Timing of H1 and H2 (after Bard et al. [2000]) is indicated by the gray bars. For the H1 light gray bar marks cold phase and the dark gray bar marks purported warming phase (explanation in the text). Except for GISP2, the locations of all sites are shown in Fig. 3.1.

The qualitative nature of our proxies makes it difficult to state clearly weather after 16.4 cal ka BP the contribution of the southern source has diminished or if it stayed at the previous level, but was counterbalanced by the growing influence of a northern source (Fig. 3.5E). The sedimentation rate in the MD04-2788/2760 is comparatively high during the red layers deposition as during most of the LGM, suggesting that the sediments from the southern provenance were rather diluted than replaced by the contribution of the northern source. In this case precipitation in NW Anatolia should have stayed at a relatively high level over that time. The lowered level of lakes in the Mediterranean region at that time points to enhanced aridity after 16.4 cal ka BP (Bartov et al., 2003; Harrison et al., 1996). However, quantitative reconstructions based on stable oxygen isotopes (Bar-Matthews et al., 1997; Jones et al., 2007) clearly suggest an increase in rainfall amount. This apparent dissonance between lake level and isotope records may arise from a different sensitivity to different components of the water balance. Since the lake level is controlled by precipitation-to-evaporation ratio, the lowering of the lake level after H1 can be explained by the temperature increase leading to higher evaporation and not necessarily by decreased precipitation. Marine Mediterranean records document a significant reorganization of the oceanic/atmospheric circulation at that time (Cacho et al., 2001; Sierro et al., 2005) including regional warming. The sharp warming phase in the Gulf of Cadiz (Fig. 3.5B) probably corresponds to a rapid northward migration of the polar front (Cacho et al., 2001). A northward retreating polar front would have had an effect opposite to the glacial situation: decreased temperature gradients between mid and low latitudes, a weakened westerly jet, and a shift the precipitation belt back north towards the continent. A readvance of woodlands in Central Europe (Atanassova, 2005) and the establishment of lowland forests in southeastern Alps (Vescovi et al., 2007) after ~16 cal ka BP point to an increase in rainfall in the north and in the west of the Black Sea.

Taken together, within the time frame of H1 (*sensu* Bard et al., 2000) only the initial decrease in precipitation amount at 18-17 cal ka BP inferred from the MD04-2788/2760 record corresponds to the North Atlantic cooling event. The following 'apparent' precipitation minima, caused by the dilution of southern provenance sediment by the enhanced contribution of the northern provenance starting at 16.4 cal ka BP, is contemporary to an increase of the Mediterranean SSTs and can be related to the northward retreat of the polar front. Sanchez Goni et al. (2000) described a three-phase pattern of Heinrich Events in the mid-latitudes of the North Atlantic region with a first cold and humid phase, then a cold and dry middle phase related to massive iceberg discharge from the Laurentidian ice-sheet and, finally, a mild and humid third phase linked to the disintegration of the European ice-sheets. Bard et al. (2000) also showed that in the Subtropical Northeast Atlantic ice rafted debris (IRD) has a different composition during the first phase of H1 than during the last phase (Fig. 3.5F), suggesting multiple origins of the ice surges (including the Fennoscandian ice-sheet). The intensification of the northern sediment/freshwater source observed in our record after 16.4 cal ka BP fits well to the scenario of European ice-sheets melting and the mitigation of the Central and Northern European climate.

CONCLUSIONS

During the Last Glacial, rainfall in western Anatolia was responding to changes in Mediterranean SSTs. Periods of reduced precipitation recorded in the Black Sea sediments correlate to Heinrich Events H1 and H2 and support the idea of a strong link between the mid- and high-latitudes. Until ~16.4 cal ka BP, precipitation associated with the Mediterranean cyclonic disturbances was controlling the supply of terrigenous material in the southern drainage of the western Black Sea

basin. Intensification of northern sediment/freshwater sources at ~16.4 cal ka BP coincides with major postglacial reorganizations of atmospheric and/or oceanic circulation patterns and our observation is coherent with other climatic records pointing to a shift in the European moisture source distribution. Our indirect record of northwest Anatolian precipitation and changes in relative contribution of southern and northern sediment sources agrees well with SST records from the Western Mediterranean (Cacho et al., 2001) and lake level records from the Eastern Mediterranean (Bartov et al., 2003; Fontugne et al., 1999) and Northern Eurasia (Harrison et al., 1996). The intensification of a northern sediment source paralleled the northward retreat of the polar fronts after ~16.4 cal ka BP accounting for warming in the Mediterranean region and more humid conditions in Central and Northern Europe.

ACKNOWLEDGMENTS

This research was sponsored by Comer Science and Education Foundation (CS&EF). We thank IPEV for logistic support during the ASSEMBLAGE I cruise (RV Marion Dufresne). We also thank M. Segl, University of Bremen, and her team for performing the stable isotope analysis, U. Röhl, University of Bremen, for support in XRF measurements and A. Hendrich, GFZ-Potsdam, for graphic assistance with the topographic map, and a Spectral Electron Microscope team; Helga Kemnitz and Juliane Herwig for introduction to the SEM facility.

4. Abrupt changes of temperature and water chemistry in the late Pleistocene and early Holocene Black Sea

André Bahr[1], Frank Lamy[2], Helge W. Arz[3], Candace Major[4], Olga Kwiecien[3] and Gerold Wefer[1]

[1]*MARUM - Center for Marine Environmental Research, University of Bremen, Germany*
[2]*Alfred Wegener Institute for Polar and Marine Research (AWI), Bremerhaven, Germany*
[3]*GeoForschungsZentrum Potsdam, (GFZ Potsdam), Germany*
[4]*Woods Hole Oceanographic Institution, Geology and Geophysics, Woods Hole, USA*

Published in: Geochemistry Geophysics Geosystems, 9 (1)

ABSTRACT *New Mg/Ca, Sr/Ca and published stable oxygen isotope and $^{87}Sr/^{86}Sr$ data obtained on ostracods from gravity cores located on the northwestern Black Sea slope were used to infer changes in the Black Sea hydrology and water chemistry for the period between 30 to 8 ka BP (calibrated radiocarbon years). The period prior to 16.5 ka BP was characterised by stable conditions in all records until a distinct drop in $\delta^{18}O$ values combined with a sharp increase in $^{87}Sr/^{86}Sr$ occurred between 16.5 and 14.8 ka BP. This event is attributed to an increased run-off from the northern drainage area of the Black Sea between Heinrich Event 1 and the onset of the Bølling warm period. While the Mg/Ca and Sr/Ca records remained rather unaffected by this inflow; they show an abrupt rise with the onset of the Bølling/Allerød warm period. This rise was caused by calcite precipitation in the surface water, which led to a sudden increase of the Sr/Ca and Mg/Ca ratios of the Black Sea water. The stable oxygen isotopes also start to increase around 15 ka BP, although in a more gradual manner, due to isotopically enriched meteoric precipitation. While Sr/Ca remains constant during the following interval of the Younger Dryas cold period a decrease in the Mg/Ca ratio implies that the intermediate water masses of the Black Sea temporarily cooled by 1-2°C during the Younger Dryas. The $^{87}Sr/^{86}Sr$ values drop after the cessation of the water inflow at 15 ka BP to a lower level until the Younger Dryas, where they reach values similar to those observed during the Last Glacial Maximum (LGM). This might point to a potential outflow to the Mediterranean Sea via the Sea of Marmara during this period. The inflow of Mediterranean water started around 9.3 ka BP, which is clearly detectable in the abruptly increasing Mg/Ca, Sr/Ca and $^{87}Sr/^{86}Sr$ values. The accompanying increase in the $\delta^{18}O$ record is less pronounced and would fit to an inflow lasting ca. 100 years.*

KEYWORDS *Black Sea; ostracods; trace elements*

INTRODUCTION

Today the Black Sea is the largest semi-enclosed basin of the world (V=537,000 km³) that is only connected with the global ocean through the ca. 36 m deep Bosphorus strait. This particular situation led to a complete disconnection with the open ocean during the last glacial period, when the global sea level was lower than the Bosphorus sill. As a consequence the Black Sea turned into a fresh or slightly brackish lake (Mudie et al., 2002a) in which its hydrology and lake level were very sensitive to environmental changes.

One of the major environmental variables is the freshwater budget of the Black Sea, which contributed to significant sea level oscillations since the glacial period (e.g. Ryan et al., 1997; 2003;

Aksu et al., 2002). Previous publications proposed the inflow of large amounts of meltwater from Scandinavian and/or Siberian ice sheets into the Black Sea after the LGM (Ryan et al., 2003; Mangerud et al., 2004; Bahr et al., 2006; Major et al., 2006) that were inferred to result in an overflow of the Black Sea into the Sea of Marmara (Kvasov, 1979; Smith et al., 2005) and to a temporary freshening of the Sea of Marmara (Mudie et al., 2004). A further direct response to climatic changes is the precipitation of calcite during the Bølling/Allerød (B/A) and early Holocene (Major et al., 2002; Bahr et al., 2005) as a result of CO_2-assimilation through enhanced phytoplankton activity during favourable climatic conditions.

Due to the large volume of the Black Sea, variations in the stable oxygen isotopic composition of the water body are slow and, during its lacustrine stage, mainly governed by changes in the isotopic composition of precipitation and run-off (Bahr et al., 2006). Stable oxygen isotope records based on ostracod and bivalve shells from different water depths (Bahr et al., 2006; Major et al., 2006) and bulk $\delta^{18}O$ data (Major et al., 2002) suggest that the effect of temperature changes is rather restricted to the uppermost water column. These data also imply that the water column experienced periods with vertical stratification, but without developing anoxic conditions in the deeper basin.

However, the effects, if any, these environmental changes had on the water chemistry and temperature evolution of the Black Sea are not well known until now. Here we present newly obtained Mg/Ca and Sr/Ca measurements on ostracod shells from the western Black Sea that, in combination with previously published $\delta^{18}O$ and $^{87}Sr/^{86}Sr$ data (on biogenic calcite), reveal abrupt changes in the water chemistry of the Black Sea in terms of its elemental composition in response to climatic and hydraulic changes between the LGM and the early Holocene. A particular focus lies in this case on the deglacial period and the reconnection of the Black Sea with the global ocean at ca. 9.3 ka cal BP. The combination of Sr/Ca and Mg/Ca ratios allows furthermore for semi-quantitative estimates on temperature variability in the deep Black Sea, which has not been assessed so far. On the basis of a newly defined age model (Kwiecien et al., 2008) we also re-evaluate the previously discussed influences of potential meltwater incursions into the Black Sea.

ENVIRONMENTAL SETTING

At present the water balance of the Black Sea is positive: freshwater sources (300 km^3yr^{-1} precipitation and 350 km^3yr^{-1} runoff, of which 190 km^3yr^{-1} is contributed by the Danube (Panin and Jipa, 2002) exceed the losses by evaporation (350 km^3yr^{-1}) (Swart, 1991). The remaining components of the freshwater budget are compensated by the net flux of warm, salty water through the Bosphorus from the Sea of Marmara (Öszoy and Ünlüata, 1997). The high amount of freshwater input to the Black Sea is also responsible for its particular hydrographic situation. A stable pycnocline between 100 and 200 m water depth separates less saline near-surface water (18‰ salinity) from the more saline (22.5‰) deep water of Mediterranean origin. Due to this stable stratification, anoxic conditions prevail below a depth of ca. 150 m. The stable isotope composition of Black Sea waters reflects the present hydrology with values around -2.8‰ in the upper 50 m and around -1.8‰ in depths >500 m (Öszoy et al., 2002). In areas with significant freshwater influence, like in our research area, $\delta^{18}O$ values are depleted (-10.5‰ near the Danube river mouth and -3‰ on the NW Black Sea shelf close to the coring sites (Öszoy et al., 2002).

The present-day values of Black Sea water for Sr/Ca (7.68 mmol/mol in 2000 m water depth, Aloisi et al., 2004) and Mg/Ca (4.55 mol/mol for the surface waters, 4.77 mol/mol in 2000 m water depth

(Manheim and Chan, 1974) approach typical marine ratios (Sr/Ca: 8.74 mmol/mol; Mg/Ca: 5.16 mmol/mol (Chester, 1990), but the freshwater influence on the upper water column is still expressed in the slightly reduced Mg/Ca ratio of surface water relative to the deep water. In areas of dominant freshwater input, like the Danube Delta, the Mg/Ca ratio can be as low as 0.612 mol/mol (Manheim and Chan, 1974). The average $^{87}Sr/^{86}Sr$ ratio of molluscs shells from core top samples from the Black Sea (0.709133±0.000015, Major et al., 2006) is close to that measured on modern shells from the fully marine Aegean Sea (0.709157±0.00001) but still indicates a slight influence of Sr brought in by rivers (Major et al., 2006).

MATERIAL AND METHODS

This study is based on five gravity cores from the NW Black Sea, retrieved during RV Meteor cruise M51-4 (Jørgensen, 2003). They are located on a depth transect ranging from the upper (465 m water depth) to the lower continental slope (1977 m) (Fig. 4.1, Tab. 4.1). The cores from the slope contain the classical sequence of the marine units I (finely laminated coccolith ooze) and II (sapropelic sediments) in the top ca. 45 cm, and the lacustrine unit III (homogeneous to (mostly) mm-scale laminated muddy clay) in the lower part of the cores (Bahr et al., 2005).

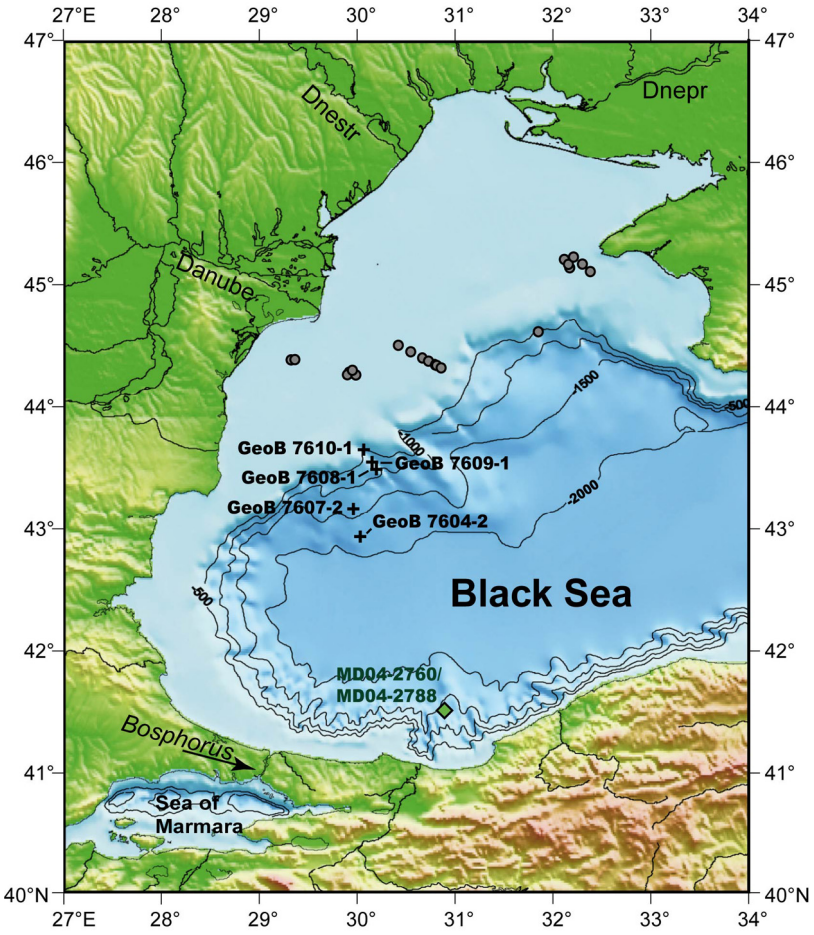

Figure 4.1: Location of gravity/piston cores retrieved during RV Meteor cruise M51-4 in 2001 (crosses) and onboard RV Marion Dufresne during the ASSEMBLAGE I cruise in 2004 (diamonds) and those published in Major et al. (2006) (circles).

All GeoB cores listed in Tab. 4.1 were analysed in 1 cm resolution with a CORTEX X-ray fluorescence (XRF) scanner measuring the K, Ca, Ti, Mn, Fe, Cu and Sr contents in counts per second, while core MD04-2760 has been scanned with an AVAATECH-Scanner giving XRF-intensities in total counts; both scanners are located at the University of Bremen (Jansen et al., 1998; Röhl and Abrams, 2000, Richter et al., 2006). Stable isotope analyses ($\delta^{18}O$ and $\delta^{13}C$) were performed on 5-8 shells of juvenile ostracods belonging to the genus *Candona* spp. at the University of Bremen (for further details see Bahr et al., 2006).

Core	Latitude N	Longitude E	Water depth (m)	Core length (m)
GeoB 7604-2	42°56.2'	30°01.9'	1977	5.92
GeoB 7607-2	43°09.7'	29°57.7'	1562	6.36
GeoB 7608-1	43°29.2'	30°11.8'	1202	6.85
GeoB 7609-1	43°32.8'	30°09.2'	941	6.55
GeoB 7610-1	43°38.9'	30°04.1'	465	8.80
MD04-2760	41°31.7'	30°53.1'	1226	41.94
MD04-2788	41°31.7'	30°53.0'	1224	6.00

Table 4.1: Location and length of the investigated gravity/piston cores.

Total carbon (TC) was measured on freeze-dried samples using a LECO SC-444 instrument. Total inorganic carbon (TIC) was determined using a CM 5012 CO_2 coulometer with a CM5140 acidification device. TOC contents were calculated from the difference between TC and TIC. These measurements were done at the ICBM, Oldenburg, Germany.

For Mg/Ca and Sr/Ca analysis 3 to 10 ostracod valves of the species *Candona schweyeri* (adult) were picked from the 150 µm fraction. Each valve was cleaned individually in a faunal slide under the microscope with a fine brush and a few drops of deionised water. The cleaning procedure was repeated three times, after each cleaning the samples were immediately dried to avoid corrosion of the shell by deionized water. Valves were subsequently dissolved in 2% HNO_3 and measured with a Finnigan Element2 ICP-MS at the Woods Hole Oceanographic Institution (WHOI). The average analytical precision from replicates was 2.9% for Mg/Ca and 1.7% for Sr/Ca.

All data are available under the name of the corresponding author through the PANGAEA server (www.pangaea.de/PangaVista).

Age model

An age model was developed for core GeoB 7608-1 based on 6 AMS ^{14}C dates calibrated to calendar years BP (1950) with the program Calib Rev 5.0.1 (Stuiver and Reimer, 1993) using the INTCAL04 calibration curve (Reimer et al., 2004) (Tab. 4.2). In the previously used stratigraphy for GeoB 7608-1 (Bahr et al., 2005, 2006) a constant 1000 years reservoir age correction throughout the record was assumed, however, new findings made modifications of this earlier stratigraphy necessary.

Sample	Core depth (cm)	^{14}C age (yr BP)	Calendar age (yr BP)	Age, tuned to MD04-2788/2760 (yr BP)	Material /source
	31		7995		Unit II/III boundary [*Lamy et al.*, 2006]
KIA 21464	34	7735 ± 50	8116 ± 100[a]		ostracods
KIA 21463	88	11,460 ± 70	12,394 ± 280[b]		gastropod
KIA 21461	158	13,350 ± 80	14,240 ± 345[b]		gastropod
KIA 21460[#§]	243	17,080 +150/-140	18,899 ± 230[c]	14,683	ostracods and bivalves
KIA 21866[§]	436	16,360 ± 70	18,257 ± 305[c]	15,795	ostracods and bivalves
KIA 21459[§]	596	20,140 +180/-170	22,197 ± 425[c]	22,567	gastropod
KIA 21457[§]	652	24,970 +310/-300	28,488 ± 485[c]	24,928	mixed mollusc shells

[a]calculated with 415 yrs reservoir correction
[b]calculated with 1000 yrs reservoir correction
[c]calculated with 1450 yrs reservoir correction (*Kwiecien et al.*, 2008)
[#]sample was discarded because of its high amount of broken and probably reworked shells (*Bahr et al.*, 2006)
[§]dates were not used because of the adoption of the stratigraphy from MD04-2760 (*Kwiecien et al.*, 2008) (see also Fig. 2)

Table 4.2: Age control points for GeoB 7608-1.

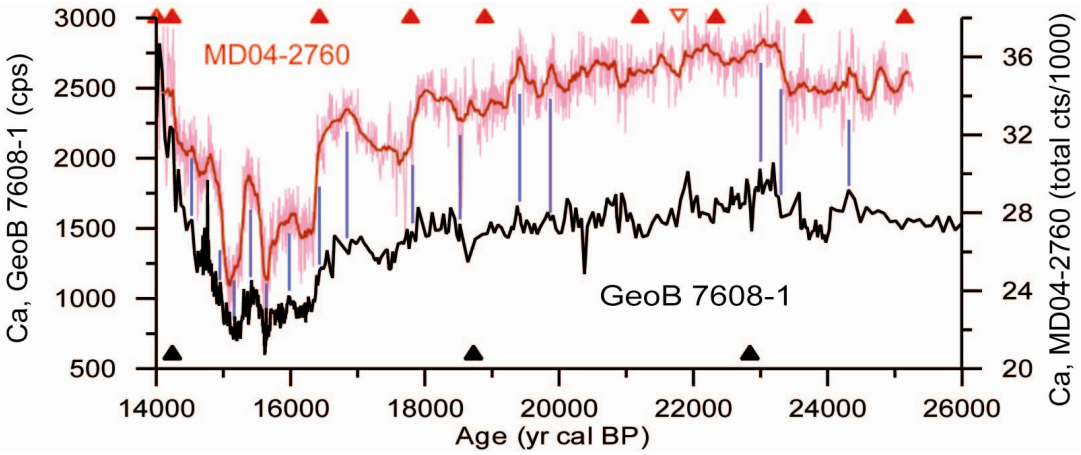

Figure 4.2: The glacial part of core GeoB 7608-1 tuned to MD04-2760 using XRF-scanning data (Ca is shown in counts per second for GeoB 7608-1 and total counts for MD04-2760 with a 21-point running average). The red triangles indicate the age control points for MD04-2760 (Kwiecien et al., 2008), the Y-2 tephra is indicated by a non-filled triangle; the black triangles are the radiocarbon dates made on GeoB 7608-1. Blue lines visualize tie-points between both Ca-records (for optical reasons not all tie-points were shown for the interval 16 to 14 ka cal BP).

The first modification is based on the discovery of the Y-2 tephra from the Cape Riva eruption of the Santorini volcano 21,780±510 cal yr BP (Eriksen et al., 1990; Pilcher and Friedrich, 1976) in core MD04-2760 from the south-western Black Sea (Fig. 4.1). Radiocarbon dated samples of ostracod shells bracketing the Y-2 tephra in core MD04-2760 imply that the reservoir age of the glacial Black Sea was approximately 1450 yrs (Kwiecien et al., 2008). Based on a comparison of MD04-2760 with the Greenland ice core records a drop of the reservoir age to 900-1000 yrs seems to occur

before the onset of the Bølling (Kwiecien et al., 2008). The sedimentary sequences of cores GeoB 7608-1 and MD04-2760 can be correlated very well using the XRF-scanning data (Kwiecien et al., 2008) (Ca-abundances are shown in Fig. 4.2; the correlation was performed visually also using K and Ti/Ca curves with the program ICC by Norbert Nowaczyk, GFZ-Potsdam).

Based on this correlation it was argued that the radiocarbon dates from 436 cm (18.257±305 yr cal BP) and 652 cm (28.488±485 cal ka BP) were much too old, perhaps by contamination with reworked shells (Kwiecien et al., 2008), while the dating from 596 cm (22.197±425 cal ka BP) lies within the error estimates, possibly a result of the better dating material (a whole gastropod shell). Following this assumption and considering the higher number of radiocarbon dates we decided to tune the pre-Bølling part (i.e. the part older than 14.240 cal ka BP; see also Tab. 4.2) of GeoB 7608-1 to MD04-2760, also discarding the dating from 596 cm for reasons of consistency.

This has important consequences for the chronological position of the reddish clay layers interpreted to be deposited during the inflow of meltwater from the Fennoscandian Ice Sheet (FIS). Based on our new stratigraphy, the deposition of the clay layers started significantly later at 16.5 and lasted until 14.8 ka cal BP (compared to 18 and 15.5 cal ka BP [Bahr et al., 2005]; see also Fig. 4.4i). The second modification affects the age of the Unit II/III boundary that was previously positioned at ca. 7.5 cal ka BP (Jones and Gagnon, 1994), using organic matter and inorganic carbon as dating material. However, new datings on a core from the south-western Black Sea (Lamy et al., 2006), performed on planktonic larval shells of the bivalve *Mytilus galloprovinciales*, suggest that this boundary is ca. 8.0 ka old. This is significantly older than the calibrated age of 7610± 40 yr BP (calculated using the 1000 year reservoir age correction) from core GeoB 7608-1 (7735±50 ^{14}C yr BP) taken just below the Unit II/Unit III boundary at 34 cm. This discrepancy might be resolved if a lower reservoir age correction is applied to this date: an extreme estimate is 415 yrs, the reservoir age calculated for the marine Black Sea (Siani et al., 2001), which would lead to a corrected age of 8116±100 yr BP, close to the ~8000 yrs for the Unit II/III boundary of Lamy et al. (2006). This is more reasonable because the entrance of marine Mediterranean water around 9.3 ka cal BP (see section: Reconnection with the Mediterranean Sea) should have lowered the reservoir age of the Black Sea. The revised age model of GeoB 7608-1 was transferred to the other cores from the slope transect through detailed correlations using XRF and colour scan data following the procedure described in (Bahr et al., 2005).

In addition to the reservoir age changing with time, water masses from shallow depth (i.e. above ca. 400 m) seem to diverge with respect to their reservoir age from those in greater depths with the beginning of the Bølling warm period (Kwiecien et al., 2008). This differs from earlier assumptions where an age offset between shallow and deep water has been proposed also for the pre-Bølling (Bahr et al., 2005). Further details on the potential mechanisms for the reservoir age evolution in the Black Sea are thoroughly discussed in Kwiecien et al. (2008).

Factors influencing the Sr/Ca and Mg/Ca ratios in ostracod shells

Since the pioneering work in the early 1980s (Chivas et al., 1983), many studies were performed to decipher the processes governing the uptake of trace and minor elements (especially Sr and Mg) into ostracod shells and to establish Mg/Ca and Sr/Ca records obtained on ostracod shells as powerful tools for reconstructing paleoenvironmental changes. Despite the steady increase in data from field and laboratory experiments, these studies had different conclusions regarding the influence of parameters like the host water's Sr/Ca and Mg/Ca ratios, Mg and Sr concentrations, temperature, pH or salinity on the ostracod shell chemistry. Chivas et al. (1985, 1986a, 1986b) first determined the

dependence of the Mg/Ca and Sr/Ca of the ostracode shell (in the following termed Mg/Ca_o and Sr/Ca_o) on the Mg/Ca and Sr/Ca ratio of the host waters (Mg/Ca_w and Sr/Ca_w). The uptake of Sr and Mg relative to Ca into the ostracod shell is controlled by the partition coefficient $D(M)_o$ (M stands for either Sr or Mg) that is defined as

$$D(M)_o=(M/Ca_o)/(M/Ca_w)$$

These authors also stated that $D(M)_o$ is the same for species belonging to the same genus and for closely related genera. This view was later contested claiming that the effect of Mg/Ca_w on Mg/Ca_o is minor and temperature is the controlling factor on Mg/Ca_o (Palacios-Fest and Dettman, 2001). This point was also addressed by a study incorporating different species belonging to the genus *Candona* (Wansard et al., 1998) which showed an important influence of Mg/Ca_w on $D(Mg)_o$: $D(Mg)_o$ is nearly constant above a Mg/Ca_w of ca. 0.1 mol/mol but increases exponentially below this threshold (Fig. 4.3). This behaviour of $D(Mg)_o$ especially affects the very low (<0.1 mol/mol) Mg/Ca_w values estimated by the measured Mg/Ca_o ratios in the glacial part of our records (see section: Glacial conditions).

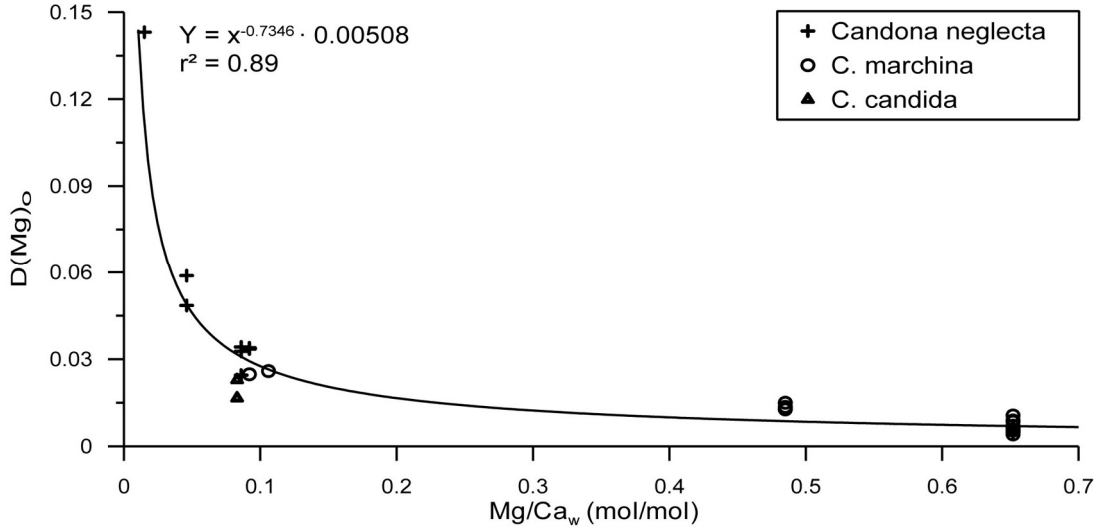

Figure 4.3: Relationship of the partition coefficient $D(Mg)_o$ of *Candona neglecta*, *C. marchina* and *C. candida* to the host water Mg/Ca_w (after Wansard et al., 1998). The best fit (r^2=0.89) is represented by the function $D(Mg)_o = (Mg/Ca_w)^{-0.73} \cdot 0.0051$.

The temperature dependence of Mg/Ca_o (with probable exceptions [Wansard et al., 1999]) has so far predominantly been used for temperature reconstructions in the marine realm (e.g. Dwyer et al., 1995; Ingram, 1998). Reconstructions in mesohaline or freshwater conditions were performed in fewer cases (Wansard, 1996; Wansard and Roca, 1997; Palacios-Fest et al., 2002; Cronin et al., 2003). Temperature reconstructions on lakes are complicated by the variability of Mg/Ca_w due to evaporation and the precipitation of different mineral phases while Mg/Ca_w in the ocean remains more or less constant on longer timescales. Engstrom and Nelson (1991) did a temperature calibration for the species *Candona rawsoni* and obtained the relation:
$T = (Mg/Ca_o - 0.004) / (Mg/Ca_w \cdot 0.0000968)$. Although later studies suggested that *C. rawsoni* might not belong to the genus *Candona*, one can assume that the temperature sensitivity of Candonids lies in the range of that observed within other genera, i.e. a rise of 1 mmol/mol Mg/Ca equals a temperature increase of 1-2 °C (Wansard, 1996; De Deckker et al., 1999; Müller, 1999;

Palacios-Fest and Dettman, 2001; Cronin et al., 2003). There were also suggestions that $D(Sr_o)$ is dependent on temperature (De Deckker et al., 1999; Majoran et al., 1999; Müller, 1999). Müller (1999) proposed that organisms building shells with a higher Sr/Ca_o ratio are generally showing a higher sensitivity of $D(Sr)_o$ towards temperature, while the temperature-dependence of Mg/Ca_o decreases simultaneously. This might help to explain why for some ostracods (e.g. *Cyprideis australensis* [De Deckker et al., 1999]) a temperature-dependent partitioning of strontium was described, but for others (e.g. *Candona* [Wansard et al., 1998]) not.

Even though there are apparent uncertainties about the interspecific or even intraspecific variability of factors controlling the Mg and Sr uptake, it seems appropriate to apply the results obtained by Wansard et al. (1998) to our record, i.e. $D(Mg)_o$ is dependent on Mg/Ca_w and temperature, whereas Sr/Ca_o only depends on Sr/Ca_w. Wansard et al.'s study is based on a broad spectrum of *Candona* species that all yielded consistent results (Wansard et al., 1998). Another important point is that the hydrological conditions in the ancient Black Sea (low salinity; low Mg/Ca_w and Sr/Ca_w, see section: Glacial conditions) are similar to the environments investigated by Wansard et al. (1998).

RESULTS

The glacial period until ~16.5 ka cal BP ('G' in Fig. 4.4) exhibits only low variability in all records with low TOC values around 0.5 wt% (with two probable outliers). The first distinct change occurred between 16.5 and 14.8 cal ka BP where consecutive drops in $\delta^{18}O$ are recorded. This period is marked by a series of reddish-brown clay layers ('RL', Fig. 4.4, 4.5) in the western Black Sea, characterised by increased concentrations of terrigenous elements (Bahr et al., 2005) and anomalous high illite and kaolinite contents (Major et al., 2002). During this interval, an increase in $^{87}Sr/^{86}Sr$ from LGM-values around 0.70870 to 0.70910 is recorded. Note, that the $^{87}Sr/^{86}Sr$ record by Major et al. (2006) was tuned to the new stratigraphy using the red layer interval and the Ca-peaks as an independent time marker (Fig. 4.4e).

Figure 4.4: Comparison of the (a) Greenland NGRIP (black, GICC05 chronology, Rasmussen et al., 2006; Vinter et al., 2006; Andersen et al., 2006)) and GISP2 (red, Grootes and Stuiver, 1997) ice core records with (b) stable oxygen isotopes of GeoB 7608-1 ($\delta^{18}O$) (Bahr et al., 2006), (c) Mg/Ca (on logarithmic scale) and (d) Sr/Ca of Candona schweyeri from core GeoB 7608-1; (e) compilation of $^{87}Sr/^{86}Sr$ measurements on ostracod and bivalve shells from 18 different cores in the western Black Sea continental slope and shelf (Major et al., 2006); the grey squares are the values plotted using the stratigraphy from Major et al. (2006), black squares those tuned to the present record; (f) salinity record from the Sea of Marmara compared to modern (Sperling et al., 2003); (g) global sea level record from Tahiti (Bard et al., 1996) and the present sill depth of the Bosphorus; (h) total organic carbon (TOC) of GeoB 7608-1 (please note the break in the scale of the axis); (i) XRF Ti/Ca of GeoB 7608-1 in the present stratigraphy (black line) and Ti/Ca applying the stratigraphy used in Bahr et al. (2006) (grey line) and (k) XRF Ca record from GeoB 7608-1 (Bahr et al., 2005). Indicated are the different lithological sections: 'S' – sapropel; 'C1'-'C3' – periods of authigenic carbonate precipitation (blue bars), interrupted by dominant clastic sedimentation during 'T' (transition, start of marine inflow; S, C1 and T are combined shown as a green bar) and 'YD' (Younger Dryas, yellow bar); 'I' – interval between C3 and 'RL' – red clay layers (red bar); 'G' – glacial part prior to ~16.5 ka BP. Dashed lines in (b) indicate the hypothetical $\delta^{18}O$-evolution of Black Sea water for a maximum flux (5475 km^3/yr), a moderate flux (500 km^3/yr) and a small inflow (80 km^3/yr) of Mediterranean/Sea of Marmara water through the Bosphorus into the Black Sea. HE1 – Heinrich Event 1, note that the timing of HE1 was chosen according to Rinterknecht et al. (2006), see also discussion (section: Glacial conditions).

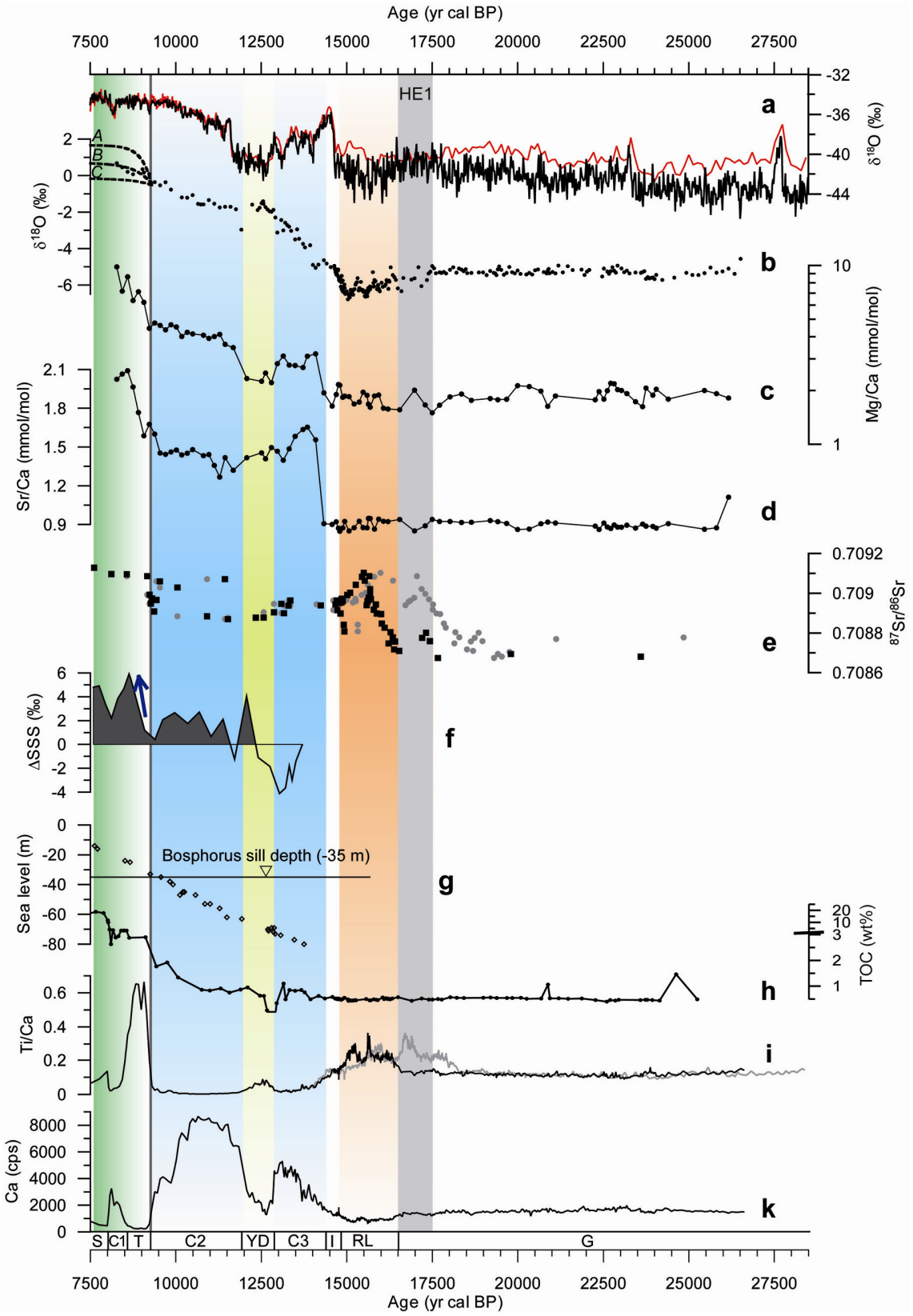
Age (yr cal BP)
7500
10000
12500
15000
17500
20000
22500
25000
27500
HE1
a
b
c
d
e
f
g
h
i
k
A
B
C
δ18O (‰)
Mg/Ca (mmol/mol)
Sr/Ca (mmol/mol)
87Sr/86Sr
ΔSSS (‰)
Sea level (m)
Bosphorus sill depth (-35 m)
TOC (wt%)
Ti/Ca
Ca (cps)
S
C1
T
C2
YD
C3
I
RL
G

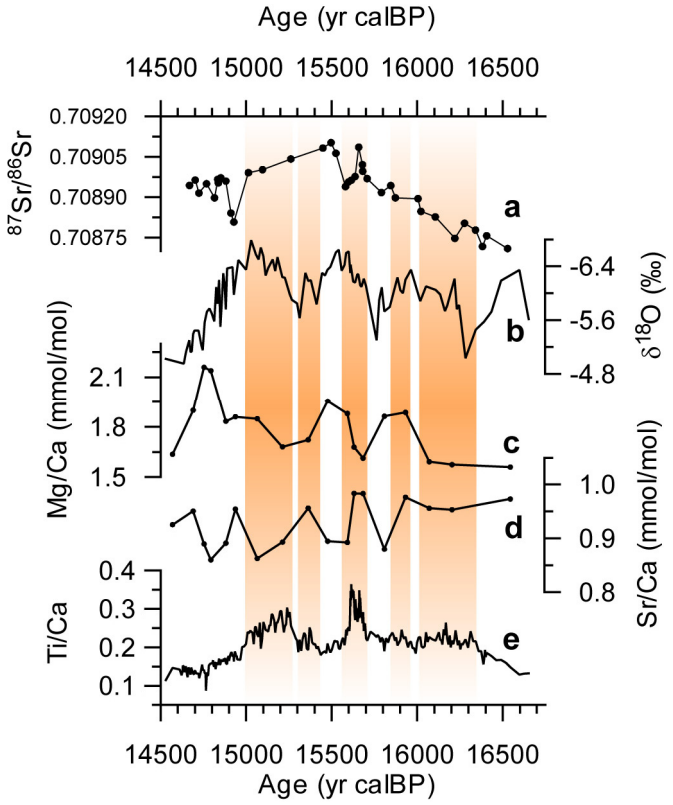

Figure 4.5: Focus on the period of red clay layer deposition: (a) $^{87}Sr/^{86}Sr$ measurements on ostracods and bivalves from (Major et al., 2006); (b) $\delta^{18}O$ (Bahr et al., 2006) of *Candona spp.*, (c) Mg/Ca and (d) Sr/Ca of *Candona schweyeri* from GeoB 7608-1; (e) Ti/Ca ratio from GeoB 7608-1 (Bahr et al., 2005). Red bars indicate periods of maximum terrigenous input (high Ti/Ca ratio).

After 14.8 ka BP $^{87}Sr/^{86}Sr$ values drop to ca. 0.70896, while $\delta^{18}O$ has a trend towards higher values, only interrupted by a relatively constant interval during the Younger Dryas ('YD'). The overall $\delta^{18}O$-shift totals ca. +7.2‰ (from ca. -6.5‰ at 14.8 cal ka BP to +0.7‰ at 8.0 cal ka BP).

Mg/Ca and Sr/Ca both increase dramatically at 14.5 cal ka BP: Mg/Ca from 1.6 to 3.2 mmol/mol; Sr/Ca from 0.9 initially to 1.65 mmol/mol, later decreasing to 1.45 mmol/mol. The change in the Mg/Ca and Sr/Ca ratios at 14.5 cal ka BP coincides with the precipitation of calcite which lasts from 14.5 to 7.5 cal ka BP (Ca-peaks 'C1'-'C3' in Fig. 4.4k), interrupted by two periods of dominant clastic deposition during the YD and around 8.5 ka BP ('YD' and 'T', Fig. 4.4). $^{87}Sr/^{86}Sr$ values remain constant until ca. 12.8 cal ka BP where it drops to 0.70888. At ca. 9.3 cal ka BP (beginning of stage 'T') Mg/Ca and Sr/Ca ratios and strontium isotopes show a final increase to maximum values. With the onset of calcite peak 'C3' the TOC content starts to increase steadily to reach values of up to 1.1 wt%, drops at the beginning of the YD interval to 0.34 wt% and then increases again to around 3 wt% at stage 'T'. Afterwards it rises sharply to a maximum of 22.3 wt% in the sapropel.

Although both, Mg/Ca and Sr/Ca, seem to covary along the record at the first glance, they do show some distinct differences, e.g. the low in Mg/Ca during the YD that is not mirrored in Sr/Ca, and the constant Sr/Ca level in the early Holocene is accompanied by a slight but steady increase in Mg/Ca.

As shown in Fig. 4.6, most of the values taken from the cores along the slope transect are in the same range. Exceptions are the measurements taken from the shallow core GeoB 7610-1. The Mg/Ca values of core GeoB 7610-1 are constantly higher until 10.5 ka BP, while Sr/Ca slightly increases between 12.5 and 10 cal ka BP. Mg/Ca measurements obtained on GeoB 7604-2 are also higher than those of the shallower cores during the YD.

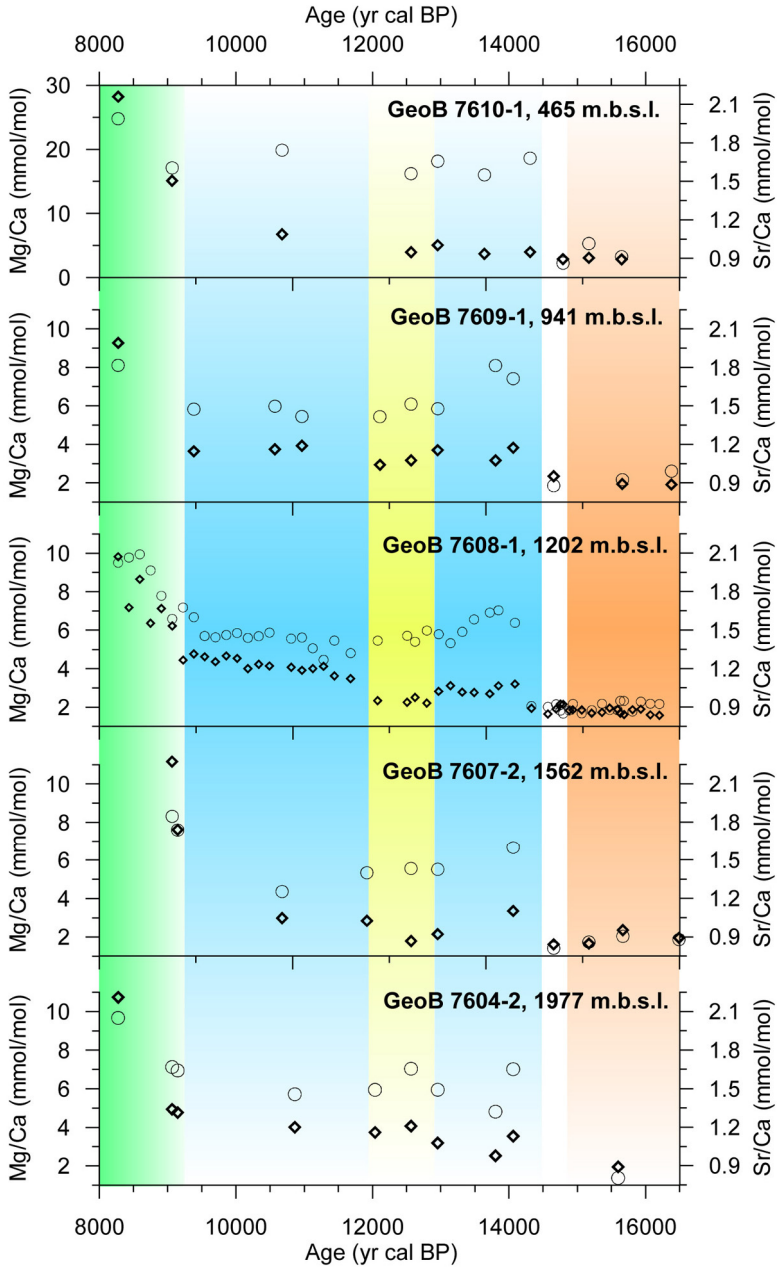

Figure 4.6: Comparison of Mg/Ca (diamonds) and Sr/Ca (circles) data of *Candona schweyeri* from different depths in the northwestern Black Sea. Core name and water depth in meters below sea level (m.b.s.l.) are given. Note that the scale for Mg/Ca of GeoB 7610-1 is different to the other. Coloured bars mark the red clay layer interval (red), Ca-peaks (blue), Younger Dryas (yellow) and inflow of Mediterranean waters (green).

INTERPRETATION AND DISCUSSION

Although $\delta^{18}O$ is a widely used parameter in paleo-studies, results and interpretations based on this proxy alone can be ambiguous, because it depends on numerous factors such as water temperature, evaporation, isotopic composition of run-off, and precipitation. With the additional use of Mg/Ca and Sr/Ca it is possible to further constrain the factors influencing $\delta^{18}O$, since Mg/Ca is temperature dependent and both Mg/Ca and Sr/Ca give insight into changes of the water chemistry. A major focus of our study is the timing of the reconnection of the Black Sea with the Mediterranean Sea via the Sea of Marmara. In this context, $^{87}Sr/^{86}Sr$ ratios give valuable results, because ocean water and fresh or slightly brackish lake water have distinctly different isotopic composition (see also Major et al. [2006]). Since the $\delta^{18}O$ and $^{87}Sr/^{86}Sr$ records have been published and discussed elsewhere ($^{87}Sr/^{86}Sr$ in Major et al. [2006]; $\delta^{18}O$ in Bahr et al. [2006]) we focus on the Mg/Ca and Sr/Ca records.

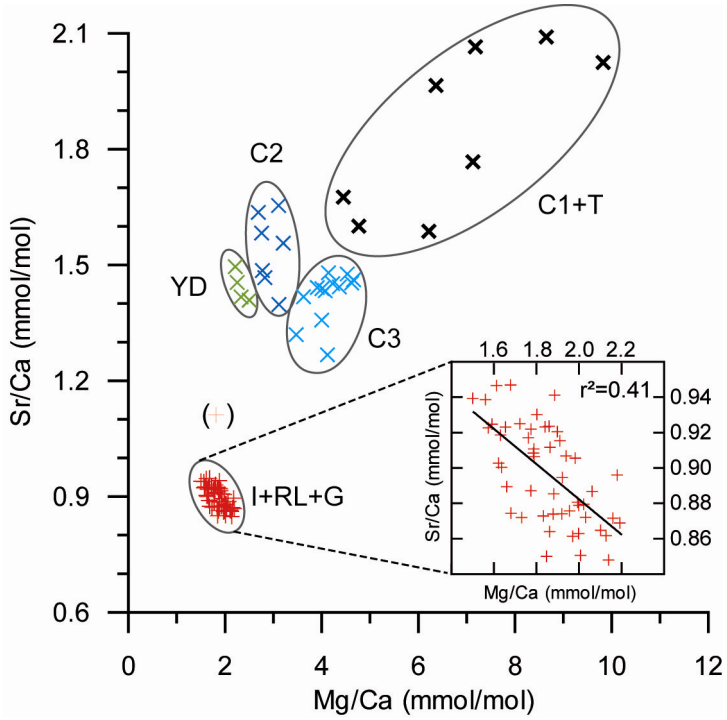

Fig. 4.7: Correlation of Mg/Ca and Sr/Ca measurements on ostracods from core GeoB 7608-1. The small insert shows an augmentation of this anticorrelation for the period before 14.5 ka BP, with a potential linear fit (r^2=0.41) of Sr/Ca = -0.100 · Mg/Ca + 1.081. Circles denote the clustering of the measurements into groups that follow the lithological sections presented in Fig. 4.4. The measurement in brackets represents the oldest sample from the glacial ('G') part, plotting outside the 'I+RL+G'-group.

Mg/Ca and Sr/Ca values measured on sediment core GeoB 7608-1 are generally positively correlated (Fig. 4.4, 4.7) and therefore suggest a common controlling factor. However, a closer inspection shows that the Mg/Ca_o and Sr/Ca_o values group into well-defined clusters (Fig. 4.7) that are related to the stratigraphic subdivision presented in Fig. 4.4. Hence, we must assume that in each of these periods different environmental conditions affected the Mg/Ca and Sr/Ca ratios found in the ostracod shells. In the following discussion we will first examine the glacial conditions until 14.5 ka BP, then the periods of the Late Glacial to early Holocene, and finally we focus on the inflow of Mediterranean waters around 9.3 cal ka BP.

Glacial conditions

Sr/Ca and Mg/Ca are constantly on a very low level until 14.5 cal ka BP (Fig. 4.4, cluster 'I+RL+G' in Fig. 4.7), implying stable environmental and hydrologic conditions throughout this time. Low Sr/Ca, Mg/Ca, $\delta^{18}O$ and $^{87}Sr/^{86}Sr$ values generally indicate fresh or slightly brackish conditions as also suggested by faunal investigations (Mudie et al., 2002a). A Sr/Ca_w ratio of 2.70 ± 0.08 mmol/mol for the glacial Black Sea water could be calculated using the obtained Sr/Ca_o values and the published $D(Sr)_o$ of 0.332 for *Candona neglecta* and *C. marchina* (Wansard et al., 1998). 2.70 mmol/mol is higher than the average Sr/Ca_w of 2.20 mmol/mol for river water entering the Black Sea (Major et al., 2006), indicating that either the partition coefficient of *Candona schweyeri* is higher than assumed for other Candonids (the $D(Sr)_o$ of *C. schweyeri* would be 0.408 in this case) or the Sr/Ca_w ratio of the glacial water was enriched relative to the calculated mean river input. Interestingly, Major et al. (2006) also calculated an unusually high D(Sr) for their Sr/Ca measurements on bivalve shells in the same time period, which might be coincidental, but could also indicate that Sr/Ca_w was higher than expected, fitting to assumptions that the glacial 'Black Lake' was not fully fresh (Mudie et al., 2002a) but enriched relative to the river composition because of evaporation.

Using the range of the $D(Mg)_o$ shown in Fig. 4.3 (ca. 0.015 to 0.15) and a Mg/Ca_o of 0.002 mol/mol yields low Mg/Ca_w values between 0.013 to 0.13 mol/mol. This indicates on one hand side freshwater conditions, but also strengthens the point that the variations in Mg/Ca_o are effected by the strong exponential gradient in $D(Mg)_o$ for Mg/Ca_w values <0.1 mol/mol (Fig. 4.3, see also section: Factors influencing the Sr/Ca and Mg/Ca ratios in ostracod shells).

The entrance of isotopically depleted water between 16.5 and 14.8 cal ka BP causes a drop in $\delta^{18}O$ (Bahr et al., 2006) ('RL' in Fig. 4.4). The observed high $^{87}Sr/^{86}Sr$ values (Major et al., 2006) and the abundance of illite and kaolinite typical for a northern sediment source (Major et al., 2002) indicate that an otherwise unimportant or inactive region contributed to a considerable extent to the sediment and water input during this time. As one of the potential sources for the incoming water the Caspian Sea has been proposed (e.g. Major et al., 2002; Ryan et al., 2003; Bahr et al., 2005), which might have spilled into the Black Sea via the Manych Depression during periods of high lake level. The timing of the highest lake level in the Caspian Sea during the late Pleistocene is subject of debate, but the present estimates suggest that it occurred either earlier than the red layer deposition at ~18 cal ka BP (Kroonenberg et al., 1997; Svitoch, 1999) or later around 12 cal ka BP (Svitoch, 2007). Thus, a Caspian source cannot be excluded, but remains speculative (see also Major et al., 2006). As an alternative Bahr et al. (2006) proposed that meltwater from the FIS might have caused the red layer deposition. However, this is unlikely since recent studies showed that the meltwater discharge was directed towards the Baltic Sea or farther west to the Bay of Biscay (Ménot et al., 2006) and the Arctic Ocean in the north (Demidov et al., 2006; Ménot et al., 2006). Interestingly it has been noted that after Heinrich Event 1 and before the warming of the Bølling, a re-advance of alpine glaciers (Gschnitz stadial) and of the FIS (Pomeranian moraine) was observed, contemporaneous to the deposition of the red layers. The paleoclimatic interpretations are contradictory, in the case of the Gschnitz stadial it was argued that extremely cold and arid conditions were prevailing (Ivy-Ochs et al., 2006), while Rinterknecht et al. (2006) propose that the extremely arid conditions were restricted to Heinrich Event 1 (HE1) dated to ca. 17.5-16.5 cal ka BP in the continental chronology used by Rinterknecht et al. (2006). Note that HE1 *sensu stricto* is related to the occurrence of detrital dolomitic carbonate grains originated from the Laurentide Ice Sheet, occurring ca. 16-15.5 cal ka BP in the eastern Atlantic (Knutz et al., 2007), but with several HE-precursors of ice-rafted debris originating from the European continent (British Ice Sheet and FIS) starting at ca. 18 cal ka BP (Knutz et al., 2007). Rinterknecht et al. (2006) explain the observed advance of the southern margin

of the Scandinavian Ice Sheet shortly before the Bølling with a slightly increased precipitation. A more positive hydrological balance might therefore account for an higher inflow of isotopically depleted water from the northern drainage area (via Dnestr and Dnepr) where the frozen soils increased the surface run-off. A dominant contribution from the alpine region is unlikely since the distinct signals of the XRF-element composition, clay mineralogy (Major et al., 2002) and $^{87}Sr/^{86}Sr$ ratio of ostracod shells (Major et al., 2006) point to a water/sediment source with characteristics considerably different from the water/sediment supplied by the Danube, which is otherwise exerting the dominant influence on the study sites in the NW Black Sea.

In contrast to $^{87}Sr/^{86}Sr$, both Mg/Ca and Sr/Ca, remain on the same level as before (Fig. 4.7), which indicates that the incoming water had Mg/Ca and Sr/Ca ratios relatively similar to that of the glacial Black Sea. The decrease of the strontium isotope ratio after the water inflow points to an outflow of the Black Sea into the Sea of Marmara: the ^{87}Sr-rich lake water would leave the Black Sea to be replaced by more ^{87}Sr depleted river water until the water balance turned negative and the Black Sea lake level dropped below the Bosphorus sill depth.

Although there is no significant correlation between the Mg/Ca and Sr/Ca records compared to the $\delta^{18}O$ or the XRF Ti/Ca ratio, the Mg/Ca and Sr/Ca ratios are to some extent inversely correlated during the glacial, especially during the red layer period (Fig. 4.5 and insert in Fig. 4.7). One possible reason could be that a slight warming (increased Mg/Ca_o) was accompanied by the input of slightly Sr/Ca-depleted water from the northern drainage area (Fig. 4.5). Compared to the full range of the climatic fluctuations one can expect that the amplitude of the temperature variability in the deeper part of the Black Sea should be reduced. If we apply the temperature estimates discussed in section 5 to the Mg/Ca ratio, a variability of ca. 0.5 mmol/mol Mg/Ca_o during the red layer period might be translated into temperature fluctuations of ca. 0.5 to 1°C in the Black Sea at 1200 m depth, however, given the sensitivity of this method and the probable influence of other factors on the Mg/Ca_o this has to be viewed with caution.

Conditions after 14.5 cal ka BP

Both Sr/Ca and Mg/Ca records from GeoB 7608-1 show a drastic shift at 14.5 ka BP, with the onset of the B/A warm period (Fig. 4.4). Since Sr/Ca and Mg/Ca are sensitive to changes in the water chemistry, it is reasonable to assume a relationship to the contemporaneous onset of calcite precipitation in the surface water, mirrored e.g. in the Ca-record (Fig. 4.4). The calcite precipitation is most likely caused by the assimilation of CO_2 in the surface water through increased phytoplankton activity during favourable climatic conditions, as corroborated by increasing TOC values with the onset of the B/A, indicating enhanced primary productivity (Fig. 4.4h). The uptake of Sr and Mg relative to Ca into the precipitated calcite (organic and inorganic) is controlled by the partition coefficient $D(M)_c$ that is defined similarly to the partition coefficient that governs the uptake of Sr and Mg into the ostracod shell:

$D(M)_c=(M/Ca_c)/(M/Ca_w)$ (Morse and Bender, 1990)

where M is either Sr or Mg.

Numerous attempts to quantify $D(Sr)_c$ and $D(Mg)_c$ for inorganic calcite (e.g. Howson et al., 1987; Morse and Bender, 1990; Burton and Walter, 1991) have shown that especially $D(Mg)_c$ is governed by a complex interaction of several parameters, including temperature, Mg/Ca_w, the Mg-concentration of the ambient water, P_{CO2}, and the calcite precipitation rate (e.g. Huang and Fairchild,

2001). For conditions that come close to the ancient Black Sea with low salinity and low to moderate alkalinity, the $D(Mg)_c$ for inorganic low-Mg calcite has been calculated to be in the range of 0.031 (for 25°C), 0.019 (15°C), and 0.012 (6.6°C) (Huang and Fairchild, 2001). The same study gives $D(Sr)_c$ values between 0.057-0.078. As these values are below 1.0, precipitating calcite would therefore be depleted in Sr and Mg relative to Ca and the upper water column would remain enriched in Sr and Mg. The data suggests that after an initial phase with overshooting Sr/Ca_w a chemical equilibrium was reached lasting until the final increase of Sr/Ca_w and Mg/Ca_w at 9.3 cal ka BP. Similar trends are also reported in the bivalve Sr/Ca record by Major et al. (2006) (Fig. 4.4e), with the difference that Sr/Ca almost returns to LGM values after the initial increase at 14.5 ka BP. However, there is a considerable scatter in this record, probably due to the fact that the sampled cores are located in different water depths (49–378 m) and the thermodynamically unstable aragonite of the bivalve shells might be more affected by diagenetic alterations than the low-Mg-calcite carapaces of the ostracod.

An important question is if the Mg/Ca_o-increase at 14.5 cal ka BP is caused exclusively by the described changes in the water chemistry, or if temperature changes add to the observed signal. The abrupt B/A warming is well documented from other regions (e.g. central Europe [Friedrich et al., 2001], Sea of Marmara [Mudie et al., 2002b]), and it seems therefore likely that the Black Sea experienced a significant warming as well. Decreasing temperatures certainly play a role for the Mg/Ca_o decrease during the YD, because if changes in the water chemistry would be responsible only, Mg/Ca_o and Sr/Ca_o would parallel each other. This is apparently not the case, except for GeoB 7604-2, which is discussed later. The observed drop of 1 mmol/mol in Mg/Ca_o in GeoB 7608-1 equals a temperature decrease of 1-2°C and explains the slightly increased $\delta^{18}O$ during the YD. If only governed by the change in the isotopic composition of the meteoric precipitation (Bahr et al., 2006), the oxygen isotope data would show a drop rather than an increase, because the $\delta^{18}O$ of meteoric almost reached its LGM-level during the YD (von Grafenstein et al., 1999a). With the evidence of a cooling during the YD, a preceding temperature increase during the B/A seems very reasonable. After the rapid temperature increase following the termination of the YD, a slight but continuous warming of the intermediate water column over the course of the early Holocene also explains the 1 mmol/mol increase of Mg/Ca_o at constant Sr/Ca_o values between 11.5 and 9.5 cal ka BP. The influence of temperature on Mg/Ca_o might therefore discriminate the periods ‘C3’, ‘YD’ and ‘C2’ into the different clusters shown in Fig. 4.7 (note that these clusters are mainly separated by different Mg/Ca_o values, while the respective Sr/Ca_o ratios are not distinctly different).

A possible stratification of the Black Sea water column during this time interval has already been discussed based on the observation of diverging ostracod-$\delta^{18}O$ trends (Bahr et al., 2006). The overall increase in $\delta^{18}O$ since ~15 cal ka BP is, at least for the B/A, mainly caused by increased $\delta^{18}O$ in the atmospheric precipitation and run-off. Nevertheless, $\delta^{18}O$ values are enriched in the deep core GeoB 7604-2 (1977 m water depth) between 14.5 and 9.3 cal ka BP, indicating that the deep water is separated to a certain extent from the intermediate water body (Bahr et al., 2006). There is, however, no significant difference in the Sr/Ca and Mg/Ca ratios for these depth levels (Fig. 4.6). This is most likely due to the different factors influencing the $\delta^{18}O$ on one side and the Mg/Ca and Sr/Ca records on the other side: the diverging trend in $\delta^{18}O$ is probably controlled by the adjustment of the deepwater to increased $\delta^{18}O$ of atmospheric precipitation (Bahr et al., 2006) that has no direct impact on the Mg/Ca or Sr/Ca record. An exception are Mg/Ca values from the deepest core GeoB 7604-2 that are higher than those in the intermediate cores during the YD, suggesting that the temperature drop during the YD did not affect the deep water. However, during the rest of the glacial/deglacial period temperatures seem to have been quite uniform in intermediate and deep water depths.

In the previous section, the $^{87}Sr/^{86}Sr$ decrease after the red layer period was linked to an outflow of Black Sea water combined with changes in the freshwater sources; the same argument could be raised for the drop in the strontium isotope ratio to almost LGM levels during the YD. A positive water balance and therefore a high lake level during the YD (in opposition to a low level during B/A and early Holocene) have also been proposed by other authors on the basis of sedimentological, geochemical, and biological evidence (e.g. Ryan et al., 2003, Major et al., 2006).

Reconnection with the Mediterranean Sea

The deglacial rise of the global sea level together with the present sill depth of the Bosphorus (-35 m) suggests that the inflow of Mediterranean water started between 9.5 and 9.0 ka BP (Fig. 4.4). It has been argued that the Bosphorus sill might have been at least 7 m shallower before the breaching of the barrier (Sperling et al., 2003), which would have postponed the inflow to about 8.7 ka BP. The final increase of Sr/Ca_o and Mg/Ca_o in our record started at 9.3 ka BP (Fig. 4.4, cluster 'C1+T' in Fig. 4.7) and is unquestionably related to the intrusion of Mediterranean water with high Sr/Ca_w and Mg/Ca_w ratios. This also fits to the abrupt $^{87}Sr/^{86}Sr$-increase (Major et al., 2006). An additional point that supports the inflow of saline Mediterranean water at ca. 9.0 ka BP are sea surface salinity (SSS) estimates from the Sea of Marmara (Sperling et al., 2003). This record shows a strong increase in SSS starting ~9 cal ka BP (Fig. 4.4) that suggests an enhanced passage of high-salinity Mediterranean water through the Sea of Marmara during the flooding of the Black Sea.

A similar question as for the 14.5 cal ka BP shift arises for the Sr/Ca and Mg/Ca increase after 9 cal ka BP: is there a temperature-component in the Mg/Ca_o signal beside the introduction of Mg and Sr-enriched Mediterranean water? The introduction of warm Mediterranean water could have increased the temperature in the deep Black Sea during this time, probably accompanied by turbulent mixing that led to a subsequent homogenisation of the water column, as indicated by the similar values found for Mg/Ca, Sr/Ca and $\delta^{18}O$ in cores from different depth (Fig. 4.6). An exception are the youngest two Mg/Ca measurement in 7610-1, which are likely to be influenced by secondary high-magnesium calcite precipitating from methane-rich fluids that caused the formation of carbonate concretions in the overlying sapropel. Any attempt to calculate the temperature-component in the final Mg/Ca_o increase is hindered by the exponential relation of $D(Mg)_o$ to Mg/Ca_w. Furthermore, it has to be taken into account, that the process of mixing of the two endmembers with different Mg/Ca_w and Sr/Ca_w ratios (Black Sea freshwater vs. Mediterranean marine water) is non-linear and the initial concentrations of Sr, Mg, and Ca in the water of the Black Sea are unknown (e.g. Anadón et al., 2002).

Despite these problems, the $\delta^{18}O$ record can be used to give a rough estimate on the volume flux during the reconnection with the Mediterranean Sea. A simple calculation with an isotopic balance model based on the program HIBAL (Benson and Paillet, 2002), modified to fit the conditions of the Black Sea (Bahr et al., 2006), was performed to calculate the hypothetical evolution of the $\delta^{18}O$ of the Black Sea water (Fig. 4.4b) during the inflow of Mediterranean water. $\delta^{18}O$ measurements obtained on the planktic foraminifera *Turborotalita quinqueloba* from the Sea of Marmara at 9.5 cal ka BP give an indication of the $\delta^{18}O$ of the inflowing water at that point of time. The values are around +1.2‰ (Sperling et al., 2003), or ~3.32‰ for our record, if the vital offset of +2.2‰ for Candoninae (von Grafenstein et al., 1999b) is taken into consideration. This yields an approximate $\delta^{18}O_{water}$ of +0.21‰ (calculated for 10°C water temperature) when using the formulas given in von Grafenstein et al. (2000). For the Black Sea water a $\delta^{18}O$ value of -4.3‰ (for 8°C) was estimated from the ostracod-$\delta^{18}O$ at 9.3 cal ka BP. The three scenarios shown in Fig. 4.4b include

a catastrophic inflow with the maximum possible flux thorough the Bosphorus (5475 km^3yr^{-1}, Myers et al., 2003), a reduced inflow of 500 km^3yr^{-1}, being equal to roughly the half of the combined amount of water (900 km^3yr^{-1}, Öszoy and Ünlüata, 1997) flowing presently in both directions through the Bosphorus, and a very low flux of 80 km^3yr^{-1}. Although the boundary conditions of the calculations are debatable, $\delta^{18}O$ is not in steady state at the point at 9.3 cal ka BP ($\delta^{18}O$ is not constant) and the simulation makes use of very simplifying assumptions (full mixing, constant inflow, steady water temperatures), it shows that a fast inflow would leave a clear signal in the $\delta^{18}O$ record (Fig. 4.4b). On the other hand, a very low inflow would not change the $\delta^{18}O$ values considerably. Since the best fit is reached with 500 km^3yr^{-1}, the volume flux of the inflow seems to be in between these extremes. Thus, if we expect a volume in the order of 40,000 km^3 to be filled (Myers et al., 2003) the flooding would last ca. 100 years, longer than the 2-3 years implied by the original 'catastrophic flooding' scenario (Ryan et al., 1997), but in geological time scales still fairly short.

CONCLUSIONS

Sr/Ca, Mg/Ca, $\delta^{18}O$ and $^{87}Sr/^{86}Sr$ records obtained on ostracod valves reveal major changes in the Black Sea hydrochemistry from the LGM to the early Holocene, driven by climatic and hydrological fluctuations. Prior to 16.5 cal ka BP, the records show little variability and thus constant environmental conditions. Between 16.5 and 14.8 cal ka BP, a series of water pulses presumably from a northern source led to the temporal depletion of the stable isotopic composition of the Black Sea water and to a significant, source-related increase in the $^{87}Sr/^{86}Sr$ ratio. At 14.5 cal ka BP major shifts in the water chemistry took place, related to the onset of the Bølling/Allerød warm period. While the $\delta^{18}O$ values are gradually increasing due to the influence of isotopically enriched atmospheric precipitation and run-off, the Sr/Ca and Mg/Ca ratios are abruptly shifting to higher values, caused by the precipitation of authigenic calcite during high phytoplankton productivity, and the associated increase in Mg and Sr concentrations in the water column. During the Younger Dryas cold period low Mg/Ca values indicate a drop of 1-2°C in the deep water, accompanied by an interruption of the calcite precipitation in the surface water due to high phytoplankton activity. A potential outflow of the Black Sea during this time is implied by the decreasing $^{87}Sr/^{86}Sr$ values. The reconnection of the Black Sea with the Mediterranean Sea via the Sea of Marmara started at 9.3 cal ka BP as marked in an increase in the Mg/Ca, Sr/Ca and $^{87}Sr/^{86}Sr$ ratios. Modelling of the $\delta^{18}O$ record indicates that it needed nearly 100 years until global and Black Sea level were adjusted.

ACKNOWLEDGMENTS

We thank captain and crew of the RV Meteor for their support during the Meteor cruise M 51-4. We also gratefully acknowledge Scott Birdwhistell for running the ICP-MS at WHOI, Monika Segl (University Bremen) and her team for doing the stable isotope measurements, and Ursula Röhl (University Bremen) for support of the XRF measurements. Bernhard Schnetger (ICBM, Oldenburg) kindly provided unpublished TOC data. A stay of A. B. at the WHOI was supported by the DAAD (ref. D/04/42992). This research was founded by the DFG grants no. LA 1273/2-1, LA 1273/2 and WE 992/47-3. RCOM No. 0517.

5. The last deglaciation as recorded in the western Black Sea: a multi-proxy study

Olga Kwiecien[1], Helge W. Arz[1], Frank Lamy[2], Birgit Plessen[1], André Bahr[3,4] and Gerald H. Haug[5]

[1]*GeoForschungsZentrum Potsdam, (GFZ Potsdam), Germany*
[2]*Alfred Wegener Institute for Polar and Marine Research (AWI), Bremerhaven, Germany*
[3]*MARUM - Center for Marine Environmental Research, University of Bremen, Germany*
[4]*now at IFM-GEOMAR, Kiel, Germany*
[5]*Swiss Federal Institute of Technology (ETH Zürich), Switzerland*

To be submitted to: Quaternary Science Reviews or Palaeogeography, Palaeoclimatology, Palaeoecology

ABSTRACT *Based on a comparison of multi-proxy sediment core records from western Black Sea, we present a comprehensive overview of the climate evolution in the Black Sea region over the last 26 ka with a special focus on the deglaciation period. Glacial sedimentation in the Black Sea was dominated by terrigenous material and characterized by high sedimentation rates. Low glacial C/N ratio values suggest a very restricted input of terrestrial organic material as the sparse vegetation cover in the drainage area (NW Anatolia) facilitated enhanced erosion rates. Early deglacial inflow of meltwater most probably originating from the disintegration of the European ice sheets (Bahr et al., 2006) strongly influenced the isotopic ($\delta^{18}O_{candona}$) but not the chemical (Sr/Ca) composition of the Black Sea water. Subsequent warming during the Bølling/Allerød (B/A) triggered changes in the basin itself and in its southern drainage area (NW Anatolia). Increasing surface water temperatures during this time-interval led to enhanced phytoplankton activity which induced precipitation of inorganic carbonates and modified the chemistry of the surface waters. Coevally, a signal of changing isotopic composition of rainfall was transmitted into the entire water column. On land, simultaneous soil development and advance of vegetation reduced run-off causing a significant decrease in sedimentation rates. During the Younger Dryas (YD) both, phytoplankton activity and vegetation advance on land were diminished but not completely ceased. Comparably, rainfall-related changes in the isotopic composition of the Black Sea water slowed down. Early Holocene conditions were similar to those of the B/A but were punctured by Mediterranean inflow which had a substantial impact on the chemical and physical properties of the Black Sea water. Comparing our data to calibrated temperature and precipitation records based on Western and Eastern Mediterranean archives, suggest that the increase in local precipitation in NW Anatolia (likely related to the early hemispheric warming) predated the increase in temperature related to the B/A warming. During the early deglaciation, we observe a decoupling of precipitation in the hinterland (NW Anatolia) and hydrological changes in the western Black Sea which may be explained by a subdued response of the Black Sea to the millennial-scale changes of the glacial atmospheric circulation. This finding has an important implication for the reconstruction of the eastward extent of a North Atlantic influence on the continental climate.*

INTRODUCTION

The long-term transition from the cold, glacial conditions of Marine Isotope Stage 2 (MIS2) to the warm, interglacial conditions of the Holocene (MIS1) was punctured by shorter-term, millennial-scale cold events, like Heinrich Event 1 (H1) and the Younger Dryas. Together with the abrupt Bølling/Allerød warming falling in between H1 and YD, these events had a significant impact on climatic conditions in much of the Northern Hemisphere (NH) (Rind et al., 1986). The Late Glacial climatic oscillations are exceptionally well recorded and dated in Greenland ice cores (Grootes et al.,

1993; Spahni et al., 2005; Mayewski et al., 1997) and marine sediment cores from the North Atlantic (Ruddiman and McIntyre, 1981; Waelbroeck et al., 2001). However, these records are often dominated by global-scale signals and offer only limited information with respect to regional climate variability in other, for example mid and low latitudinal continental parts of the NH.

A more comprehensive understanding of processes and feedbacks taking place at the termination of the last ice age requires an integration and comparison of ice core, marine and terrestrial records. Such an approach enables the assessment of possible leads and lags between climate changes as recorded in different archives. In particular comparing marine and terrestrial proxies from the same sediment core circumvents dating uncertainties and facilitates a high-resolution marine-terrestrial correlation.

Such coupled atmosphere-ocean-land studies of the last glacial have been successfully performed in the Central and Western Mediterranean region which is influenced by both low and high-latitude climatic systems. In the past, this mid-latitudinal region has witnessed oscillations of the Polar Front and associated changes in the trajectory and strength of moisture-bearing westerly winds. These changes were reflected in both, hydrological properties of the Mediterranean basin and in evolving humid/arid conditions on land. Western Mediterranean marine records show decreased sea surface temperatures (SST) (Cacho et al., 1999), decreased deep-water temperatures and intensified ventilation (Cacho et al., 2006) corresponding to cold Heinrich Events (HEs). Pollen data and terrigenous fraction data from the same marine cores document synchronous arid and cold conditions over Western Europe (Combourieu Nebout et al., 2002; Combourieu Nebout et al., 1998; Moreno et al., 2005; Moreno et al., 2002; Sanchez Goni et al., 2002). These multidisciplinary approaches demonstrated that both, marine circulation and Mediterranean climate were strongly related to the North Atlantic ocean-atmosphere system during the last glacial cycle.

In the Eastern Mediterranean region spatial and temporal coverage of paleoclimatic data is lower and multi-proxy records integrating information on ocean-atmosphere-land systems virtually do not exist. The available data from this region have been recently summarized by Robinson et al. (2006) showing that all of the major NH climatic shifts of the last 25 ka are present in the marine and terrestrial archives but while the LGM and early Holocene have received considerable attention, the data availability for the transition between these two climatic stages is poorer. Additionally, the existing Eastern Mediterranean climate records are partly ambiguous, particularly regarding changes of the regional water balance at the last glacial-interglacial transition (see review, Tzedakis, 2007). The geomorphological evidence from Lake Konya in central Anatolia (Roberts, 1983) and Lake Lisan (the present Dead Sea) (Bartov et al., 2003) show higher than today lake levels before/during the LGM and a lowering (to drying out) trend after H1 (~16.5 cal ka BP). On the contrary, pollen records from Central and Eastern Mediterranean region point to conditions drier than modern during the LGM (e.g. Peyron et al., 1998) and more humid conditions starting after H1. Opposing humidity trends in records from Mediterranean and North European lakes during the LGM were explained by the northward retreat of the westerly jet (Harrison et al., 1996). However, even a compilation of the lake level data is still a discrete information difficult to extrapolate over wider areas. Moreover there are no lake data from Central Europe that would allow a detailed reconstruction of shifts in the Late Glacial circulation regime along the European continent.

During the last glacial a decrease in the global sea level disconnected the Black Sea from the Mediterranean Sea and transformed it into a closed lacustrine basin. Considering the Black Sea a lake, its enormous size and a landlocked location perfectly qualifies it to record environmental and hydrologic changes in the continental interior of Central and Eastern Europe and Asia Minor. The potential of the Black Sea as a climatic archive was demonstrated by recent studies (Bahr et al.,

2005, 2006; Major et al., 2002, 2006). Kwiecien et al., (submitted) showed that the in the full glacial the relative precipitation changes in NW Anatolia were related to Mediterranean SST variations (e.g. Cacho et al. 2001) and as such were teleconnected to the North Atlantic climate regime. Paleohydrological properties of the basin inferred from sediment composition and stable isotopes variability revealed that the Black Sea water has undergone significant changes during and after the last glacial-interglacial transition (Bahr et al., 2005, 2006; Major et al., 2002, 2006). In the course of the early deglaciation, evolving hydrological conditions of the Black Sea basin were related to the inflow of meltwater (Bahr et al., 2006; Major et al., 2006). Subsequently, the Black Sea water experienced temperature changes which were in-phase with a North Hemispheric trend (B/A, YD, Early Holocene) (Bahr et al., 2008).

In this paper we present new proxy data from the southwestern Black Sea together with published data from the north- and southwestern basin in order to compile a comprehensive overview of the climate evolution in the Black Sea region over the last glacial-interglacial transition. First we discuss our proxy-data with respect to lake and drainage (NW Anatolia) conditions during climatic changes. Than we compare our results with those available from other calibrated records of temperature (Western Mediterranean SSTs [Cacho et al., 2001]) and precipitation (based on stable oxygen isotopes of inorganic carbonates from Eastern Mediterranean [Bar-Matthews et al., 1997; Jones et al., 2007]) in the Mediterranean region. Finally, we aim to show differences in the responses of the Black Sea basin and the adjacent continent (NW Anatolia) to climatic oscillations during the glacial and deglacial/Early Holocene mode.

MATERIAL AND METHODS

Material

Our proxy records are based on two cores: MD04-2788/2760, recovered in the southwestern Black Sea onboard R/V *Marion Dufresne* during the ASSEMBLAGE I cruise (Fig. 5.1), and GeoB 7608-1, recovered in the northwestern Black Sea during the R/V *Meteor* cruise M51-4 (Fig. 5.1). Since the focus of the present work concerns only the lacustrine phase of the Black Sea history, we have restricted our study to the time window before the reconnection with the Mediterranean Sea (8-26 cal ka BP) (Lamy et al., 2006). A detailed discussion of the age model of this time interval can be found in Kwiecien et al. (2008).

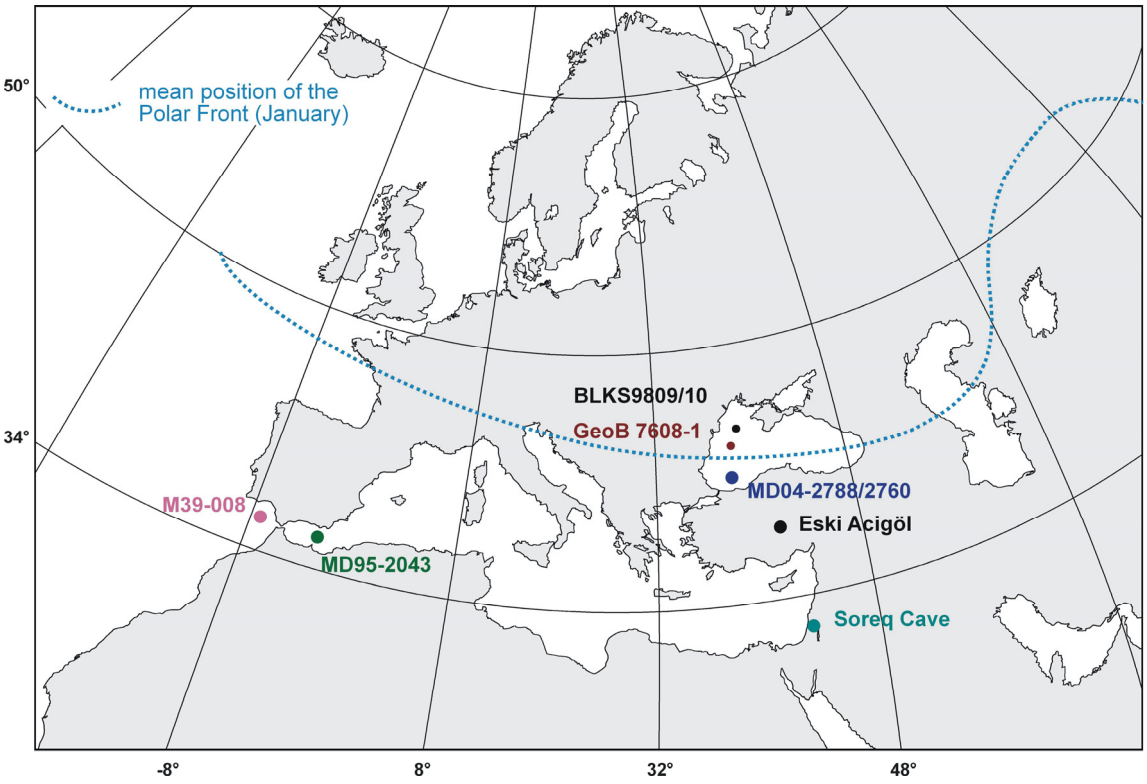

Figure 5.1: Locations of the sites relevant for the study. Mediterranean marine records: MD95-2043 (Cacho et al., 2001); M39-008 (Cacho et al., 2001); Black Sea records: MD04-2788/2760 this study; GeoB 7608-1 (Bahr et al., 2005); BLKS9809/10 (Major et al., 2002); Eastern Mediterranean continental records: Soreq Cave (Bar-Matthews et al., 1997); lake Eski Acigöl (Jones et al., 2007). Present mean position of the Polar Front after Wigley and Farmer (1982).

Chronology

Briefly, the age model for MD04-2788/2760 is based on 14 calibrated and reservoir-corrected AMS ^{14}C dates and the clearly identified Y-2 tephra layer (Fig. 5.2). The detailed examination of the XRF Ca-intensity signal and $CaCO_3$ concentrations allowed a precise correlation of MD04-2788/2760, GeoB 7608-1, and a previously published record from core BLKS9809/10 located in the NW Black Sea (Major et al., 2002) (Fig. 5.1) (Kwiecien et al., 2008). The proxy records from the three sites are presented on the MD04-2788/2760 time scale. We would like to stress that the fine tuning was performed using only the XRF Ca-intensity/$CaCO_3$ concentrations, and the very good correspondence of other proxies (e.g. $\delta^{18}O_{candona}$) confirms the accuracy of our alignment.

Applied proxies

Site MD04-2788/2760 is located on the southwestern slope of the Black Sea basin (1206 m water depth) in close vicinity of the Sakarya River mouth. Consequently, the recovered sediments provide information on environmental changes in the drainage of the Sakarya River (NW Anatolia) but also record the evolution of inherent basin conditions. Changes in the Ca-intensity record determined by means of X-ray fluorescence (XRF) core logging (Fig. 5.2B) can be closely correlated to the bulk carbonate concentration along the profile (Kwiecien et al., submitted), suggesting that Ca primarily represents carbonates. The complexity of the Ca record consists in the diverse nature of the carbonates. Until ~14.3 cal ka BP, the carbonate content is almost exclusively dominated by terrigenous input of carbonate detritus from carbonate bearing rocks outcropping in the Sakarya

River drainage area, while inorganically-precipitated calcite in the lake causes high carbonate concentrations after ~14.3 cal ka BP (Kwiecien et al. submitted).

Total organic carbon content (TOC weight %, Fig. 5.2C) is used to reconstruct concentrations of organic matter related to either *in situ* lake productivity or detrital input. The aquatic or terrestrial origin of organic matter deposited in lacustrine environment can be generally inferred from its composition (we use the C/N ratio shown in Fig. 5.2D) (Lamb et al., 2004; Lamb et al., 2007).

If measured on authigenic carbonates which precipitate in isotopic equilibrium with the lake water, $\delta^{18}O_{bulk}$ records $\delta^{18}O$ variations of continental waters (Leng and Marshall, 2004). In our case the carbonate subfractions (detrital and inorganic precipitates) were not isolated and $\delta^{18}O_{bulk}$ is actually a function of the two components. Therefore in a first approach, our $\delta^{18}O_{bulk}$ record represents changing proportions of detrital and inorganically precipitated carbonates (Fig. 5.2E).

Data obtained from shells of benthic ostracods (Sr/Ca ratio and $\delta^{18}O_{candona}$) reflect the evolving hydrochemistry of water column. The Sr/Ca ratio of ostracod shells (Fig. 5.2F) reflects the Sr/Ca ratio of the water that is influenced by changes in water input sources or geochemical processes within the water column (Bahr et al., 2008). The $\delta^{18}O$ of water incorporated in the ostracod shells (Fig. 5.2G) may respond to changes in evaporation-to-precipitation ratio and modifications in the isotopic composition of either atmospheric precipitation or run-off. Sr/Ca measurements were performed only for core GeoB 7608-1 (Bahr et al., 2008), while $\delta^{18}O_{candona}$ analyses were done on both cores GeoB 7608-1 (Bahr et al., 2006) and MD04-2788/2760 (Kwiecien et al., submitted).

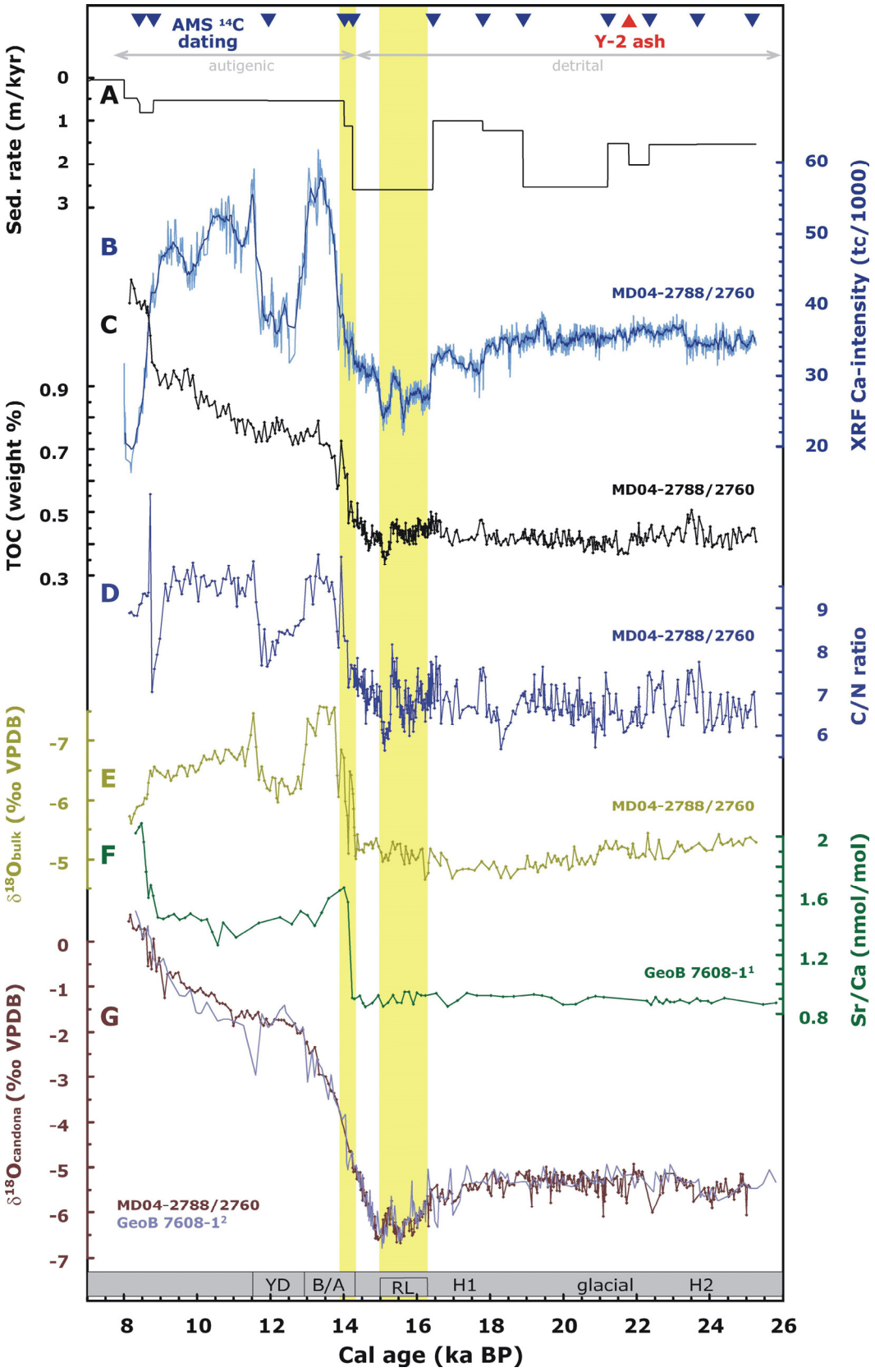

Figure 5.2: Paleoclimate records from the southern (A-D, G) and northern (E-G) Black Sea cores. Please note that the sedimentation rate (A) is plotted on an inverse scale. The chronology of the core MD04-2788/2760 is based on reservoir-corrected calibrated ^{14}C ages (Kwiecien et al., 2008). In (B) thin light blue line represents original data and thick dark blue line represents a 7-point moving average. Horizontal gray arrows refer to the nature of a dominant carbonate fraction. Thick yellow bar marks a period of meltwater discharge. Thin yellow bar indicates abrupt Bølling warming.

CHANGES IN THE WESTERN BLACK SEA BASIN AND ITS SOUTHERN DRAINAGE AREA (NW ANATOLIA)

Glacial period and red layers interval (26 to 14.5 cal ka BP)

All proxy data clearly point to relatively stable conditions during the glacial interval from 26 to ~16.4 cal ka BP. Glacial sedimentation in the Black Sea was dominated by terrigenous supply and the carbonate-poor sediments at site MD04-2788/2760 are continuously laminated and show 1 to 5 mm-scale alternations of light-colored clay to darker-colored clay/fine silt or fine sand. Kwiecien et al. (submitted) related the concentration of detrital carbonates in the glacial to relative precipitation changes in NW Anatolia. Two minima in the XRF Ca-intensity record centered at 24 and 17.5 cal ka BP (Fig. 5.2B) correlate to SST minima in western Mediterranean (Cacho et al., 2001) and were interpreted in terms of reduced regional rainfall during H1 and H2 (Kwiecien et al., submitted).

Between 15 and 16.4 cal ka BP, the XRF Ca-intensity and the stable oxygen isotope record obtained on ostracod shells ($\delta^{18}O_{candona}$) (Fig. 5.2B, 5.2G) display significant changes. A gradual $\delta^{18}O_{candona}$ depletion (Fig. 5.2G) indicates a concomitant increase of meltwater flux into the Black Sea basin (Bahr et al., 2006) most probably originating from the Late Glacial disintegration of the European ice sheets (Bahr et al., 2006). A third Ca-minimum contemporary to the $\delta^{18}O_{candona}$ depletion (16.4-15 cal ka BP) is lithologically characterized by pronounced reddish clay layers and is related to an activation of the northwest-northeast European sediment sources. The enhanced contribution from the northern Black Sea drainage areas resulted in maximum sedimentation rates at site MD04-2788/2760 (Fig. 5.2A) and thus the Ca-minimum is best explained by dilution. Activation of Northern European sediment sources related to increased meltwater flux represents the onset of the overall hemispheric warming and mitigation of the Central and Northern European climate (Kwiecien et al., submitted). Such early warming, significantly predating the abrupt Oldest Dryas/Bølling transition, has also been reported from other locations in the circum North Atlantic region (Denton et al., 1999). Noteworthy any precipitation/temperature related changes of the Black Sea water isotopic composition at that time were likely to be imprinted by the inflow of isotopically depleted meltwater. In contrast to the gradual changes in $\delta^{18}O_{candona}$, stable Sr/Ca values (Fig. 5.2F) suggest that the Sr/Ca ratio of the inflowing meltwater and that of the Black Sea water must have been relatively similar (Bahr et al., 2008).

Following the arguments above, the relatively high values of $\delta^{18}O_{bulk}$ (Fig. 5.2E) during the interval between 14.5-26 cal ka BP can be interpreted as reflecting the isotopic composition of detrital carbonates. Generally low TOC values (Fig. 5.2C) may result from low productivity due to unfavorable climate conditions and/or bad preservation due to well ventilated waters and oxic condition at the bottom of the Black Sea 'Lake' (Pelet and Debyser, 1977). C/N ratios of 4-10 are characteristic for aquatic vegetation, while values between 10-20 represent a mixture of aquatic and higher plants material (Lamb et al., 2004; Lamb et al., 2007). Glacial C/N ratio values below 8 (Fig. 5.2D) suggest a very restricted input of terrestrial organic material. This may in turn indicate a poor soil development and a sparse vegetation cover in the Sakarya River catchment (NW Anatolia).

Bølling/Allerød

The postglacial sediments deposited after ~14.3 cal ka BP consist of homogenous clays composed of up to 50% carbonates, originating mostly from inorganic precipitation in the water column induced by massive phytoplankton blooms marking the Bølling/Allerød warming (Bahr et al., 2005).

Increased phytoplankton activity related to the B/A warming is recorded by a significant increase in TOC values (Fig. 5.2C). Phytoplankton blooms increase the CO_2 uptake and oversaturate surface waters with respect to $CaCO_3$ which leads to inorganic carbonate precipitation (Kelts and Hsü, 1978). The latter process can be traced by changes in the $\delta^{18}O_{bulk}$ (Fig. 5.2D) that in a first order represent the changing proportion between inorganically precipitated and detrital carbonates.

However, the parallel increase in Sr/Ca ratio (Fig. 5.2F) suggests that increasing temperature was the main factor driving abrupt postglacial $\delta^{18}O_{bulk}$ change at 14.3 cal ka BP. As the Sr/Ca ratio remained unaffected by changes in the Black Sea freshwater sources (Fig. 5.2F) it may be considered independent from detrital input/run-off changes. A simultaneous change in Sr/Ca and $\delta^{18}O_{bulk}$ corroborates the concept that biologically triggered precipitation of inorganic carbonates at 14.3 cal ka PB led to a sudden increase of the Sr concentration of the Black Sea water by modifying the chemistry of the surface waters. Subsequently this signal propagated into the Black Sea deep-water (Bahr et al., 2008). Therefore, though not in a conventional way, postglacial changes in $\delta^{18}O_{bulk}$ can be used as indicative for relative changes in the surface water temperature.

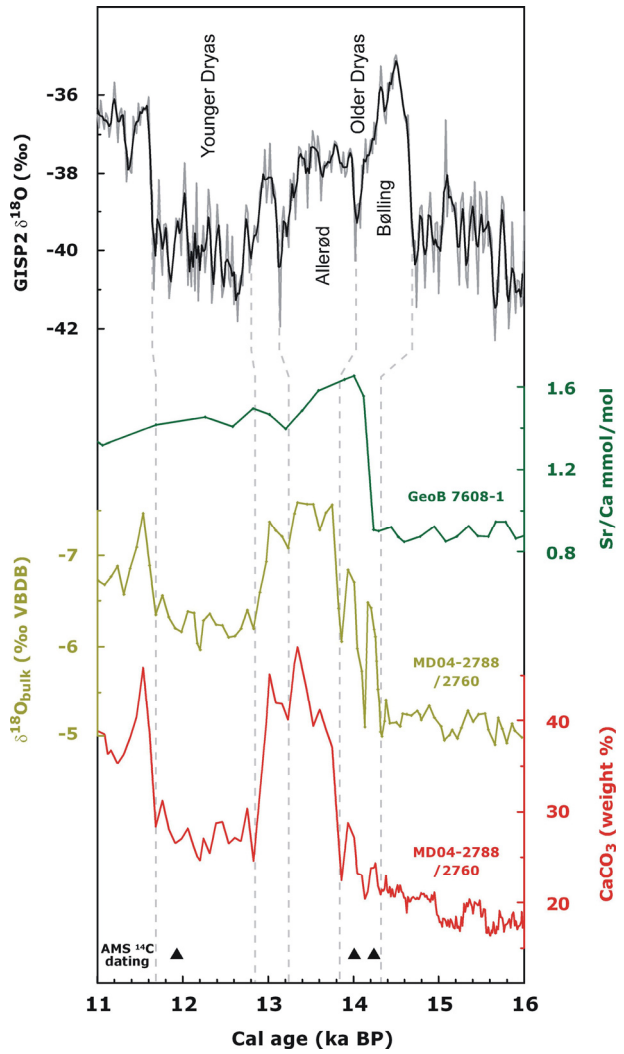

Figure 5.3: Comparison of the Black Sea records and the GISP2 chronology (Grootes et al., 1993). As the XRF Ca-intensity correlates to $CaCO_3$ content (weight %) (Kwiecien et al., submitted), we present, for the period of deglaciation, $CaCO_3$ content record which has the same resolution as $\delta^{18}O_{bulk}$ record.

Our coupling of $\delta^{18}O_{bulk}$ and Sr/Ca records (Fig. 5.2E, 5.2F) and relating them to the surface water processes suggests that until ~14.3 ka BP no significant precipitation of inorganic carbonates has occurred. With the onset of the Bølling warming, the surface water of closed large lakes like the Black Sea during that time, responded immediately to hemispheric-scale changes in atmospheric temperature. Consequently, considering dating and reservoir-correction uncertainties (Kwiecien et al., 2008) we correlate an abrupt shift in $\delta^{18}O_{bulk}$ and Sr/Ca at 14.3 cal ka BP to the Bølling warming (Fig. 5.3) recorded in ice cores (Grootes et al., 1993). A brief change towards glacial conditions recorded in the Ca-intensity, $\delta^{18}O_{bulk}$ but also in TOC content (Fig. 5.2C) and C/N ratio (Fig. 5.2D) may correspond to the cold Older Dryas interruption (Fig. 5.3). In the Sr/Ca record this interruption may be beyond the limit of detection due to lower time resolution of core GeoB 7608-1.

Though we favour a major role of temperature increase in abrupt postglacial $\delta^{18}O_{bulk}$ change, we are aware that this pronounced shift may be attributed to a mixed effect of increasing inorganic calcite precipitation (as a result of increasing surface water temperatures leading to enhanced phytoplankton activity) and decreasing detrital carbonate input.

The supply of detrital carbonate is mainly controlled by precipitation and vegetation cover in the catchment area. A drastic decrease in sedimentation-rates at the beginning of the B/A implies a substantial decrease in detrital input. The homogenous nature of the B/A muds clearly contrasts with the finely laminated glacial sediments (perhaps seasonal alternating) and suggests that the transport of coarser sized particles (silt, sand) was reduced. The generally higher C/N ratios (Fig. 5.2D) during the B/A point to enhanced input of terrestrial higher plants remains, although the aquatic vegetation was still dominant. Specific component analysis of both lacustrine and marine Black Sea sediments showed that the contribution of aquatic phytoplankton has always been greater than the contribution of terrestrial plants (Pelet and Debyser, 1977; Shimkus and Trimonis, 1974). Our interpretation of relative C/N ratio changes is consistent with pollen records from the Eastern Mediterranean region (Fontugne et al., 1999; Zonneveld, 1996) and eastern Anatolia (Landmann 1997) that suggest an advance of woodlands with the beginning of the B/A. Expanding vegetation cover in the southern drainage of the Black Sea could have hindered surface outwash and the supply of detrital material into the Black Sea basin. Additionally, Robinson et al. (2006) proposed that during the glacial much of the precipitation over the Anatolian uplands fell as snow and was later on released in a spring thaw. Spring thaws, supplying detrital material in a concentrated surge, could have played an essential role in the formation of the glacial lamination at our site. Additionally in regions where most of the precipitation falls in form of snow relatively short growing season can limit development of vegetation. Thus a shift from snow to rain at the Oldest Dryas/Bølling could have contributed to the changes observed in our record, like disappearance of lamination and increase in C/N ratio.

Interestingly, we observe a delay of ~200 yr in the significant increase of C/N ratio compared to the shift in $\delta^{18}O_{bulk,}$ corresponding to a weakly laminated interval. This interval may represent a time-lag required for the vegetation to respond to the B/A warming. A similar delay in woodland expansion has already been observed for the Bølling in Northwestern Europe (see review Walker, 1995).

Finally a pronounced trend towards heavier values in $\delta^{18}O_{candona}$ (Fig. 5.2G) can be primarily the effect of increasing $\delta^{18}O$ of run-off and on-lake precipitation as well as enhanced evaporation (Bahr et al., 2006). The well-documented 3.5‰ increase in $\delta^{18}O$ of atmospheric precipitation between Oldest Dryas and B/A in Central Europe (von Grafenstein et al., 1999a) could e.g. almost alone account for the whole shift of ca. 4‰ that occurred in the Black Sea records since the end of the red layers period (Bahr et al., 2006).

Younger Dryas

A change towards glacial conditions is clearly visible in decreased Ca-intensity (Fig. 5.2B) and heavier $\delta^{18}O_{bulk}$ (Fig. 5.2E), however, none of these proxies reaches its glacial values. The Ca-intensity during the YD is higher than the average glacial level (Fig. 5.2B) and $\delta^{18}O_{bulk}$ falls between glacial and B/A values. Thus, even if by analog we assume that detrital supply was as high as during the glacial, the total carbonate concentration must have been compensated by inorganically-precipitated carbonates. The inorganic carbonate precipitation, though strongly reduced, probably did not cease as suggested by microscopic investigations of smear slides that proved the presence of inorganic calcite crystals. Additionally, the rapid change in $\delta^{18}O_{bulk}$ towards heavier values corresponds to only a general decrease in Sr/Ca ratio. Although the assessment of a potential contribution of surface water temperature changes to the $\delta^{18}O_{bulk}$ signal during the YD is impossible, parallel Mg/Ca measurements on ostracods suggest 1-2 °C cooling of the Black Sea deep-water (Bahr et al., 2008). Such a cooling signal must have been transmitted from the surface waters to the entire water column. Following this argument, with possible cooling of surface waters, the phytoplankton activity may have been reduced. Also the C/N ratio implies reduced input of terrestrial organic material, though the TOC content does not decrease within the YD (Fig. 5.2C). However, the plateau observed in the TOC record may be related to abundant diatoms, which has been reported also from other Black Sea cores over this time period (Ryan et al., 2003).

The reappearance of lamination together with relatively lower C/N ratio values (Fig. 5.2D) implies that a short-lived retreat of vegetation (due to climatic deterioration) might have led to an increased input of detrital material. Interruption of woodlands advance during the YD is well documented in the Eastern Mediterranean region (Fontugne et al., 1999; Zonneveld, 1996). A similar situation is observed at Lake Van where the decline of vegetation led to increased siliciclastic input and higher sediment deposition rates (Landmann et al., 1996). Our age model does however not resolve an increase in sedimentation-rates in the Black Sea during the YD (Fig. 5.2A).

The isotopic plateau observed in $\delta^{18}O_{candona}$ values during the YD (Fig. 5.2G) may represent inertia of a basin as large as the Black Sea, due to the long residence time, in a response to shorter-scale climate oscillations like the YD.

Early Holocene

Early Holocene sediments are, like in the B/A interval, composed of homogenous clays with mostly authigenic carbonates. After the YD interruption, the Ca-intensity increases suggesting enhanced carbonate precipitation. The $\delta^{18}O_{bulk}$ values are lighter than during the YD but heavier than during the B/A. This trend towards heavier $\delta^{18}O$ values, parallel in both the bulk and the ostracod records, implies that either increasing $\delta^{18}O$ of atmospheric precipitation or enhanced evaporation (or both) affected the surface and deep-water in a similar way. C/N ratios reaching again B/A values point to a readvance of vegetation. Early Holocene tree colonization has been widely observed in Southern Europe (Allen et al., 1999; Vescovi et al., 2007). The single C/N-peak at 8.72 cal ka BP was confirmed by re-measuring and may represent a plant macro-rest present in the sample. A final increase in the stable isotope composition of bulk and ostracods, TOC and the Sr/Ca ratio is associated with the hydrological changes in the basin subsequent to the initial inflow of marine Mediterranean waters (Bahr et al., 2008) which had a substantial impact on the chemical and physical properties of the Black Sea water. Interestingly, the C/N ratio is the only proxy which shortly returns to its pre-connection values. As the other proxies (e.g. Sr/Ca), show only the onset of

the initial Mediterranean inflow a duration of C/N negative excursion may illustrate the duration of this event. However, this interpretation is only tentative.

WIDER IMPLICATIONS FOR THE RECONSTRUCTION OF MEDITERRANEAN CLIMATE

In the full glacial (26-14.5 cal ka BP), relative precipitation changes in NW Anatolia expressed by detrital carbonate concentration (Kwiecien et al., submitted) (Fig. 5.4E) were related to Mediterranean SSTs variability (Cacho et al., 2001) (Fig. 5.4A, 5.4B). Notably, glacial changes in the relative rainfall amount are associated with relative stable temperature conditions (Fig. 5.4F, 5.4G). Fig. 5.4 shows a comparison to two quantitative precipitation reconstructions based on stable oxygen isotopes; a stalagmite record from Israel (Bar-Matthews et al., 1997, modified after Jones et al., 2007) and an authigenic carbonate record from a crater lake in central Anatolia (Jones et al., 2007). The quantitative data are based on a hydrological model that covers five time-periods from the last glacial to the early Holocene, each of which is characterized by relatively stable isotopic values (thus the model is not designed to test sub-millennial climate variability but long-term trends). Eastern Mediterranean precipitation inferred from lake Eski Acigöl (Fig. 5.4H) and Soreq Cave (Fig. 5.4I) was low until 16.4 cal ka BP. Relatively high sedimentation rates in the southwestern Black Sea at the same time may be explained by the relatively sparse vegetation cover in NW Anatolia favoring erosion and effective sediment transport to the slope. A dominance of the southern sediment source during the full glacial (Fig. 5.4C) is most likely accompanied by a diminished contribution from the northern source areas of the western Black Sea basin. During the same period generally low level of North European lakes (Harrison et al., 1996) confirms cold and arid conditions in Northern and Central Europe (Atanassova, 2005; Florineth and Schlüchter, 2000) which likely accounted for limited northern rivers runoff.

The first symptom for an early warming of the northern Black Sea drainage is a reactivation of the northern source (Fig. 5.4C) at ~16.4 cal ka BP probably linked to meltwater discharge originating most from the disintegration of European ice sheets (Bahr et al., 2006; Major et al., 2002). Higher than average sedimentation rates during the subsequent red layers interval (Fig. 5.4D) suggest that our core site received a significant amount of sediment not only from local sources but also from reactivated sources in the northern drainage areas of the Black Sea. The significant supply from the south is consistent with more humid conditions reconstructed for the Eastern Mediterranean region (Fig. 5.4H, 5.4I) and increased Mediterranean SSTs (Fig. 5.4A, 5.4B).

Notably, neither the Black Sea surface water processes (Fig. 5.4F) nor deep-water proxies (Fig. 5.4G) show any response to an early warming as indicated from western Mediterranean SST records (Fig. 5.4A, 5.4B). The entire Black Sea water column reacts later, but particularly strong, at the abrupt B/A transition (Fig. 5.4E, 5.4F). A decrease in sedimentation rates at about this time (Fig. 5.4D) only apparently contradicts increasing precipitation as recorded in Eski Acigöl and Soreq Cave (Fig. 5.4H, 5.4I). The general climate amelioration during the B/A in NW Anatolia resulted in an expanded vegetation cover, probably hindering erosion and lowering the terrigenous supply to the southwestern Black Sea. In a similar way widespread development of vegetation during the B/A could have added to a temperature effect in lowering the level of Mediterranean and Turkish lakes. This may be conceivable through the effect of expanding woodlands on regional evapotranspiration in which evolving soils could retain more moisture and therefore reduce run-off, while higher temperatures increased evaporation.

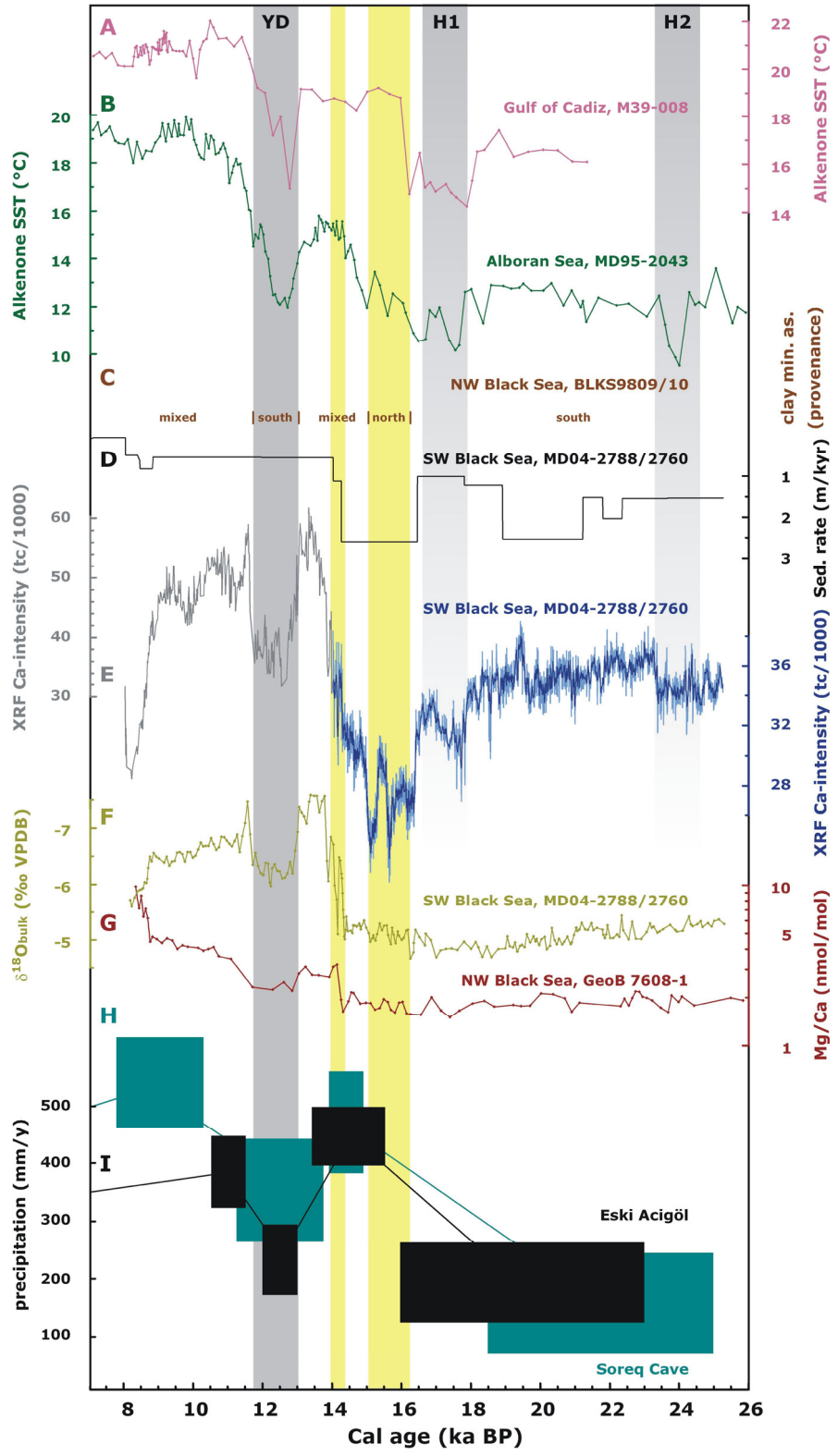

Figure 5.4: Juxtaposition of selected climatic records from the Mediterranean region from 26 to 8 cal ka BP. Location of all the sites is shown on the Figure 5.1. (A) M39-008 (Cacho et al., 2001); (B) MD95-2043 (Cacho et al., 2001); (C) BLKS9809/10 (Major et al., 2002); (D-F) MD04-2788/2760 this study, please note that the sedimentation rate (D) is plotted on an inverse scale; (G) GeoB 7608-1 (Bahr et al., 2008); (H) Soreq Cave (Bar-Matthews et al., 1997, modified after Jones et al., 2007); (I) lake Eski Acigöl (Jones et al., 2007). Thick yellow bar marks a period of most significant precipitation increase recorded in the Black Sea. Thin yellow bar indicates period of abrupt warming recorded in the Black Sea. Gray bars indicate HEs and YD respectively.

During the YD, precipitation recorded in Eski Acigöl and Soreq Cave (Fig. 5.4H, 5.4I) has reduced. Both, Mediterranean SSTs (Fig. 5.4A, 5.4B) and the Black Sea deep-water record (Fig. 5.4G) also point to a temperature decrease. A dominance of the southern sediment provenance in the northern Black Sea (Fig. 5.4C) may be a result of 'blocking' of the northern provenance, a situation analogous to the full glacial conditions (Kwiecien et al., submitted). Finally the Early Holocene warming trend is recorded in Mediterranean SSTs (Fig. 5.4A, 5.4B), Black Sea intermediate water temperature (Fig. 5.4G), and correlates to the precipitation increase in the Eastern Mediterranean (Fig. 5.4H, 5.4I).

A decoupling of precipitation (NW Anatolia) and temperature signals (W Black Sea basin) during the last glacial and the early deglaciation may be explained by a subdued basin response to the millennial-scale changes of the glacial atmospheric circulation. The interval around the Last Glacial Maximum was the time of maximum ice volume and minimum NH summer insolation (Mix et al., 2001). This period was characterized by reduced temperature variability over Greenland (Chapman and Maslin, 1999) and, in comparison to MIS3, generally reduced amplitude of millennial-scale climate variability. During the full glacial, the southward shifted Polar Front and jet stream likely resulted in reduced latitudinal temperature gradients over the Black Sea and thus little additional impact of Heinrich Events.

Climate models based on the CLIMAP reconstructions (CLIMAP, 1981) show that during the glacial much of the precipitation over the Anatolian uplands fell as snow (Robinson et al., 2006). Thus climatic settings generated for the south-western cost of the Black Sea suggest that, in this region glacial winter conditions were significantly colder than the modern ones. This agrees with our conclusion that the Black Sea basin was locked in the glacial mode and glacial temperature changes in its region might have been below the detection limit of our proxies. The difference in response of the Western Mediterranean and Black Sea temperatures may come from a direct amplifying impact of the North Atlantic. During Heinrich Events (H1 and H2), changes of the Mediterranean SSTs were attributed primarily to the effect of inflowing cold North Atlantic waters (Cacho et al., 1999; Sierro et al., 2005) and to a smaller extent to atmospheric cooling.

CONCLUSIONS

Summarizing observations from different climatic archives suggests that precipitation changes not only in NW Anatolia but also in the wider eastern Mediterranean region respond to changes in the North Atlantic/Western Mediterranean SSTs during the last glacial-interglacial transition. Calibrated quantitative data from the Eastern Mediterranean demonstrate that the most significant precipitation increase experienced by the eastern Mediterranean region in the last 26 ka took place approximately at 16 ka BP (Bar-Matthews et al., 1997; Jones et al., 2007). This change, coinciding with maximum sedimentation rates in the Black Sea, was concomitant to mitigation of Northern and Central European climate. During this time interval, we observe little changes in surface water temperatures (reflecting the temperature of the air aloft) suggesting that the Black Sea was locked in the glacial mode until the Bølling warming. Starting with the B/A warming and proceeding through the YD cold interval and the Early Holocene warming, the Black Sea temperature signal corresponds to the precipitation and temperature changes recorded in the wider Mediterranean region. This implies that the Bølling warming released the Black Sea basin out of is previous glacial steady-state and was decisive enough to induce internal changes within the basin itself and the adjacent land (NW Anatolia).

ACKNOWLEDGMENTS

This research was sponsored by Comer Science and Education Foundation (CS&EF). We thank IPEV for logistic support during the ASSEMBLAGE I cruise (RV *Marion Dufresne*).

6. Laminated glacial sediments from the southwestern Black Sea - a preliminary study

Olga Kwiecien[1], Helge W. Arz[1], Frank Lamy[2], Peter Dulski[1], Norbert Nowaczyk[1] and Gerald H. Haug[3]

[1]*GeoForschungsZentrum Potsdam, (GFZ-Potsdam), Germany*
[2]*Alfred Wegener Institute for Polar and Marine Research (AWI), Bremerhaven, Germany*
[3]*Swiss Federal Institute of Technology (ETH-Zürich), Switzerland*

ABSTRACT *Glacial lacustrine Black Sea sediments recovered off northwestern Anatolia are characterized by continuous mm-scale lamination of predominantly detrital origin. We analyzed a sequence of ~500 years within the Last Glacial Maximum (LGM) anchored between two calibrated radiocarbon dates in order to investigate the nature of the lamination that potentially reflects seasonal changes in sedimentation. We combined results of optical and scanning electron microscopy and image-based layer counting with the radiocarbon chronology and suggest that the light/fine and dark/coarse layer couplets may have been deposited in an annual cycle. We further propose that the light/fine laminae represent the fall and winter season, while dark/coarse laminae form during the spring thawing. To investigate a potential relationship between the flux of clastic material, the supply of detrital carbonates, and general trends in grain sizes, we compare the varve thickness, the μXRF Ca-intensity, and the magnetic susceptibility records. Kwiecien et al. (submitted) suggested that on the millennial time-scales concentration of detrital carbonates in the glacial Black Sea sediments was positively correlated to the relative precipitation changes in NW Anatolia. Outcome of our exercise suggests that this relation is valid also for the short-term variability.*

INTRODUCTION

A sedimentary environment needs to fulfill two essential criteria to sustain the development of laminated sequences; (1) variations in input, chemical composition, or biological activity that will result in compositional changes of the sediment; and (2) conditions that will preserve the laminated sediment fabric from bioturbation (Kemp, 1996). The modern anoxic Black Sea basin matches these requirements superbly. In summer and fall phytoplankton blooms (coccoliths) supply biogenic carbonate while in winter and spring peak river discharge result in enhanced input of terrigenous material which is subsequently bind by spring diatom blooms (Hay, 1988). Oxygen-free bottom conditions circumvent bioturbation. Effectively the Black Sea lamination, represented by intercalated white (biogenic carbonates) and dark (terrigenous material) layers, manifests seasonal changes (Pilskaln and Pike, 2001).

During the last glacial, the decreased global sea level disconnected the Black Sea from the Mediterranean Sea. Thus, sedimentary conditions in the isolated Black 'Lake' were different than today. The glacial Black Sea phytoplankton was adapted to much lower salinities (Mudie et al., 2002b), biogenic and organic production was subordinate (Kwiecien et al., in prep), and as result of an intense ventilation Black Sea bottom waters were most probably well oxygenated (Bahr et al., 2006). Despite the lack of significant amounts of biogenic components, the presence of fine

lamination in the glacial Black Sea sediments highlights the substantial role of changes in the terrigenous supply on the laminae formation.

The Black Sea site MD04-2788/2760, located on the upper slope off western Anatolia (Fig. 6.1) represents an ideal setting to study laminated sediments. The proximity of the Sakarya River mouth contributes to very high sedimentation rates, while the location on an isolated topographic elevation, away from the path of turbidity currents, secures undisturbed deposition. A strong positive relation between sediment load of the Sakarya River and regional precipitation (Algan et al., 1999) encourages studies of the terrigenous input variability as a mean to reconstruct past changes in NW Anatolian hydrology. Today, the region drained by the Sakarya River (NW and central Anatolia) is influenced by Mediterranean climate and receives most of its rain during winter. The incipient work of (Hurrell, 1995) introduced the North Atlantic Oscillation (NAO) as a seesaw of atmospheric pressure difference between the Icelandic Low and the Azores High dominating present day winter temperatures and precipitation in the circum-North Atlantic region. During low NAO index years, week meridional pressure gradient guides northwesterly mid-latitudes, bringing higher precipitation to the Mediterranean, whereas during high NAO index years the situation is inverse and the North Atlantic depression tracks are deflected north bringing humidity to central and northern Europe. Since the original publication (Hurrell, 1995), ample studies have demonstrated the sensitivity of the Mediterranean and Middle East regions either to the NAO mode in modern days, or to NAO-like analogs in the past (Cullen and deMenocal, 2000; Felis et al., 2004; Prasad et al., 2004).

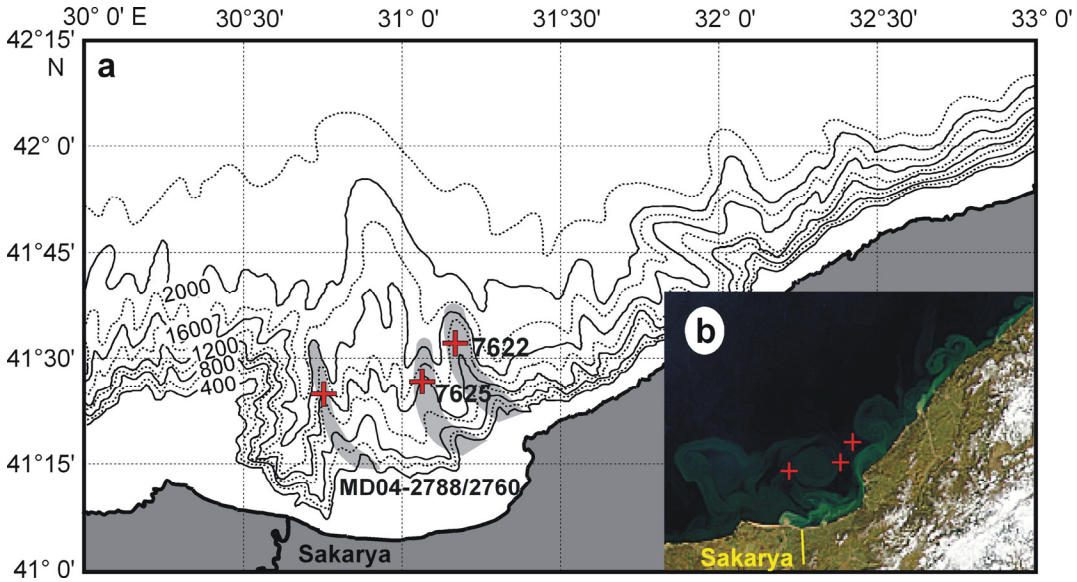

Figure 6.1: Regional setting of the Black Sea. (a) Detailed bathymetric map of the study area showing the location of core MD04-2788/2760 and cores GeoB 7622-2 and 7625-2 (modified after Lamy et al., 2006). All three sites are located on topographic ridges (gray shading) and should therefore not be influenced by resedimentation processes such as turbidity currents. (b) Satellite image of the Sakarya River mouth with the location of the sediment cores showing that the coring sites receive large amounts of suspended sediment originating from the river (source: http://visibleearth.nasa.gov/).

Modern data from hydrologic stations in the drainage basin of the Sakarya River document interannual to decadal-scale rainfall changes that are strongly coupled to NAO variability (Türkes and Erlat, 2005). Consequently, sedimentary records of changes in the terrigenous supply may primarily reflect modifications in river run-off that potentially could relate to the NAO. The

frequency of clay layers from two neighboring Black Sea sites northeast of the Sakarya River, GeoB 2722-2 and 2725-2 (Fig. 6.1), provide evidence for NAO–like atmospheric changes during the Holocene (Lamy et al., 2006) on the centennial timescales.

Compositional changes in the glacial Black Sea sediments have been related to variations in the Sakarya River run-off, suggesting changes in NW Anatolian precipitation that were coupled - at least on the millennial time scales - to the major North Atlantic climate evolution (Kwiecien et al., submitted). Following this argument, and considering a seasonal character of the marine Holocene sediments, we aim to examine the nature of the Black Sea glacial lamination and its potential as a tool to reconstruct patterns of short-term climate change under conditions very different from today.

MATERIAL AND METHODS

Material

The composite record MD04-2788/2760 consists of two cores, gravity core MD04-2788 and piston core MD04-2760 (Kwiecien et al., 2008) recovered in the southwestern Black Sea off northwestern Anatolia from a water depth of ~1200m (Fig. 6.1). The age model for MD04-2788/2760 is based on 14 calibrated and reservoir-corrected AMS ^{14}C dates and the clearly identified Y-2 tephra layer (Kwiecien et al., 2008). The interval sampled for this study (2649-2816 cm original depth, 2192-2311 cm composite depth) is bracket by two dated horizons, the Y-2 tephra layer and an ostracod sample. The full-glacial lacustrine deposits are characterized by very high sedimentation rates ranging from 1.5 m/ka to 2.5 m/ka and are laminated throughout revealing 1 to 5 mm-scale alternations of light-colored clay to darker-colored clay/fine silt (or sporadically fine sand) of detrital origin.

Sample preparation and image analysis

A total of 15 samples, each 10 cm in length including a 2 cm overlap were taken from the full-glacial section of the core MD04-2760. After freeze-drying, the samples were embedded in epoxy resin in order to prepare thin-sections and polished blocks. To allow a detailed evaluation of the lamination pattern, the polished blocks were scanned at a resolution of 600 dpi. The quality of the images was subsequently enhanced by optimizing contrast and brightness. The image processing included grayscale analysis along carefully selected profiles (3 for each image) perpendicular to the lamination. Disturbed or bended intervals were avoided. The grayscale curves were averaged, smoothed, and superimposed on the respective image. Subsequently, the grayscale maxima (light laminae) were identified manually, and counted. This technique allowed determining the exact position of overlap between consecutive samples essential to assembly the complete profile. Repeated marking of grayscale maxima performed on the same section yielded a standard deviation of +/- 6% of the overall amount of counted layers. Further, the grayscale profiles served as an additional reference to digitize the thickness of individual laminae.

Scanning Electron Microscope imaging

The scanning electron microscope (SEM, Carl Zeiss NTS, DSM 962 at GFZ-Potsdam, Germany) equipped with an energy-dispersive system (EDS) was employed to obtain high resolution and

element distribution images of the laminated sediments. Before analysis, the respective thin section was highly polished and coated with carbon. Back-scattered electron (BSE) images show compositional contrasts due to differences of the mean atomic weight of the analyzed mineral grain or aggregate. Grains consisting of elements with a high atomic weight appear brighter than those with a lower one. EDS X-ray mapping (400 x 400 µm) was repeated three times along the same laminae. EDS-based element distribution images on pre-selected light and dark couplets helps to qualitatively identify differences in a distribution of the major elements (e.g. Ca, Fe, Al, K, Si).

Profiling measurements

The XRF-scanning is a non-destructive method providing bulk intensities of major elements (e.g. Al, Si, S, K, Ca, Ti, Mn, and Fe; [Jansen et al., 1998]). The whole length of the core MD04-2760 was scanned in 1 cm resolution with an AVAATECH X-ray fluorescence scanner at the University of Bremen, Germany. The particular section of the core (2649-2816 cm, original depth; 2192-2305 cm, composite depth) was re-scanned in 500 µm resolution with an EDAX Eagle III BKA Spectrometer at the GFZ Potsdam, Germany. These two XRF core scanners provide different measurement units: the EDAX operates in counts per second (cps) while the AVAATECH in total counts (tc) thus values for the intensity of the same element may differ in order of magnitudes.

Magnetic susceptibility is a commonly used magnetic parameter directly proportional to the quantity and grain size of ferro- and ferri-magnetic materials in the sample (Verosub and Roberts, 1995). Within the investigated interval magnetic susceptibility was measured every 1 mm at a precision of 10^{-6} SI units with a Bartington MS2E spot-reading sensor mounted to a fully automatic (GFZ-developed) core logging system at the GFZ Potsdam, Germany. The drift of the sensor was monitored by readings in air after every 10th reading on the sediments, and was subsequently subtracted from these data by linear interpolation (e.g. Nowaczyk, 2001).

RESULTS

General observations and sedimentary microfacies

The analyzed interval is composed of carbonate- and organic-poor terrigenous muds. Total organic carbon (TOC) content and $CaCO_3$ concentration (in 8 cm sampling resolution) were reported by Kwiecien et al. (submitted, in prep). They showed a TOC content of less than 0.5 wt% being of predominantly aquatic origin and an average carbonate content of ~23 wt%. SEM imaging and $\delta^{18}O_{bulk}$ analysis proved that throughout the glacial the major portion of the carbonate fraction is of detrital origin.

Selected thin sections were investigated with an optic microscope and revealed that both, light and dark laminae consist predominately of detrital nonfossilferous clays, silts, and sporadically fine sands, and differ primarily in color and grain size. The detrital fraction in both light and dark layers includes quartz, feldspar, micas, clay minerals, and to lesser extent carbonates. In general, the lighter laminae consist of better sorted and finer material than the dark ones. Mineral grains in the coarse silt-rich dark laminae are contiguously distributed within a clay matrix; no grading has been observed (Fig. 6.2). Single tests with the fluorescence microscope did not show increased amount of organic matter confined to either coarse/dark or fine/light layers. However, close inspection of exceptionally well preserved dark/coarse laminae suggests that often the coarser minerogenic

material is embedded in finer darker matrix which may contain slightly increased amounts of organic material (Fig. 6.2).

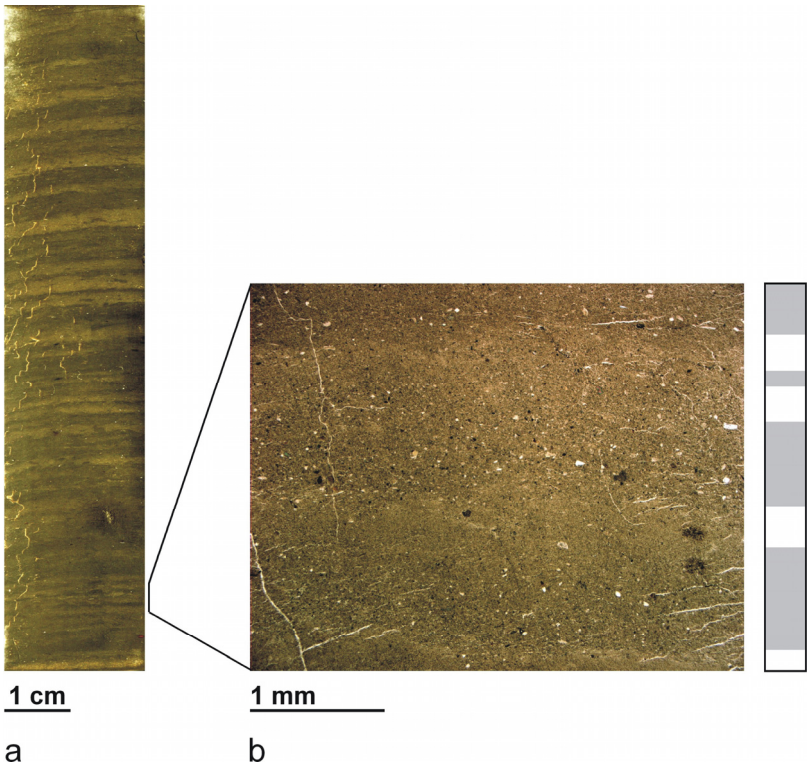

Figure 6.2: Laminated glacial Black Sea sediments: (a) image of a polished epoxy block; (b) optical microscope image of a thin section showing the alternation of dark, coarse silt-rich laminae with probably higher organic content (gray key), and lighter clay laminae (white key).

The sequence of clastic rhythmites is best recognized visually and on the polished epoxy block images. Optical microscopy shows that the boundaries between consecutive layers are not sharp features. According to the image analysis, couplets are on average 2.14 mm thick. The thickness of individual dark and light lamina falls into a range of 0.23 mm to 2.96 mm, with an average thickness of ~1 mm.

Scanning Electron Microscope imaging

We performed SEM imaging and EDS X-ray mapping to verify whether the glacial Black Sea lamination is mainly grain size induced. The BSE scanning shows no significant compositional changes between light and dark layers (Fig. 6.3a and b) and confirms differences in grain size as the main control on laminae formation. Additionally, systematical EDS X-ray mapping also suggests that consecutive couplets of light and dark layers do not vary statistically in the major elements distribution (Fig. 6.3c).

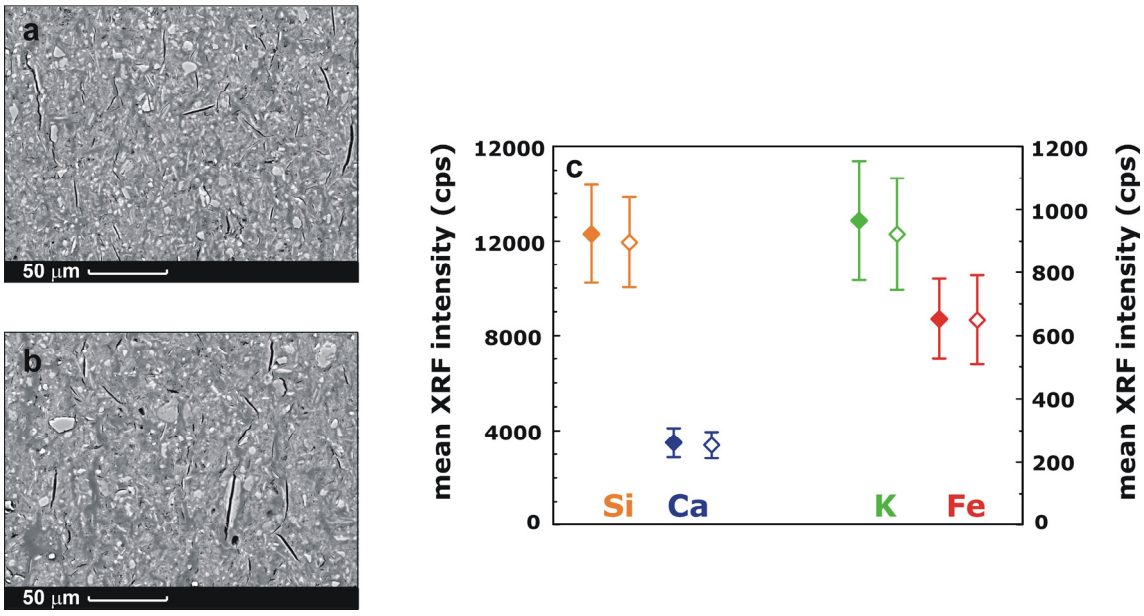

Figure 6.3: Samples of back-scattered electron (BSE) images showing no compositional difference in the minerogenic components of: (a) fine/light layer and (b) coarse/dark layer. (c) Results of EDS-based element distribution results. The mean and the standard deviation of all measurements for coarse/dark (closed diamonds) and fine/light (open diamonds) laminae. EDS X-ray mapping (400x400 µm) was repeated three times along the same laminae for 8 selected couplets.

Floating chronology

Presently, MD04-2788/2760 reaching back to ~26 cal ka BP and is the best-dated Black Sea record available (Kwiecien et al. 2008). According to the chronology, which is based on calibrated reservoir-corrected AMS ^{14}C ages and the Y-2 tephra layer, the investigated interval falls into the Last Glacial Maximum (LGM). Relatively large dating and reservoir-correction uncertainties valid for the glacial sediments result in a wide calibration probability range of the two anchoring points (21.27-22.29 cal ka BP for the Y-2 tephra and 21.74-22.92 cal ka BP for the ostracod sample). The calibration to the calendar time scale allocates the radiocarbon dates on the absolute time scale but adds additional uncertainty to the radiocarbon dating error itself. Normally, the calibration affects only to a minor extent the absolute interval between consecutive dates. In case of our chronology, the implementation of a mean Y-2 Cape Riva age (calculated from 4 different AMS ^{14}C dates, Fig. 6.4) into the age model results in a difference of ~70 yr in the duration of the investigated interval (480 ^{14}C years vs. 550 calibrated years).

To check the relation of our potential varve chronology to the radiocarbon-constrained one we applied following approach: (1) By extracting grayscale we obtained a semi-objective tool necessary to perform layer counting. Subsequently, the results of the grayscale-based layer counting were tested and re-proved by digitizing the thickness of the individual layers. As the results of our layer counting fit well within the errors of the reservoir-corrected uncalibrated age model (Fig. 6.4) we compared in a next step (2) the results of our layer counting to the calibrated age model. The respective time span constrained by the calibrated age model (550 yrs) matches very well our layer counting (522 couplets +/- 6%). We anchored our varve chronology arbitraly to the younger of the two bracketing dates (Y-2 Cape Riva age).

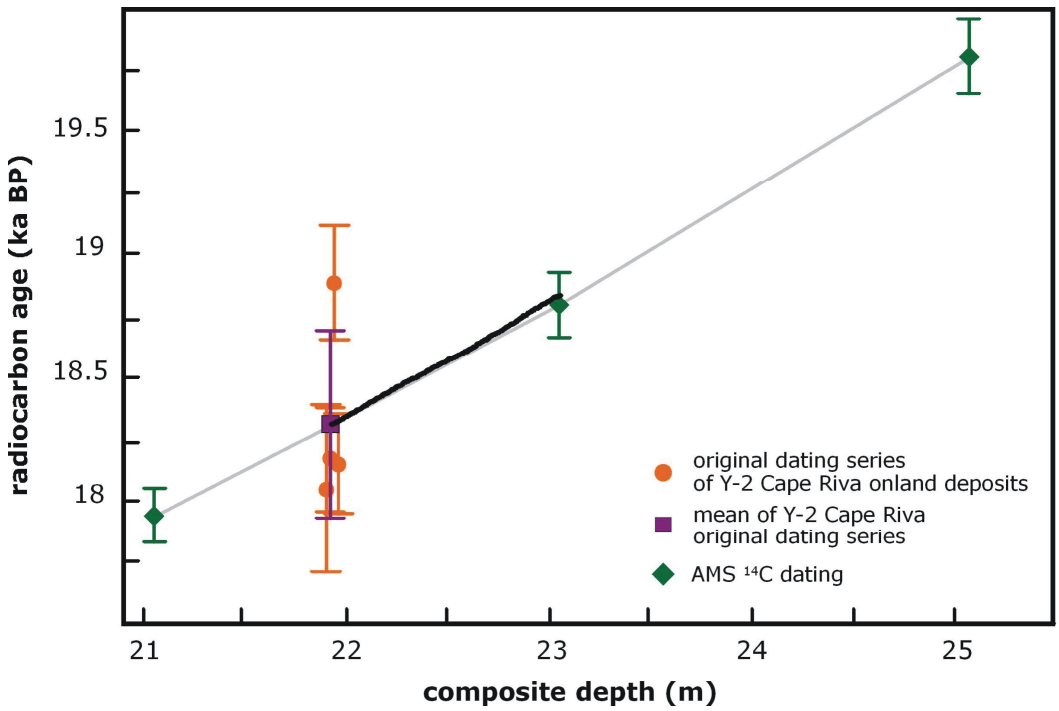

Figure 6.4: Age-depth relation for the investigated interval in MD04-2788/2760. The radicarbon dates from MD04-2788/2760 are reservoir corrected. The black line represents the cumulative thickness of the couplets and is plotted against the age by assuming that the deposition of couplets represents an annual cycle. The gray line shows the linear interpolation between the mean value of 4 calibrated Y-2 tephra ages (Eriksen et al., 1990; Pilcher and Friedrich, 1976) and the reservoir-corrected calibrated ostracod dating sample (Kwiecien et al, 2008).

Profiling measurements

The µXRF Ca-intensity record follows very closely the lower-resolution signal (Fig. 6.5B). The low-amplitude change of the µXRF signal is comparable with the amplitude of the lower-resolution measurements and yet provides far more detailed information. The correlation between the intensity-pattern of other elements (e.g. K, Fe, Si) measured with low- and high- resolution is similarly very good (not shown). The comparison between µXRF intensity and respective high resolution images of laminated blocks does, however, not bring a satisfactory fit (Fig. 6.6). Two instrumental limitations can account for this discrepancy: (1) µXRF measurements were conducted on the core sections in the central part of the core while the samples for epoxy blocks were taken from the core margins. Thus, we cannot exclude peripheral deformation of the lamination pattern visible in blocks. (2) If the supposition about the annual character of the lamination is correct, then the resolution of 500 µm (resulting in 4 measuring points per year) may be not sufficient to clearly depict intra-annual changes.

The magnetic susceptibility values are relatively low (between 160 and 330 10^{-6} SI) (Fig. 6.5D). Very high values (up to 6000) mark the occurrence of secondary greigite and were removed from the record. The amplitude of changes in the greigite-corrected magnetic susceptibility record is relatively low but the pattern corresponds very well to the µXRF Ca-intensity record.

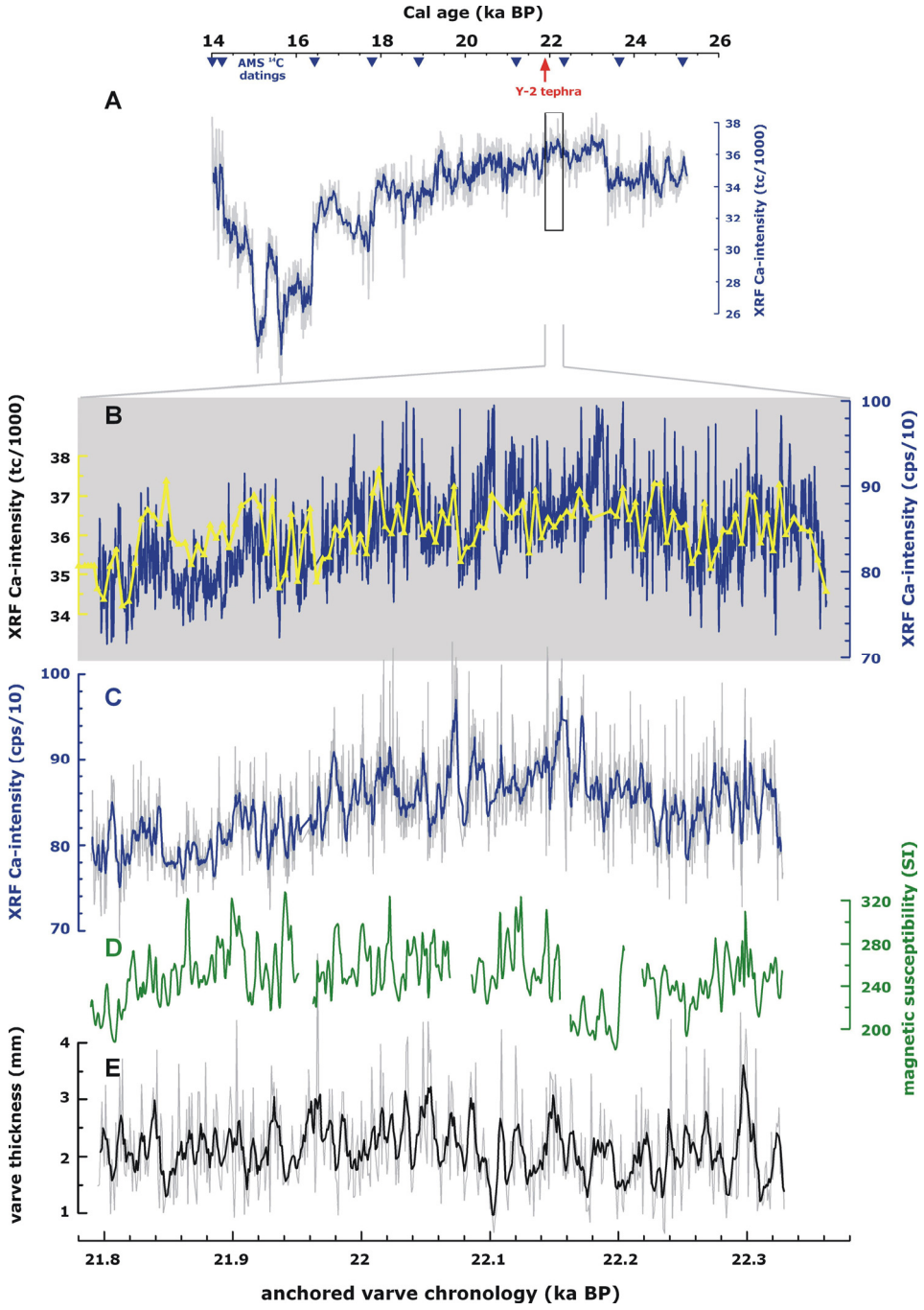

Figure 6.5: Comparison of the MD04-2788/2760XRF, µXRF, magnetic susceptibility, and varve thickness records from the analyzed interval. The chronology is based on reservoir-corrected calibrated ^{14}C ages (Kwiecien et al., 2008). A and B are presented on a linearly interpolated time scale, whereas C, D and E are presented on a 'varve years' time scale anchored to the calibrated age of the Y-2 tephra. (A) Data obtained from the AVAATECH scanner at 1 cm resolution. The gray line represents the original data and the blue line represents a 7-point moving average. (B) Correlation of the data obtained from the AVAATECH scanner at 1 cm resolution (yellow) and the EDAX Eagle III scanner at 500 µm resolution (blue). (C) µXRF Ca-intensity. The gray line represents the original data, the blue and red line represents 9-point running averages. (E) Greigite-corrected magnetic susceptibility data. (D) Varve thickness. The gray line represents the original data and the black line the 5-point running average.

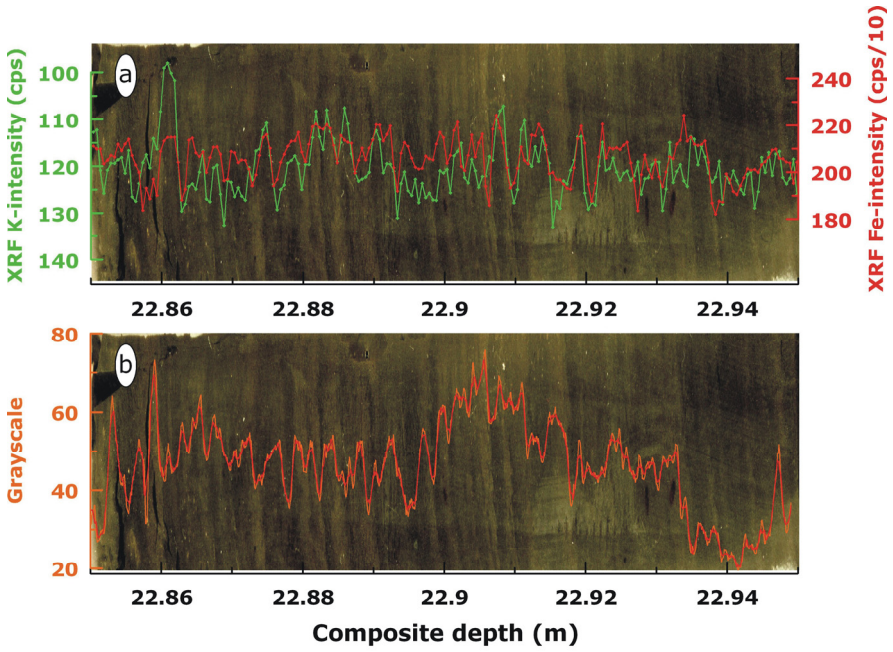

Figure 6.6: An example of (a) µXRF scanning results; in red XRF Fe intensity; in green XRF K intensity; (b) grayscale analysis juxtaposed on the image of the respective block.

DISCUSSION

Nature of the glacial lamination

Our analyses suggest that the glacial lamination in the Black Sea is predominantly grain-size controlled. The contrasting colors may attribute to secondary effects related to the differences in grain-sizes, because coarser layers are more porous thus appearing darker in the epoxy blocks, while more homogenous fine grained layers appear lighter. Additionally, changes in color may relate to some extend to minor changes in the organic carbon content. EDS X-ray mapping of consecutive laminae (Fig. 6.3c) suggest that the material of coarse and fine layers is of the same composition and probably provenance.

A typical example of laminae defined by changes in color and terrigenous grain size are clastic varves first described by de Geer (1912) and since then found in many glacio-lacustrine environments e.g. (Brauer and Casanova, 2001; Petterson, 1996). In case of clastic varves, coarse layers result from the spring meltwater discharge and alternate with finer sediment deposited during winter in a potentially ice covered lake environment. It seams reasonable that laminated sediments deposited in periglacial environments, under much more extreme climatic conditions, display much stronger contrasts in color and grain size than in the Black Sea sediments. Noteworthy, similar differences in grain size may be also produced by a variety of depositional mechanisms, not related to processes operating in annual cycles (e.g. settling from distant turbidity currents or detached turbid layers [O'Brien, 1996; Schieber et al., 2007]). However as the site MD04-2788/2760 is located on a bathymetric ridge, well below the storm base it remains unaffected by redeposition processes. Additionally, the glacial Black Sea was probably well mixed (Bahr et al., 2006) whereas the formation of detached turbid layers requires stratification. After excluding other than annual depositional processes we verified the number of layers/couplets with the radiocarbon time frame of the respective interval (Fig. 6.4). The very good agreement of AMS ^{14}C uncalibrated and calibrated

dates with the couplets thickness curve confirms the assumption that one couplet was deposited during one year.

The deposition of intercalating couplets following the annual cycle calls for a seasonal mechanism forcing changes in grain sizes. During the glacial, in the Mediterranean region seasonal precipitation gradient between winter and summer was similar or possibly stronger than today (Prentice et al., 1992). Therefore, seasonal changes in the Sakarya River run-off could account for producing laminated sediments with the coarse layer representing the higher energy regime related to winter/spring increased precipitation. We favor an alternative scenario suggested by a modeling study of (Robinson et al., 2006) and claiming that in the glacial much of the precipitation over the Anatolian uplands fell as snow. In that case, the coarser dark layer could correspond to the spring thaw season with increased higher-energy river discharge, while the finer light layer would deposit during the fall and winter. The dark color of the coarser layers (which may be also resulting from higher content of organic material) promotes the concept of spring thaw associated with blooms of non-calcifying phytoplankton.

Climatic implications

(Kwiecien et al., submitted) suggested that the glacial Ca-intensity record of core MD04-2788/2760 represents precipitation-related changes in the supply of detrital carbonates. Accordingly, higher carbonate contents relate to more intense regional precipitation in the Sakarya River catchment. Using the millennial-scale reconstruction (Kwiecien et al., submitted) as an analog, the μXRF Ca-intensity may also be translated in terms of detrital carbonate content.

Magnetic susceptibility measurements are valuable for sediment studies as they can indicate temporal variation in the concentration and grain size of terrigenous material deposited in aquatic environment. In many lacustrine sediments receiving material from a single catchment higher magnetic susceptibility values reflect enhanced/coarser terrigenous input (Verosub and Roberts, 1995). As the SEM results suggest no compositional differences within the investigated interval we assume that changes in the magnetic susceptibility predominantly illustrate grain size variability. Good correspondence between magnetic susceptibility and μXRF Ca-intensity suggest that enhanced detrital carbonate supply was accompanied by input of coarser magnetic material. Both, μXRF Ca-intensity and magnetic susceptibility measurements show significant parallel changes on decadal to sub-decadal scale (e.g. Ca-intensity, fig. 6.5C, 6.5D), however, they do not follow precisely the visual lamination pattern (Fig. 6.6).

While the difference in mineralogical composition of dark and light layers seems to be statistically not significant, the interannual/decadal variations in the μXRF intensities and magnetic susceptibility point to significant changes in the sediment fluxes. Interannual/decadal changes in sediment flux can also be reflected by the variations in varve thickness (Fig. 6.5C). In order to examine this potential relationship we re-plotted the μXRF and magnetic susceptibility data using a non-linear 'varve year' scale as time axis. μXRF Ca-intensity and magnetic susceptibility data show patterns roughly similar to the varve thickness record (Fig. 6.5C-6.5.E) implying that higher carbonate content and generally coarser material correspond to relatively higher sediment flux. Additional support for this concept comes from a clear anti-correlation of the μXRF Ca- and K-intensities (Fig. 6.7). During the full glacial K is associated mostly with clay minerals and therefore the fine sediment fraction. We expect that higher intensites of K point to a relatively increased clay content during periods of weaker river transport-capacity and decreased sediment flux. The variable sediment flux to our core site can be seen as a derivative of the erosion rates in the Sakarya River drainage basin and the general river

transport-capacity. These features are dependant on the precipitation regime (in form of snow and/or rain). Our results tend to confirm our previous interpretation that e.g. changes in the detrital carbonate content reflect changes in precipitation also for the longer time scales (Kwiecien et al., submitted).

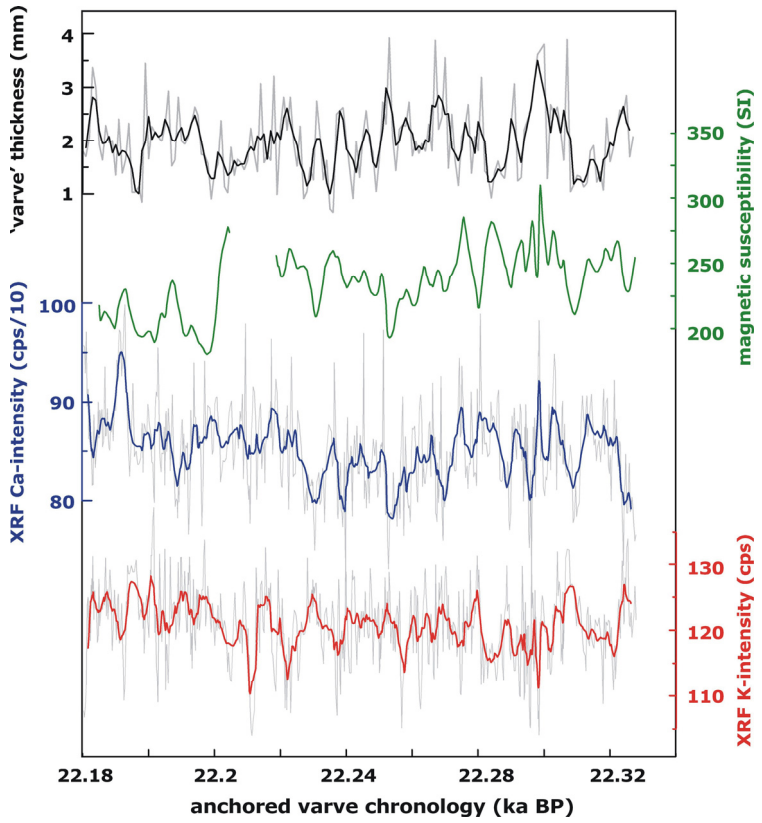

Figure 6.7: Comparison of the μXRF Ca- and K- intensities, magnetic susceptibility, and varve thickness records from the ~150 yrs within analyzed interval. All of the proxies are presented on a 'varve years' time scale anchored to the calibrated age of Y-2 tephra. For the varve thickness, the gray line represents the original data and the black line represents the 3-point running average. For the Ca- and K-intensity the gray line represents the original data and the blue and red line represent the 9-point running average.

The bracketing calibrated radiocarbon ages are placing the investigated ~500 yr interval within the Last Glacial Maximum. This period was characterized by generally reduced amplitude of millennial/centennial-scale climate variability (Mix et al., 2001). Today, the Mediterranean region receives most of its rainfall in winter, and the precipitation pattern is strongly (though not exclusively) influenced by the North Atlantic Oscillation. Some studies of glacial Mediterranean climate (e.g. Moreno et al., 2005) compare relatively mild and humid Dansgaard-Oeschger (D/O) interstadials to low NAO index conditions and dry D/O stadials and Heinrich Events to a high NAO index. Noteworthy, the glacial boundary conditions (e.g. pressure gradients related to the continental and sea ice extent and the location of the major permanent low and high pressure cells) were very different from today. Nevertheless, a similar atmospheric phenomenon related to pressure gradients might have been operating in the glacial period. Consequently, long-term persisting positive/negative phase of such a mode in LGM could have reduced precipitation variability in Mediterranean region over longer time scales. Our ~500 yr record shows relatively stable glacial conditions on the longer time scale, yet clearly suggests short-term changes in regional precipitation in NW Anatolia. Spectral analysis (performed with the Analyseries 1.2 software [Paillard et al.,

1996]) of µXRF Ca-intensity data and the varve thickness record indicate significant power in the frequency range of 3 to 10 years (Fig. 6.8) suggesting significant interannual to decadal time-scale processes influencing regional precipitation in NW Anatolia.

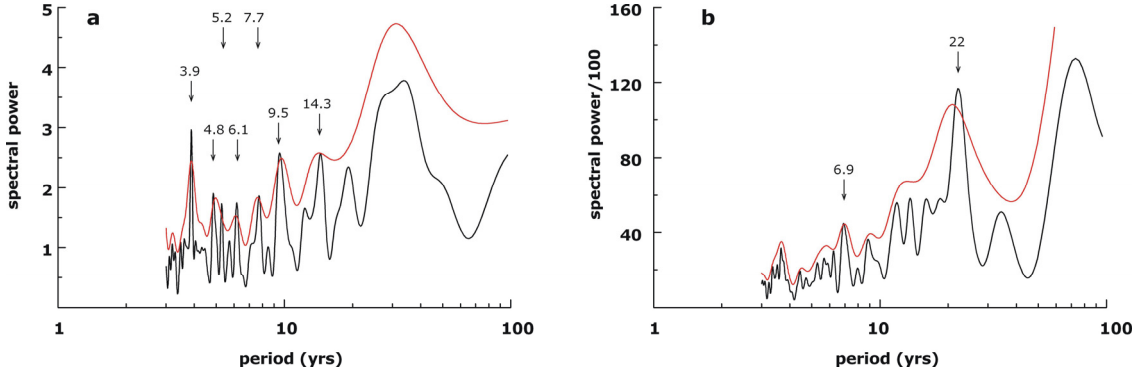

Figure 6.8: Blackman–Tukey spectrum of the (a) varve thickness and (b) detrended µXRF Ca-intensity for the analyzed interval. Before analysis µXRF data were allocated on the varve year time scale. Analyses were performed with the Analyseries software (black line: one sided confidence interval at the 80% level, red line: low-resolution spectrum).

CONCLUSIONS AND OUTLOOK

The presence of a grain size induced lamination in the Black Sea glacial sediments suggests significant changes in runoff-related terrigenous supply. Results of layer counting compared to the linearly interpolated age model confirm the annual character of the lamination. Consequently, the couplets represent clastic varves whit the coarse/dark layers depositing during the spring thaw likely associated with non-calcifying phytoplankton blooms, and the fine/dark layers forming during fall and winter.

In order to fully exploit the potential of the Black Sea laminated sequences it is important to present results of high-resolution measurements (like µXRF analysis and magnetic susceptibility) not on a linearly interpolated time scale but on a constructed 'varve year' time axis. Providing a floating chronology anchored to calibrated radiocarbon ages allows a more detailed study of inter-annual and decadal scale changes. As the older part of the glacial Black Sea sequence has satisfactory AMS^{14}C age control, the study of short-term climate variability could be extended to ~26 cal ka BP. The interannual variability within millennial-scale hemispheric cooling events, like the Heinrich Event 2 (centered at ~23.5 cal ka BP [Bard et al., 2000]) may improve our understanding of short term-climate dynamics.

ACKNOWLEDGMENTS

This research was sponsored by Comer Science and Education Foundation (CS&EF). We thank IPEV for logistic support during the ASSEMBLAGE I cruise (RV *Marion Dufresne*). We thank Michael Köhler and Gabi Arnold for the preparation of blocks and thin-sections and a Spectral Electron Microscope team, Helga Kemnitz and Juliane Herwig for introduction to the SEM facility.

7. Summary

7.1. Main results

Each of the manuscripts that are part of my thesis concentrates either on a specific issue, like chronostratigraphy *(Manuscript 1)*, Black Sea water temperature and chemistry changes *(Manuscript 3)*, nature of the Black Sea glacial lamination *(Manuscript 5)*, or a certain time frame, like 14-26 cal ka BP *(Manuscript 2)*, or the deglaciation *(Manuscript 4)*. Here I present in a chronological order a synthesis of the most important results.

Glacial sedimentation in the Black Sea was dominated by terrigenous input and characterized by high sedimentation rates. At the site MD04-2788/2760 the supply of carbonate- and organic poor material was mainly controlled by precipitation-dependant local river run-off. Fine alternations of light-colored clays and darker-colored silts most likely represent annual deposition cycles with the darker coarser layers deposited during spring thaws. Low glacial C/N ratio values suggest a very restricted input of terrestrial organic material. Sparse vegetation cover in the Black Sea drainage most likely facilitated enhanced minerogenic input and favored erosion of also carbonatic rocks leading to a contamination of the Black Sea water body with old, in terms of radiocarbon, 'dead' carbon. The recognition of the Y-2 tephra, which originated from the Cape Riva eruption, allowed to estimate the glacial apparent reservoir age of the Black Sea to be ~1450 ^{14}C yr. A comparison of records from different water depths implies that this age offset was characteristic for a fairly well homogenized glacial water column. During the full glacial, the southward-shifted Polar Front reduced the moisture transport to the northern - European drainage of the Black Sea and let the southern – Mediterranean drainage become dominant in freshwater and sediment supply to the basin. The good correspondence between rainfall intensity in NW Anatolia (reconstructed from changes in the terrigenous supply by the Sakarya River) and past Mediterranean SSTs implies that during the glacial the regional precipitation variability was controlled, like today, by Mediterranean cyclonic disturbances. Connected to the Mediterranean SSTs, the regional precipitation decreased in response to the North Atlantic cooling events H1 and H2. In contrast to the reconstructed changes in precipitation, the hydrological properties of the Black Sea (like the surface temperature, isotopic composition and chemistry of the water) remained relatively stable suggesting that the Black Sea was locked in a glacial steady-state.

Significant changes in the Black Sea hydrology took place around 16.4 cal ka BP and were the first symptoms of the deglacial warming. Meltwater pulses, derived most probably from the disintegrating European ice sheets, led to a temporal depletion of the Black Sea δ^{18}O and decreased the apparent age of the Black Sea water to ~1000 ^{14}C yr. At about that point, northern sediment sources were reactivated and increased the supply of fine-grained material prompting the deposition of characteristic reddish layers. Together with the sediment supply from the southern drainage, this contributed to generally higher sedimentation rates in the southwestern Black Sea. This intensification of sediment supply is consistent with other geomorphological (lake level) and pollen records from the Mediterranean region and points to a major reorganization of the atmospheric circulation patterns, affecting the hydrology of the European continent. At approximately the same time sea surface temperatures in the Western Mediterranean show an abrupt warming (Cacho et al., 1999) and precipitation in the Eastern Mediterranean a significant increase (Bar-Matthews et al., 1997; Jones et al., 2007).

These changes related to the deglacial northward retreat of the oceanic and atmospheric polar fronts signalized a mitigation of the Northern European and Mediterranean climate. However, a decisive

increase in local temperature in the Black Sea region took place only later at the transition from the Oldest Dryas to the Bølling around 14.6 cal ka BP. A likely warming of the Black Sea surface led to massive phytoplankton blooms, which in turn induced precipitation of inorganic carbonates. This biologically triggered process is well documented in abrupt changes in the $\delta^{18}O_{bulk}$ and Mg/Ca and Sr/Ca ratios of ostracod shells. Additionally, it could have accounted for a contemporary reduction of the apparent age of the upper water column to nearly 0 yr. Mg/Ca and Sr/Ca ratios determined on benthic ostracod shells changed rapidly within the entire water column, while the signal of enriched isotopic composition of rainfall propagated more gradually to the Black Sea intermediate and deep water. Similarly, the soil development and response of the vegetation in NW Anatolia was not immediate and postdated the Bølling warming by ~200 years. Vegetation-related changes in the drainage basin reduced the run-off and caused a significant decrease in local sedimentation rates. Paralleling the changes in Black Sea water chemistry, this could have diminished the hardwater effect by decreasing a supply of 'old' carbon. Latest from the Allerød on, the apparent ages of the intermediate and upper water column were probably evolving divergently.

A decoupling of precipitation in the hinterland (NW Anatolia) and hydrological changes in the western Black Sea which can be observed during the early deglaciation may be explained by a subdued response of the Black Sea to the millennial-scale changes of the glacial atmospheric circulation. Starting with the B/A warming and proceeding through the YD cold interval and the Early Holocene warming, the Black Sea temperature signal corresponds to the precipitation and temperature changes recorded in the wider Mediterranean region. This implies that only the Bølling warming could release the Black Sea basin from its previous glacial steady-state situation, triggering internal changes in the basin and on the adjacent continent (NW Anatolia).

During the Younger Dryas cold period the ostracod Mg/Ca ratios imply a 1-2°C cooling of the Black Sea deep water. A much stronger surficial cooling may be inferred from diminished phytoplankton activity during this period and a general vegetation retreat in the Mediterranean region. Comparably, rainfall-related changes in the isotopic composition of the Black Sea water slowed down.

Early Holocene conditions were similar to those of the Bølling/Allerød but were punctured by the marine inflow from the Mediterranean at ~9.3 cal ka BP, which initiated the end of the lacustrine phase of the Black Sea. This reconnection had a substantial impact on the chemical, biological, and physical properties of its water. The modern reservoir age of the Black Sea water established after the reconnection with the Mediterranean Sea and is a result of processes clearly different from those operating in the closed, glacial Black 'Lake' basin. In contrast to the glacial conditions, the recent permanent stratification and isolation of the intermediate and deep water from atmospheric CO_2 favor not an apparent but a real increased reservoir age of the deeper water column.

7.2. Conclusions

Sediment cores retrieved along a N-S transect in the western Black Sea provide comprehensive information on the environmental changes that took place in the basin and on the adjacent continents. The analysis of a new record MD04-2788/2760 from the southwestern Black Sea improved our understanding of the climatic changes of the last 26 ka in the Black Sea region and shed light on the role of the North Atlantic climate regime and the connection between the climatic evolution of Western and Eastern Mediterranean region during this period. The most important findings of my thesis include:

- Conceptual model of temporal and spatial changes in the reservoir age of the glacial Black Sea water masses. Once applied to dates obtained on biogenic Black Sea samples, the model may serve as a chart for estimating reservoir ages and provide information on the possible range of corrections for radiocarbon ages.

- Mechanism linking changes in glacial precipitation pattern in NW Anatolia to abrupt North Atlantic cooling events (Heinrich Events). A decrease in rainfall intensity in NW Anatolia observed during H1 and H2 was likely related to the cooling of Mediterranean Sea surface which in turn inhibited formation of moisture-bearing winter cyclones.

- Evidence for the mitigation of the Northern and Central European climate after ~16.4 cal ka BP, simultaneous to a warming in the Mediterranean region. This early deglacial changes were related to a northward retreat of the polar fronts.

- Constraining the time of the initial Mediterranean inflow into the Black Sea to ~9.3 cal ka BP.

- Spatial constraints on the eastward extent of the North Atlantic climate influence on the continental climate variability during the MIS2 and transition to MIS1. Late Glacial decoupling of the precipitation in the southern Black Sea drainage area (NW Anatolia) and the temperature-related changes in the hydrology of the basin itself suggests a subdued response of the Black Sea to millennial-scale changes of the glacial atmospheric circulation. The Black Sea was released from its relatively stable glacial mode at the onset of the decisive Bølling warming.

7.3. Outlook

The paleoclimatic investigations presented in my thesis demonstrate the potential of the Black Sea for paleoenvironmental reconstruction. The nature, location, and the enormous size of the basin open a wide spectrum of possibilities for future paleoclimatic studies.

A further improvement of the chronostatigraphic framework remains one of the most important tasks. Sediment cores from intermediate water depths (ca. 1200 m) present complete and undisturbed sequences but are difficult to date due to the scarcity of suitable dating material. On the contrary, large bivalve shells - excellent dating material - are abundant in cores from shallower water depths, but these cores often contain hiatuses. In the course of the thesis I showed, using a multi-proxy approach, that within the western Black Sea basin certain processes were synchronous. This knowledge may not only be used to correlate new cores from different water depths, but is essential for comparison of independently dated records in order to test the proposed model of reservoir age changes. Another point worth examining concerns indirectly inferred changes in the vegetation cover. An additional direct method, like pollen analysis, could produce interesting results and improve the comparison between lake conditions and processes taking place in the drainage area.

The N-S Black Sea transect gave way to investigate local environmental changes (NW Anatolia, Eastern Central Europe) but also provided information about large-scale regional climate oscillations. Focusing future Black Sea research on the eastern basin and initiating a W-E transect may bring comprehensive insight into the past climate of the northern Middle-East.

Initial examination of newly retrieved sediment cores from the eastern Black Sea (R/V *Meteor* cruise 72/5, unpublished data) brought very promising results. Cores recovered from the northern Black Sea, south of the Sea of Azov show high sedimentation rates which predestine them to record with detail the late glacial period. On the other hand, the discovery of a pre-Holocene sapropel (most likely Eemian) in the southeastern Black Sea suggests that these sediments cover the complete last glacial-interglacial cycle and record environmental changes resembling the high-amplitude Daansgard-Oeschger variability in the early part of MIS 3. In light of these preliminary results, the Black Sea emerges as an even more valuable continental archive.

While disconnected from the global ocean, the glacial Black Sea must have been similar to the modern Caspian Sea. Extending the scope of interest even further east into the Caspian Sea to test if/how hydrology of this basin reacted on climatic changes of a last glacial/deglaciation might be a truly compelling quest.

Finally yet importantly, the youngest reconnection history with the Mediterranean Sea stays an intriguing issue. Combining the western Black Sea profiles with the newly recovered sediment cores from the eastern basin may shed more light on a spatial development of the last lacustrine/marine transition. A detailed geochemical investigation together with microfacies analysis will provide more information on the dynamics of the reconnection process. Moreover, southeastern cores give a chance, for the first time, to investigate scrupulously the inverse process, namely the desalinification of the Black Sea basin that accompanied the transition from the ‘Eemian’ marine to the last lacustrine phase. Although precise and direct dating of the last interglacial Black Sea sediments is challenging, new data are likely to contribute to the understanding of the Black Sea hydrological evolution.

8. References

Aksu, A. E., Hiscott, R. N., Yasar, D., Isler, F. I., and Marsh, S. (2002). Seismic stratigraphy of Late Quaternary deposits from the southwestern Black Sea shelf: evidence for non-catastrophic variations in sea-level during the last 10 000 yr. *Marine Geology* 190, 61-94.

Algan, O., Gazioglu, C., Cagatay, M. N., Yücel, Z. Y., and Gonencgil, B. (1999). Sediment and water influxes into the Black Sea by Anatolian rivers. 43, 61-67.

Algan, O., Gokasan, E., Gazioglu, C., Yücel, Z. Y., Alpar, B., Guneysu, C., Kirci, E., Demýrel, S., Sari, E., and Ongan, D. (2002). A high-resolution seismic study in Sakarya Delta and Submarine Canyon, southern Black Sea shelf. *Continental Shelf Research* 22, 1511-1527.

Allen, J. R. M., Brandt, U., Brauer, A., Hubberten, H.-W., Huntley, B., Keller, J., Kraml, M., Mackensen, A., Mingram, J., Negendank, J. F. W., Nowaczyk, N. R., Oberhansli, H., Watts, W. A., Wulf, S., and Zolitschka, B. (1999). Rapid environmental changes in southern Europe during the last glacial period. *Nature* 400, 740-743.

Aloisi, G., Drews, M., Wallmann, K., and Bohrmann, G. (2004). Fluid expulsion from the Dvurechenskii mud volcano (Black Sea): Part I. Fluid sources and relevance to Li, B, Sr, I and dissolved inorganic nitrogen cycles, *Earth and Planetary Science Letters*, 225, 347-363.

Anadón, P., Gliozzi, E., and Mazzini, I. (2002), Paleoenvironmental reconstruction of marginal marine environments from combined paleoecological and geochemical analyses on ostracods. *In Holmes, J.A. (Ed): Ostracoda: Applications in Quaternary Research, Geopyhs. Monogr. Ser, vol. 113, pp. 227-247 AGU, Washington D. C.*

Andersen, K. K., Svensson, A. M., Johnsen, S. J., Rasmussen, S. O., Bigler, M., Rothlisberger, R., Ruth, U., Siggaard-Andersen, M.-L., Peder Steffensen, J., Dahl-Jensen, D., Vinther, B. M., and Clausen, H. B. (2006). The Greenland Ice Core Chronology 2005, 15-42 ka. Part 1: constructing the time scale. *Quaternary Science Reviews* 25, 3246-3257.

Arz, H. W., Pätzold, J., and Wefer, G. (1998). Correlated Millennial-Scale Changes in Surface Hydrography and Terrigenous Sediment Yield Inferred from Last-Glacial Marine Deposits off Northeastern Brazil. *Quaternary Research* 50, 157-166.

Atanassova, J. (2005). Palaeoecological setting of the western Black Sea area during the last 15000 years. *The Holocene* 15, 4, 576-584.

Bahr, A. (2005). Late Glacial to Holocene Paleoenvironmental Evolution of the Black Sea. *PhD Thesis*, 121 pp. Universität Bremen

Bahr, A., Arz, H. W., Lamy, F., and Wefer, G. (2006). Late glacial to Holocene paleoenvironmental evolution of the Black Sea, reconstructed with stable oxygen isotope records obtained on ostracod shells. *Earth and Planetary Science Letters* 241, 863-875.

Bahr, A., Lamy, F., Arz, H. W., Major, C. O., Kwiecien, O., and Wefer, G. (2008). Abrupt changes of temperature and water chemistry in the late Pleistocene and early Holocene Black Sea. *Geochemistry Geophisics Geosystems* 9, Q01004, doi:10.1029/2007GC001683

Bahr, A., Lamy, F., Arz, H., Kuhlmann, H., and Wefer, G. (2005). Late glacial to Holocene climate and sedimentation history in the NW Black Sea. *Marine Geology* 214, 309-322.

Bard, E., Hamelin, B., Arnold, M., Montaggioni, L., Cabioch, G., Faure, G., and Rougerie, F. (1996). Deglacial sea-level record from Tahiti corals and the timing of global meltwater discharge. *Nature* 382, 241-244.

Bard, E., Rostek, F., Turon, J.-L., and Gendreau, S. (2000). Hydrological Impact of Heinrich Events in the Subtropical Northeast Atlantic. *Science* 289, 1321-1324.

Bar-Matthews, M., Ayalon, A., and Kaufman, A. (1997). Late Quaternary Paleoclimate in the Eastern Mediterranean Region from Stable Isotope Analysis of Speleothems at Soreq Cave, Israel. *Quaternary Research* 47, 155-168.

Bartov, Y., Goldstein, S. L., Stein, M., and Enzel, Y. (2003). Catastrophic arid episodes in the Eastern Mediterranean linked with the North Atlantic Heinrich events. *Geology* 31, 439-442.

Benson, L., and Paillet, F. (2002). HIBAL: a hydrologic-isotopic-balance model for application to paleolake systems. *Quaternary Science Reviews* 21, 1521-1539.

Bond, G., Broecker, W. S., Johnsen, S. J., McManus, J., Labeyrie, L., Jouzel, J., and Bonani, G. (1993). Correlations between climate records from North Atlantic sediments and Greenland ice. *Nature* 365, 143-147.

Bourdeau, B. P., and Leblond, P. H. (1989). A simple evolutionary model for water and salt in the Black Sea. *Paleoceanography* 4, 157-166.

Brauer, A., and Casanova, J. (2001). Chronology and depositional processes of the laminated sediment record from Lac d'Annecy, French Alps. *Journal of Paleolimnology* 25, 163-177.

Burton, E. A., and Walter, L. M. (1991), The effects of PCO_2 and temperature on magnesium incorporation in calcite in seawater and $MgCl_2$-$CaCl_2$ solutions, *Geochimica et Cosmochimica Acta*, 55, 777-785.

Cacho, I., Grimalt, J. O., Canals, M., Sbaffi, L., Shackleton, N. J., Schönfeld, J., and Zahn, R. (2001). Variability of the western Mediterranean Sea surface temperature during the last 25 000 and its connection the Northern Hemisphere climatic changes. *Paleoceanography* 16, 40-52.

Cacho, I., Grimalt, J. O., Pelejero, C., Canals, M., Sierro, F. J., Flores, J. A., and Shackleton, N. (1999). Daansgard-Oeschger and Heinrich event imprints in Alboran Sea paleotemperatures. *Paleoceanography* 14, 689-705.

Cacho, I., Grimalt, J. O., Sierro, F. J., Shackleton, N., and Canals, M. (2000). Evidence for enhanced Mediterranean thermohaline circulation during rapid climatic coolings. *Earth and Planetary Science Letters* 183, 417-429.

Cacho, I., Shackleton, N., Elderfield, H., Sierro, F. J., and Grimalt, J. O. (2006). Glacial rapid variability in deep-water temperature and $\delta^{18}O$ from the Western Mediterranean Sea. *Quaternary Science Reviews* 25, 3294-3311.

Chapman, M. R., and Maslin, M. A. (1999). Low-latitude forcing of meridional temperature and salinity gradients in the subpolar North Atlantic and the growth of glacial ice sheets. *Geology* 27, 875-878.

Chester, R. (1990), *Marine Geochemistry*, 698 pp., Unwyn Hyman, London,

Chivas, A. R., De Deckker, P., and Shelley, J. M. G. (1983). Magnesium, strontium and barium partitioning in nonmarine ostracod shells and their use in paleoenvironmental reconstructions - a preliminary study, in *Applications of Ostracoda,* edited by R. F. Maddocks, pp. 238-249, Univ. Houston Geosci., Houston.

Chivas, A. R., De Deckker, P., and Shelley, J. M. G. (1986a). Magnesium and strontium in non-marine ostracod shells as indicators of palaeosalinity and palaeotemperature, *Hydrobiologia*, 143, 135-142.

Chivas, A. R., De Deckker, P., and Shelley, J. M. G. (1985). Strontium content of ostracods indicates lacustrine palaeosalinity, *Nature*, 316, 251.

Chivas, A. R., De Deckker, P., and Shelley, J. M. G. (1986b). Magnesium content of non-marine ostracod shells: a new palaeosalinometer and palaeothermometer, *Palaeogeography, Palaeoclimatology, Palaeoecology*, 54, 43-61.

CLIMAP (1981). Seasonal reconstructions of the earth's surface at the last glacial maximum. *Geological Society of America Map and Chart Series* MC-36.

Cloething, S., Spadini, G., Van Wees, J. D., and Beekman, F. (2003). Thermo-mechanical modelling of Black Sea Basin (de)formation. *Sedimentary Geology* 156, 169-184.

Combourieu Nebout, N., Paterne, M., Turon, J.-L., and Siani, G. (1998). A high-resolution record of the last deglaciation in the Central Mediterranean Sea: Palaeovegetation and Palaeohydrological Evolution. *Quaternary Science Reviews* 17, 303-317.

Combourieu Nebout, N., Turon, J. L., Zahn, R., Capotondi, L., Londeix, L., and Pahnke, K. (2002). Enhanced aridity and atmospheric high-pressure stability over the western Mediterranean during the North Atlantic cold events of the past 50 k.y. *Geology* 30, 863-866.

Cortijo, E., Labeyrie, L., Elliot, M., Balbon, E., and Tisnerat, N. (2000). Rapid climatic variability of the North Atlantic Ocean and global climate: a focus of the IMAGES program. *Quaternary Science Reviews* 19, 227-241.

Cronin, T. M., Dwyer, G. S., Kamiya, T., Schwede, S, .and Willard, D. A. (2003). Medieval Warm Period, Little Ice Age and 20th century temperature variability from Chesapeake Bay, *Global and Planetary Change*, 36, 17-29.

Crusius, J., and Anderson, R. F. (1992). Inconsistencies in accumulation rates of Black sea sediments inferred from records of laminae and ^{210}Pb. *Paleoceanography* 7, 215-227.

Cullen, H. M., and deMenocal, P. (2000). North Atlantic Influence on Tigris-Euphrates streamflow. *International Journal of Climatology* 20, 853-863.

De Deckker, P., Chivas, A. R., and Shelley, J. M. G. (1999). Uptake of Mg and Sr in the euryhaline ostracod Cyprideis determined from in vitro experiments, *Palaeogeography, Palaeoclimatology, Palaeoecology*, 148, 105-116.

De Geer, G. (1912). A geochronology of the last 12000 years. *In '11th International Geological Congress' Stockholm*, pp. 241-253.

Demidov, I. N., Houmark-Nielsen, M., Kjaer, K. H., and Larsen, E. (2006). The last Scandinavian Ice Sheet in northwestern Russia: ice flow patterns and decay dynamics. *Boreas* 35, 425 - 443.

Denton, G. H., Heusser, C. J., Lowell, T. V., Moreno, P. I., Andersen, B. G., Heusser, L., Schlüchter, C., and Marchant, D. R. (1999). Interhemispheric linkage of paleoclimate during the last deglaciation. *Geografiska Annaler* 81, 107-153.

Deuser, W. G. (1972). Late-Pleistocene and Holocene history of the Black Sea as indicated by stable-isotope studies. *Journal of Geophysical Research* 77, 1071-1077.

Dwyer, G. S., Cronin, T. M., Baker, P. A., Raymo, M. E., Buzas, J. S., and Corrège, T. (1995). North Atlantic Deepwater Temperature Change During Late Pliocene and Late Quaternary Climatic Cycles. *Science* 270, 1347-1351.

EIE State General Directory of Electrical Research Works. (1993). Sediment data and sediment transport amount for surface waters in Turkey. Ankara, Turkey, EIE.

Engstrom, D. R. and Nelson, S. (1991), Paleosalinity from trace metals in fossil ostracodes compared with observational records at Devils Lake, North Dakota, *Palaeogeography, Palaeoclimatology, Palaeoecology*, 83, 295-312.

Eriksen, U., Friedrich, W. L., Buchardt, B., Tauber, H., and Thomsen, M. S. (1990). The stronghyle Caldera: Geological, palaeontological and stable isotope evidence from radiocarbon dated stromatolites from Santorini. *In Hardy, D.A., Keller, J. (Eds.): Thera and the Aegean World. Santorini, Greece 1990*, 139-150.

Federman, A. N., and Carey, S. N. (1980). Electron microprobe correlation of tephra layers from Eastern Mediterranean abyssal sediments and the Island of Santorini. *Quaternary Research* 13, 160-171.

Felis, T., Lohmann, G., Kuhnert, H., Lorenz, S. J., Scholz, D., Pätzold, J., Al-Rousan, S. A., and Al-Moghrabi, S. M. (2004). Increased seasonality in Middle East temperatures during the last interglacial period. *Nature* 429, 164-168.

Florineth, D., and Schlüchter, C. (2000). Alpine Evidence for Atmospheric Circulation Patterns in Europe during the Last Glacial Maximum. *Quaternary Research* 54, 295-308.

Fontugne, M., Kuzucuoglu, C., Karabiyikoglu, M., Hatte, C., and Pastre, J.-F. (1999). From Pleniglacial to Holocene: a ^{14}C chronostratigraphy of environmental changes in the Konya Plain, Turkey. *Quaternary Science Reviews* 18, 573-591.

Friedrich, M., Kromer, B., Kaiser, K. F., Spurk, M., Hughen, K. A., and Johnsen, S. J. (2001). High-resolution climate signals in the Bolling-Allerod Interstadial (Greenland Interstadial 1) as reflected in European tree-ring chronologies compared to marine varves and ice-core records. *Quaternary Science Reviews* 20, 1223-1232.

Friedrich, W. L., Kromer, B., Friedrich, M., Heinemeier, J., Pfeiffer, T., and Talamo, S. (2006). Santorini Eruption Radiocarbon Dated to 1627-1600 B.C. *Science* 312, 548-551.

Geological Research Department of the General Directorate of Mineral Research and Exploration. (2002). Geological Map of Turkey.

Grootes, P., and Stuvier, M. (1997). Oxygen $^{16/18}$ variablilty in Greenland snow and ice with 10^{-3} to 10^{-5}-year time resolution. *Journal of Geophysical Research* 102, 26,455-26,470.

Grootes, P., Stuvier, M., White, J. W. C., Johnsen, S. J., and Jouzel, J. (1993). Comparison of oxygen isotope records from the GISP2 and GRIP Greeenland ice cores. *Nature* 366, 552-554.

Guichard, F., Carey, S., Arthur, M. A., Sigurdsson, H., and Arnold, M. (1993). Tephra from the Minoan eruption of Santorini in sediments of the Black Sea. *Nature* 363, 610-612.

Hajdas, I., Zolitschka, B., Ivy-Ochs, S. D., Beer, J., Bonani, G., Leroy, S. A. G., Negendank, J. W., Ramrath, M., and Suter, M. (1995). AMS radiocarbon dating of annually laminated sediments from lake Holzmaar, Germany. *Quaternary Science Reviews* 14, 137-143.

Hammer, C. U., Clausen, H. B., Friedrich, W. L., and Tauber, H. (1987). The Minoan eruption of Santorini in Greece dated to 1645 BC? *Nature* 328, 517-519.

Harrison, S. P., Yu, G., and Tarasov, P. E. (1996). Late Quaternary Lake-Level Record from Northern Eurasia. *Quaternary Research* 45, 138-159.

Hay, B. J. (1988). Sediment accumulation in the central western Black Sea over the past 5100 years. *Paleoceanography* 3, 491-508.

Hay, B. J., Honjo, S., Kempe, S., Venugoplan, A., Degens, E. T., Konuk, T., and Izdar, E. (1990). Interannual variability in particle flux in the southwestern Black Sea. *Deep-Sea Research* 37, 911-928.

Howson, M. R., A. D. Pethybridge and W. A. House (1987). Synthesis and distribution coefficient of low-magnesium calcites, *Chemical Geology*, 64, 79-87.

Huang, Y., and Fairchild, I. J. (2001). Partitioning of Sr^{2+} and Mg^{2+} into calcite under karst-analogue experimental conditions, *Geochimica et Cosmochimica Acta*, 65, 47-62.

Hughen, K. A., Baillie, M. G. L., Bard, E., Beck, J.W., Bertrand, C. J. H., Blackwell, P. G., Buck, C. E., Burr, G. S., Cutler, K. B., Damon, P. E., Edwards, R. L., Fairbanks, R. G., Friedrich, M., Guilderson, T. P., Kromer, B., McCormac, G., Manning, S., Ramsey, C. B., Reimer, P. J., Reimer, R. W., Remmele, S., Southon, J. R., Stuiver, M., Talamo, S., Taylor, F. W., van der Plicht, J., and Weyhenmeyer, C. E. (2004). Marine04 marine radiocarbon age calibration, 0-26 cal kyr BP. *Radiocarbon* 46.

Hughen, K. A., Southon, J. R., Lehman, S. J., and Overpeck, J. T. (2000). Synchronous Radiocarbon and Climate Shifts During the Last Deglaciation. *Science* 290, 1951-1954.

Hurrell, J. W. (1995). Decadal Trends in the North Atlantic Oscillation: Regional Temperatures and Precipitation. *Science* 269, 676-679.

Ingram, C. (1998). Palaeoecology and geochemistry of shallow marine ostracoda from the Sand Hole formation, Inner Silver Pit, southern North Sea, *Quaternary Science Reviews*, 17, 913-929.

Ivy-Ochs, S., Kerschner, H., Kubik, P. W., and Schlüchter, C. (2006). Glacier response in the European Alps to Heinrich Event 1 cooling: the Gschnitz stadial. *Journal of Quaternary Science* 21, 115-130.

Jaccard, S. L., Haug, G. H., Sigman, D. M., Pedersen, T. F., Thierstein, H. R., and Röhl, U. (2005). Glacial/Interglacial Changes in Subarctic North Pacific Stratification. *Science* 308, 1003-1006.

Jansen, J. H. F., Van der Gaast, S. J., Koster, B., and Vaars, A. J. (1998). CORTEX, a shipboard XRF-scanner for element analyses in split sediment cores. *Marine Geology* 151, 143-153.

Jones, G. A. (1991). Constraining the initiation and evolution of anoxia in the Black Sea by AMS radiocarbon dating. *Radiocarbon* 33, 211-213.

Jones, G. A., and Gagnon, A. R. (1994). Radiocarbon chronology of Black Sea sediments. *Deep Sea Research Part I: Oceanographic Research Papers* 41, 531-557.

Jones, M. D., Roberts, C. N., and Leng, M. J. (2007). Quantifying climatic change through the last glacial-interglacial transition based on lake isotope palaeohydrology from central Turkey. *Quaternary Research* 67, 463-473.

Jørgensen, B. B. (2003). Cruise 51, Leg 4, Istanbul - Istanbul, *METEOR-Berichte*, 03-1, 1-57.

Kalicki, T., and Sanko, A. F. (1998). Palaeohydrological changes in the Upper Dneper Valley, Belarus, during the last 20,000 years. *In: Benito, G., et al. (Eds.), Palaeohydrology and Environmental Change* Wiley, Chichester, England, 125-135.

Karrow, P. F., and Anderson, T. W. (1975). Palynological studies of lake sediments profiles from SW New Brunswick: Discussion. *Canadian Journal of Earth Science* 12, 1808-1812.

Keller, J., Ryan, W.B.F., Ninkovich, D., Altherr, R. (1978). Explosive volcanic activity in the Mediterranean over the past 200 000 yr as recorded in deep-sea sediments. *Geol. Soc. Am. Bull*. 89, 591-604.

Kelts, K., and Hsü, K. J. (1978). Freshwater carbonate sedimentation. *In Leman, A. (Ed.): Lakes Chemistry, Geology, Physics Springer-Verlag, New York* 295-323.

Kemp, A. E. S. (1996). Laminated sediments as palaeo-indicators. *In Kemp, A.E.S. (Ed.): Palaeoclimatology and Palaeoceanography from Laminated Sediments. Special Publication-Geological Society of London* 116, vii.

Knutz, P. C., Zahn, R. and Hall, I. R. (2007). Centennial-scale variability of the British Ice Sheet: Implications for climate forcing and Atlantic meridional overturning circulation during the last deglaciation, *Paleoceanography*, 22*,* PA1207.

Kostopoulou, E., and Jones, P. D. (2007). Comprehensive analysis of the climate variability in the eastern Mediterranean. Part II: relationships between atmospheric circulation patterns and surface climatic elements. *International Journal of Climatology* 27, 1351-1371.

Kroonenberg, S. B., Rusakov, G. V., and Svitoch, A. A. (1997). The wandering of the Volga delta: a response to rapid Caspian sea-level change. *Sedimentary Geology* 107, 189-209.

Kvasov, D. (1979). *The late-quaternary history of large lakes and inland seas of Eastern Europe*, Annales Academiae Scientiarum Fennicae 157, 71 pp.

Kwiecien, O., Arz, H. W., Lamy, F., Plessen, B., Bahr, A., and Haug, G. H. North Atlantic control on precipitation patterns in the Eastern Mediterranean/Black Sea region during the Last Glacial: new insights from the Black Sea sediments. *Quaternary Research, submitted*.

Kwiecien, O., Arz, H. W., Lamy, F., Plessen, B., Bahr, A., and Haug, G. H. The last deglaciation as recorded in the western Black Sea: a multi-proxy approach. *In preparation*.

Kwiecien, O., Arz, H. W., Lamy, F., Wulf, S., Bahr, A., Röhl, U., and Haug, G. H. (2008). Estimated reservoir ages of the Black Sea since the Last Glacial. *Radiocarbon* 50, 99-118.

Lamb, A. L., Leng, M. J., Umer Mohammed, M., and Lamb, H. F. (2004). Holocene climate and vegetation change in the Main Ethiopian Rift Valley, inferred from the composition (C/N and $\delta^{13}C$) of lacustrine organic matter. *Quaternary Science Reviews* 23, 881-891.

Lamb, A. L., Vane, C. H., Wilson, G. P., Rees, J. G., and Moss-Hayes, V. L. (2007). Assessing $\delta^{13}C$ and C/N ratios from organic material in archived cores as Holocene sea level and palaeoenvironmental indicators in the Humber Estuary, UK. *Marine Geology* 244, 109-128.

Lamy, F., Arz, H. W., Bond, G., Bahr, A., and Pätzold, J. (2006). Multicentennial-scale hydrological changes in the Black Sea and northern Red Sea during the Holocene and the Arctic/North Atlantic Oscillation. *Paleoceanography* 21, PA1008, doi:10.1029/2005PA001184

Lamy, F., Kaiser, J., Ninnemann, U., Hebbeln, D., Arz, H. W., and Stoner, J. (2004). Antarctic Timing of Surface Water Changes off Chile and Patagonian Ice Sheet Response. *Science* 304, 1959-1962.

Landmann, G., Reimer, A., Lemcke, G., and Kempe, S. (1996). Dating Late Glacial abrupt climate changes in the 14,570 yr long continuous varve record of Lake Van, Turkey. *Palaeogeography, Palaeoclimatology, Palaeoecology* 122, 107-118.

Leng, M. J., and Marshall, J. D. (2004). Palaeoclimate interpretation of stable isotope data from lake sediment archives. *Quaternary Science Reviews* 23, 811-831.

Major, C. O., Goldstein, S. L., Ryan, W. B. F., Lericolais, G., Piotrowski, A. M., and Hajdas, I. (2006). The co-evolution of Black Sea level and composition through the last deglaciation and its paleoclimatic significance. *Quaternary Science Reviews* 25, 2031-2047.

Major, C., Ryan, W., Lericolais, G., and Hajdas, I. (2002). Constraints on Black Sea outflow to the Sea of Marmara during the last glacial-interglacial transition. *Marine Geology* 190, 19-34.

Majoran, S., S. Agrenius and G. S. Dwyer (1999). The effect of temperature on the geochemical composition of the shells of the ostracod species Krithe praetexta praetexta, *GEOSOUND*, 35, 93-113.

Mangerud, J., Jakobsson, M., Alexanderson, H., Astakhov, V. I., Clarke, G. K. C., Henriksen, M., Hjort, C., Krinner, G., Lunkka, J.-P., and Moller, P. (2004). Ice-dammed lakes and rerouting of the drainage of northern Eurasia during the Last Glaciation. *Quaternary Science Reviews* 23, 1313-1332.

Manheim, F. T., and Chan, K. M. (1974). Interstitial waters of Black Sea sediments: new data and review. *In Degens, E.T., Ross, D.A. (Eds.): The Black Sea - Geology, Chemistry, and Biology, AAPG, Tulsa, OK*, 155-180.

Mayewski, P. A., Meeker, L. D., Twickler, M. S., Whitlow, S., Yang, S., Lyons, W. B., and Prentice, M. (1997). Major features and forcing of high-latitude northern hemisphere atmospheric circulation using a 110,000-year-long glaciochemical series. *Journal of Geophysical Research* C102, 26,345-26,366.

Menot, G., Bard, E., Rostek, F., Weijers, J. W. H., Hopmans, E. C., Schouten, S., and Damste, J. S. S. (2006). Early Reactivation of European Rivers During the Last Deglaciation. *Science* 313, 1623-1625.

Mix, A. C., Bard, E., and Schneider, R. (2001). Environmental processes of the ice age: land, oceans, glaciers (EPILOG). *Quaternary Science Reviews* 20, 627-657.

Moreno, A., Cacho, I., Canals, M., Grimalt, J. O., Sanchez-Goni, M.-F., Shackleton, N., and Sierro, F. J. (2005). Links between marine and atmospheric processes oscillating on a millennial time-scale. A multi-proxy study of the last 50,000 yr from the Alboran Sea (Western Mediterranean Sea). *Quaternary Science Reviews* 24, 1623-1636.

Moreno, A., Cacho, I., Canals, M., Prins, M. A., Sanchez-Goni, M.-F., Grimalt, J. O., and Weltje, G. J. (2002). Saharan Dust Transport and High-Latitude Glacial Climatic Variability: The Alboran Sea Record. *Quaternary Research* 58, 318-328.

Morse, J. W., and Bender, M. (1990). Partition coefficients in calcite: examination of factors influencing the validity of experimental results and their application to natural systems, *Chemical Geology*, 82, 265-277.

Mudie, P. J., Rochon, A., Aksu, A. E., and Gillespie, H. (2002b). Dinoflagellate cysts, freshwater algae and fungal spores as salinity indicators in Late Quaternary cores from Marmara and Black seas. *Marine Geology* 190, 203-231.

Mudie, P. J., Rochon, A., Aksu, A. E., and Gillespie, H. (2004). Late glacial, Holocene and modern dinoflagellate cyst assemblages in the Aegean-Marmara-Black Sea corridor: statistical analysis and re-interpretation of the early Holocene Noah's Flood hypothesis. *Review of Palaeobotany and Palynology* 128, 143-167.

Mudie, P. J., Rochon, A., and Aksu, A. E. (2002a). Pollen stratigraphy of Late Quaternary cores from Marmara Sea: land-sea correlation and paleoclimatic history. *Marine Geology* 190, 233-260.

Müller, A. (1999). Mg/Ca- und Sr/Ca-Verhältnisse in biogenem Carbonat planktischer Foraminiferen und benthischer Ostracoden, *PhD Thesis*, Universität Kiel

Müller, G., and Stoffers, P. (1974). Mineralogy and petrology of the Black Sea basin sediments. *In Degens, E.T., Ross, D.A. (Eds.): The Black Sea - Geology, Chemistry, and Biology, AAPG, Tulsa, OK*, 200-248.

Murray, J. W., Top, Z., and Özsoy, E. (1991). Hydrographic properties and ventilation of the Black Sea. *Deep-Sea Research* 38, Suppl. 2, 663-689.

Myers, P. G., Wielki, C., Goldstein, S. B., and Rohling, E. J. (2003). Hydraulic calculations of postglacial connections between the Mediterranean and the Black Sea. *Marine Geology* 201, 253-267.

Nadeau, M.J., Schleicher, M., Grootes, P.M., Erlenkeuser, H., Gottdang, A., Mous, D.J.W., Sarnthein, J.M., Willkomm, H. 1997. The Leibniz-Labor AMS facility at the Christian-Albrechts University, Kiel., Germany. *Nuclear Instruments and Methods in Physics Research* 123, 22-30.

Nowaczyk, N. R. (2001). Logging of magnetic susceptibility. *In Last ,W.M. and Smol, J.P. (Eds): Tracking environmental change using lake sediments. Kluwer Academic Publishers, Dordrecht*, pp. 155-170.

O'Brien, N. R. (1996). Shale lamination and sedimentary processes. *In Kemp, A.E.S. (Ed.): Palaeoclimatology and Palaeoceanography from Laminated Sediments. Special Publication-Geological Society of London* 116, 23-36.

Östlund, H. G., and Dyrssen, D. (1986). Renewal rates of the Black Sea deep water. *Report on chemistry of the Seawater. XXXIII* proceedings of the chemical and physical oceanography of the Black Sea, Göteborg, 1986.

Özsoy, E., and Unluata, U. (1997). Oceanography of the Black Sea: a review of some recent results. *Earth-Science Reviews* 42, 231-272.

Özsoy, E., Rank, D., and Salihoglu, I. (2002). Pycnocline and Deep Mixing in the Black Sea: Stable Isotope and Transient Tracer Measurements. *Estuarine, Coastal and Shelf Science* 54, 621-629.

Palacios-Fest, M. R. and Dettman, D. L. (2001). Temperature controls monthly variation in ostracod valve Mg/Ca: Cypridopsis vidua from a small lake in Sonora, Mexico, *Geochimica et Cosmochimica Acta*, 65, 2499-2507.

Palacios-Fest, M., Carreno, A. L., Ortega-Ramirez, J. R., and Alvarado-Valdéz, G. (2002). A paleoenvironmental reconstruction of Laguna Babicore, Chihuahua, Mexico based on ostracod paleoecology and trace element shell chemistry, *Journal of Paleolimnology*, 27, 185-206.

Panin, N., and Jipa, D. (2002). Danube River Sediment Input and its Interaction with the North-western Black Sea. *Estuarine, Coastal and Shelf Science* 54, 551-562.

Pelet, R., and Debyser, Y. (1977). Organic Geochemistry of Black Sea cores. *Geochimica et Cosmochimica Acta* 41, 1575-1577.

Petit, J. R., Jouzel, J., Raynaud, D., Barkov, N. I., Barnola, J.-M., Basile, I., Bender, M., Chappellaz, J., Davis, M., Delaygue, G., Delmotte, M., Kotlyakov, V. M., Legrand, M., Lipenkov, V. Y.,

Lorius, C., Pepin, L., Ritz, C., Saltzman, E., and Stievenard, M. (1999). Climate and atmospheric history of the past 420,000 years from the Vostok ice core, Antarctica. *Nature* 399, 429-436.

Petterson, G. (1996). Varved sediments in Sweden; a brief review. *In Kemp, A.E.S. (Ed.): Palaeoclimatology and Palaeoceanography from Laminated Sediments. Special Publication-Geological Society of London* 116, 73-78.

Peyron, O., Guiot, J., Cheddadi, R., Tarasov, P., Reille, M., de Beaulieu, J.-L., Bottema, S., and Andrieu, V. (1998). Climatic Reconstruction in Europe for 18,000 YR B.P. from Pollen Data. *Quaternary Research* 49, 183-196.

Pilcher, H., and Friedrich, W. (1976). Radiocarbon dates of Santorini volcanics. *Nature* 262, 373-374.

Pilskaln, C. H., and Pike, J. (2001). Formation of Holocene sedimentary laminae in the Black Sea and the role of the bentic flocculent layer. *Paleoceanography* 16, 1-19.

Prasad, S., Vos, H., Negendank, J. F. W., Waldmann, N., Goldstein, S. L., and Stein, M. (2004). Evidence from Lake Lisan of solar influence on decadal- to centennial-scale climate variability during marine oxygen isotope stage 2. *Geology* 32, 581-584.

Prentice, I. C., Guiot, J., and Harrison, S. P. (1992). Mediterranean vegetation, lake levels and paleoclimate at the Last Glacial Maximum. *Nature* 360.

Rasmussen, S. O., Andersen, K.K., Svensson, A. M., Steffensen, J. P., Vinther, B. M., Clausen, H. B., Siggaard-Andersen, M.-L., Johnsen, S. J., Larsen, L. B., Dahl-Jensen, D., Bigler, M., Röthlisberger, R., Fischer, H., Goto-Azuma, K., Hansson, M. E., and Ruth, U. (2006). A new Greenland ice core chronology for the last glacial termination. *Journal of Geophysical Research* 111.

Reimer, P. J., Baillie, M. G. L., Bard, E., Bayliss, A., Beck J.W.,Bertrand, C. J. H., Blackwell, P. G., Buck, C. E., Burr, G. S., Cutler, K. B., Damon, P. E., Edwards, R. L., Fairbanks, R. G., Friedrich, M., Guilderson, T. P., Hogg, A. G., Hughen, K. A., Kromer, B., McCormac, G., Manning, S., Ramsey, C. B., Reimer, R. W., Remmele, S., Southon, J. R., Stuiver, M., Talamo, S., Taylor, F. W., van der Plicht, J., and Weyhenmeyer, C. E. (2004). IntCal04 terrestrial radiocarbon age calibration, 0-26 cal kyr BP. *Radiocarbon* 43, 1029-1085.

Renssen, H., and Bogaart, P. (2003). Atmospheric variability over the ~14.7 kyr BP stadial-interstadial transition in the North Atlantic region as simulated by an AGCM. *Climate Dynamics* 20, 301-313.

Richter, T. O., van der Gaast, S., Koster, B., Vaars, A., Gieles, R., de Stigter, H. C., de Haas, H., and van Weering, T. C. E. (2006). The Avaatech XRF Core Scanner: technical description and application to the NE Atlantic sediments. *in Rothwell, R.G. 'New techniques in sediment core analysis'. Geological Society, London, Special Publications, 267*, 39-50.

Rind, D., Peteet, D., Broecker, W. S., McIntyre, A., and Ruddiman, W. F. (1986). The impact of cold North Atlantic sea surface temperatures on climate: Implications for the Younger Dryas cooling (11-10 k). *Climate Dynamics* 1, 3-33.

Rinterknecht, V. R., Clark, P. U., Raisbeck, G. M., Yiou, F., Bitinas, A., Brook, E. J., Marks, L., Zelcs, V., Lunkka, J.-P., Pavlovskaya, I. E., Piotrowski, J. A., and Raukas, A. (2006). The Last Deglaciation of the Southeastern Sector of the Scandinavian Ice Sheet. *Science* 311, 1449-1452.

Roberts, N. (1983). Age, palaeoenvironments, and climatic significance of late Pleistocene Konya lake, Turkey. *Quaternary Research* 19, 154-171.

Robinson, S. A., Black, S., Sellwood, B. W., and Valdes, P. J. (2006). A review of palaeoclimates and palaeoenvironments in the Levant and Eastern Mediterranean from 25,000 to 5000 years BP: setting the environmental background for the evolution of human civilisation. *Quaternary Science Reviews* 25,, 1517-1541.

Röhl, U., and Abrams, L. J. (2000). High-resolution, downhole and nondestructive core measurements from sites 999 and 1001 in the Caribbean Sea: application to the late Paleocene

thermal maximum. In. Leckies, R.M., Sigurdsson, H., Acton, G.D., Draper, G. (Eds.), *Proceedings of the ODP Scientific Results*. 165, 191–203

Rohling, E. J., Hayes, A., Kroon, D., De Rijk, S., Zachariasse, W. J., and Eisma, D. (1998). Abrupt cold spells in the NW Mediterranean. *Paleoceanography* 13, 316-322.

Ross, D. A., and Degens, E. T. (1970). Black sea: Recent Sedimentary History. *Science* 170, 163-165.

Ross, D. A., and Degens, E. T. (1974). The Black Sea: Geology, Chemistry, and Biology. *E.T. Degens and D.A. Ross (Editors), AAPG, Tulsa, OK*.

Ruddiman, W. F., and McIntyre, A. (1981). The North Atlantic Ocean during the last deglaciation. *Palaeogeography, Palaeoclimatology, Palaeoecology* 35, 145-215.

Ryan, W., Major, C., Lericolais, G., and Goldstein, S. L. (2003). Catastrophic Flooding of the Black Sea. *Annual Revievs of Earth and Planetary Science* 31, 525-554.

Ryan, W., Pitman, C. W., Major, C., Shimkus, K., Moskalenko, V., Jones, G. A., Dimitrov, P., Gorur, N., Sakinc, M., and Yüce, H. (1997). An abrupt drowning of the Black Sea shelf. *Marine Geology* 138, 119-126.

Sanchez Goni, M. F., Cacho, I., Turon, J. L., Guiot, J., Sierro, F. J., Peypouquet, J. P., Grimalt, J. O., and Shackleton, N. J. (2002). Synchroneity between marine and terrestrial responses to millennial scale climatic variability during the last glacial period in the Mediterranean region. *Climate Dynamics* 19, 95-105.

Sanchez Goni, M. F., Turon, J.-L., Eynaud, F., and Gendreau, S. (2000). European Climatic Response to Millennial-Scale Changes in the Atmosphere-Ocean System during the Last Glacial Period. *Quaternary Research* 54, 394-403.

Schieber, J., Southard, J., and Thaisen, K. (2007). Accretion of Mudstone Beds from Migrating Floccule Ripples. *Science* 318, 1760-1763.

Schrader, H. J. (1979). Quaternary paleoclimatology of the Black Sea basin. *Sedimentary Geology* 23, 165-180.

Shimkus, K. M., and Trimonis, E. S. (1974). Modern Sedimentation in Black Sea. *In Degens, E.T., Ross, D.A. (Eds.): The Black Sea - Geology, Chemistry, and Biology, AAPG, Tulsa, OK*, 249-278.

Siani, G., Paterne, M., Arnold, M., Bard, E., Metivier, B., Tisnerat, N., and Bassinot, F. (2000). Radiocarbon reservoir ages in Mediterranean Sea and Black Sea. *Radiocarbon* 42, 271-280.

Sierro, F. J., Hodell, D. A., Curtis, H. J., Flores, J. A., Reguera, I., Colmenero-Hidalgo, E., Barcena, M. A., Grimalt, J. O., Cacho, I., Frigola, J., and Canals, M. (2005). Impact of iceberg melting on Mediterranean thermohaline circulation during Heinrich events. *Paleoceanography* 20, 1-13.

Spahni, R., Chappellaz, J., Stocker, T. F., Loulergue, L., Hausammann, G., Kawamura, K., Fluckiger, J., Schwander, J., Raynaud, D., Masson-Delmotte, V., and Jouzel, J. (2005). Atmospheric Methane and Nitrous Oxide of the Late Pleistocene from Antarctic Ice Cores. *Science* 310, 1317-1321.

Sperling, M., Schmiedl, G., Hemleben, C., Emeis, K. C., Erlenkeuser, H., and Grootes, P. M. (2003). Black Sea impact on the formation of eastern Mediterranean sapropel S1? Evidence from the Marmara Sea. *Palaeogeography, Palaeoclimatology, Palaeoecology* 190, 9-21.

Starkov, J. J. (1951). Outline of carbonate accumulation in modern reservoirs. *in Schatskiy NS. Memorials to Academican A. D. Arcgangielskiy, Moscow Izv. Akad. Nauk SSSR* 487-567.

Stuiver, M., Reimer, P. J., and Reimer, R. W. (2005). Calib 5.0. (www pragram and documentation). *URL: http://calib.qub.ac.uk/calib/*

Sur, H. I., and Özsoy, E. (1996). Costal/deep ocean interactions in the Black sea an their ecological/environmental impacts. *Journal of Marine Systems* 7, 293-320.

Svitoch, A. A. (1997). Caspian Sea level in the Pleistocene: hierarchy and position in the paleogeographic and chronological records. *Oceanology* 39, 94-1001.

Svitoch, A. A. (2007). On the nature of the Khvalynian transgression of the Caspian Sea. *Oceanology* 47, 282-289.

Swart, P. K. (1991). The oxygen and hydrogen isotopic composition of the Black Sea. *Deep-Sea Research (Black Sea Oceanography)* 38, supplement, 761-772.

Tjallingii, R., Röhl, U., Kölling, M., and Bickert, T. (2007). Influence of the water content on X-ray fluorescence corescanning measurements in soft marine sediments. *Geochemistry Geophysics Geosystems* 8. Q02004, doi:10.1029/2006GC001393

Top, Z., and Clark, W. B. (1983). Helium, neon and tritium in the Black Sea. *Journal of Marine Research* 41, 1-17.

Touchan, R., Akkemik, U., Hughes, M. K., and Erkan, N. (2007). May-June precipitation reconstruction of southwestern Anatolia, Turkey during the last 900 years from tree rings. *Quaternary Research* 68, 196-202.

Türkes, M., and Erlat, E. (2005). Climatological responses of winter precipitation in Turkey to variability of the North Atlantic Oscillation during the period 1930–2001. *Theoretical and Applied Climatology* 81, 45-69.

Tzedakis, P. C. (2007). Seven ambiguities in the Mediterranean palaeoenvironmental narrative. *Quaternary Science Reviews* 26, 2042-2066.

Verosub, K. L., and Roberts, A. P. (1995). Environmental magnetism: Past, present and future. *Journal of Geophysical Research* 100, 2175-2192.

Vescovi, E., Ravazzi, C., Arpenti, E., Finsinger, W., Pini, R., Valsecchi, V., Wick, L., Ammann, B., and Tinner, W. (2007). Interactions between climate and vegetation during the Lateglacial period as recorded by lake and mire sediment archives in Northern Italy and Southern Switzerland. *Quaternary Science Reviews* 26, 1650-1669.

Vinci, A. (1985). Distribution and chemical composition of tephra layers from Eastern Mediterranean abyssal sediments. *Marine Geology* 64, 143-155.

Vinther, B. M., Clausen, H. B., Johnsen, S. J., Rasmussen, S. O., Andersen, K. K., Buchardt, S. L., Dahl-Jensen, D., Seierstad, I. K., Siggaard-Andersen, M.-L., Steffensen, J. P., Svensson, A. M., Olsen, J., and Heinemeier, J. (2006). A synchronized dating of three Greenland ice cores throughout the Holocene. *Journal of Geophysical Research* 111, D13102, doi:10.1029/2005JD006921.

von Grafenstein, U., Eicher, U., Erlenkeuser, H., Ruch, P., Schwander, J., and Ammann, B. (2000). Isotope signature of the Younger Dryas and two minor oscillations at Gerzensee (Switzerland): palaeoclimatic and palaeolimnologic interpretation based on bulk and biogenic carbonates. *Palaeogeography, Palaeoclimatology, Palaeoecology* 159, 215-229.

von Grafenstein, U., Erlenkeuser, H., Brauer, A., Jouzel, J., and Johnsen, S. J. (1999a). A Mid-European Decadal Isotope-Climate Record from 15,500 to 5000 Years B.P. *Science* 284, 1654-1657.

von Grafenstein, U., Erlernkeuser, H., and Trimborn, P. (1999b). Oxygen and carbon isotopes in modern fresh-water ostracod valves: assessing vital offsets and autecological effects of interest for palaeoclimate studies. *Palaeogeography, Palaeoclimatology, Palaeoecology* 148, 133-152.

Waelbroeck, C., Duplessy, J.-C., Michel, E., Labeyrie, L., Paillard, D., and Duprat, J. (2001). The timing of the last deglaciation in North Atlantic climate records. *Nature* 412, 724-727.

Walker, M. J. C. (1995). Climatic changes in Europe during the last glacial/interglacial transition. *Quaternary International* 28, 63-76.

Wansard, G. (1996), Quantification of paleotemperature changes during isotopic stage 2 in the La Draga continental sequence (NE Spain) based on the Mg/Ca ratio of freshwater ostracods, *Quaternary Science Reviews*, 15, 237-245.

Wansard, G. and Roca, J. P. (1997), Ètude expérimentale de l'incorporation du strontium et du magnesium dans le valves d'un ostracode d'eau douce, Heterocypris brevicaudata (Crustacea, Ostracoda), *Comptes Rendus de l'Académie des Sciences,* 325*,* 403-409.

Wansard, G., Roca, J. P., and Mezquita, F. (1999). Experimental determination of strontium and magnesium partitioning in calcite of the freshwater ostracod Herpetocypris intermedia, *Archiv für Hydrobiologie*, 145, 237-253.

Wansard, G., De Deckker, P. and Julia R. (1998). Variability in ostracod partition coefficients D(Sr) and D(Mg): Implications for lacustrine palaeoenvironmental reconstructions, *Chemical Geology*, 146, 39-54.

Wigley, T. M. L., and Farmer, G. (1982). Climate of the Eastern Mediterranean and the Near East. *In Bintliff, J.L. et al. (Eds.), Paleoclimates, Paleoenvironments and Human Communities in the Eastern Mediterranean Region in Later Prehistory*, *Oxford* 3-37.

Wulf, S., Kraml, M., Keller, J. Towards a detailed distal tephrostratigraphy in the Mediterranean: the last 20 kyrs record of Lago Grande di Monticchio. *Journal of Volcanology and Geothermal Research,* in press.

Wulf, S., Kraml, M., Kuhn, T., Schwarz, M., Inthorn, M., Keller, J., Kuscu, I., and Halbach, P. (2002). Marine tephra from the Cape Riva eruption (22 ka) of Santorini in the Sea of Marmara. *Marine Geology* 183, 131-141.

Zeebe, R. E., and Wolf-Gladrow, D. (2001). CO_2 in seawater: equilibrium, kinetics, isotopes. *Elsevier oceanography series,* 17-83.

Zonneveld, K. A. F. (1996). Palaeoclimatic reconstruction of the last deglaciation (18-8 ka B.P.) in the Adriatic Sea region; a land-sea correlation based on palynological evidence. *Palaeogeography, Palaeoclimatology, Palaeoecology* 122, 89-106.